JPL Publication 90-9

A Novel Multireceiver Communications System Configuration Based on Optimal Estimation Theory

R. Kumar

February 1, 1990

Prepared for

California State University,
Long Beach

and

National Aeronautics and
Space Administration

by

Jet Propulsion Laboratory
California Institute of Technology
Pasadena, California

JPL Publication 90-9

A Novel Multireceiver Communications System Configuration Based on Optimal Estimation Theory

R. Kumar

February 1, 1990

Prepared for

California State University,
Long Beach

and

National Aeronautics and
Space Administration

by

Jet Propulsion Laboratory
California Institute of Technology
Pasadena, California

The research described in this publication was carried out by the Jet Propulsion Laboratory, California Institute of Technology, and was sponsored by the California State University, Long Beach, and the National Aeronautics and Space Administration.

ABSTRACT

This publication presents a novel multireceiver configuration for the purpose of carrier arraying and/or signal arraying. Such a problem arises for example, in the NASA Deep Space Network where the same data-modulated signal from a spacecraft is received by a number of geographically separated antennas and the data detection must be efficiently performed on the basis of the various received signals. The proposed configuration is arrived at by formulating the carrier and/or signal arraying problem as an optimal estimation problem. Two specific solutions are proposed.

The first solution is to simultaneously and optimally estimate the various phase processes received at different receivers with coupled phase-locked loops (PLLs) wherein the individual PLLs acquire and track their respective receivers' phase processes, but are aided by each other in an optimal manner. The coupled PLL estimator is followed by simple addition of the quadrature-phase components of the mixers from various receivers for the purpose of data detection. Such signal combining, of course, requires the transmission of high information rate (the rate related to the data transmission rate) baseband signals from all the receivers to one of the selected receivers, as expected. For relatively strong correlation among various phase processes, the detection performance as measured in terms of radio loss is near optimal; in this case the phase error processes themselves are also highly correlated.

However, when the phase processes are relatively weakly correlated, coupling among loops is of only marginal significance (in the limit the improvement due to coupling is zero for zero cross-correlation). In this case, most of the gain is expected to result from the post-loop combining. However, simple combining of baseband signals

is far from optimal in this case as the residual phase errors from different loops are highly uncorrelated. For this case, and for the case of relatively high values of symbol energy-to-noise spectral density ratio (E_s/N_0), we propose a novel configuration for combining the data-modulated, loop-output signals.

The scheme can be extended to the case of low (E_s/N_0) case by performing the combining/detection process over a multisymbol period. Such a configuration results in the minimization of the effective radio loss at the combiner output, and thus a maximization of energy per bit to noise-power spectral density ratio is achieved.

CONTENTS

1. INTRODUCTION 1

2. SIGNAL MODEL AND RECEIVER STRUCTURE 5

3. OPTIMUM ESTIMATION VIA COUPLED, PHASE-LOCKED LOOPS . 9

4. AN EVALUATION OF THE PROPOSED CONFIGURATION 11

5. PERFORMANCE COMPUTATION VIA RECURSIVE SOLUTION 17

6. A NOVEL SIGNAL-COMBINING CONFIGURATION FOR COUPLED RECEIVERS 21

7. CONCLUSIONS 31

8. SUGGESTIONS FOR FUTURE RESEARCH 35

REFERENCES 37

APPENDICES

Appendix A: Extended Kalman Filter Equations for the Signal Model (5–8) 39

Appendix B: Steady State Performance Equations for a Dual-Receiver Communications System 43

FIGURES

1. (a) Proposed Estimation–Detection Scheme 1 51
   (b) Proposed Estimation–Detection Scheme 2 52

2. (a) Multireceiver Configuration With N = 2 53
   (b) An Equivalent Implementation for the Case of Diagonal Matrix F and n = 2 54

3. Digital Filter Implementation of G^{11} (z) 55

4. An Equivalent Implementation of a Two-Receiver Configuration 56

5. Implementation of the Multivariable Digital Filter, S_1 57

CONTENTS (cont'd)

6. Normalized Loop Noise Bandwidth of the Second-Order Filter vs. (σ_a^2/σ_v^2) 58

7. Normalized Phase Error Variance vs.(σ_a^2/σ_v^2) 59

8. Comparison of Filter Performance With and Without Process Noise 60

9. Improvement Due to Arraying; $\rho = 0.995$ 61

10. Improvement Due to Arraying; $\rho = 0.999$ 62

11. Improvement Due to Arraying; T = 0.5, $\sigma_a^2/\sigma_v^2 = 1.0$ 63

12. Improvement Due to Arraying; T = 0.5, $\rho = 0.999$ 64

13. Improvement Due to Arraying With a Two-Receiver Configuration; T = 0.5 65

14. Improvement Due to Arraying With a Two-Receiver Configuration; T = 0.1 66

15. Improvement Due to Arraying With a Two-Receiver Configuration; T = 0.01 67

16. Improvement Due to Arraying With a Three-Receiver Configuration (Equal CNR; $\sigma_a^2/\sigma_v^2 = 0.1$) 68

17. Improvement Due to Arraying With a Three-Receiver Configuration (Equal CNR; $\sigma_a^2/\sigma_v^2 = 10$) 69

18. Improvement Due to Arraying With a Three-Receiver Configuration (Equal CNR; T = $0.01s$) 70

19. Improvement Due to Arraying With a Three-Receiver Configuration (Equal CNR; T = $0.5s$) 71

20. Improvement Due to Arraying With a Three-Receiver Configuration and a 1:1:4 Ratio (Receiver 1) 72

21. Improvement Due to Arraying With a Three-Receiver Configuration and a 1:4:4 Ratio (Receiver 1) 73

22. Improvement Due to Arraying With a Three-Receiver Configuration and a 1:4:4 Ratio (Receiver 2) 74

CONTENTS (cont'd)

23. Improvement Due to Arraying With a Three-Receiver Configuration and a 1:1:4 Ratio (Receiver 3) 75

24. Improvement Due to Arraying With a Three-Receiver Configuration and a 1:4:16 Ratio (Receiver 3) 76

25. Improvement Due to Arraying With a Three-Receiver Configuration and a 1:1:4 Ratio (Receiver 1) 77

26. Improvement Due to Arraying With a Four-Receiver Configuration; Equal CNR Case 78

27. Improvement Due to Arraying With a Four-Receiver Configuration and a 1:1:1:4 Ratio (Receiver 1) 79

28. Improvement Due to Arraying With a Four-Receiver Configuration and a 1:1:4:4 Ratio (Receiver 1) 80

29. Improvement Due to Arraying With a Four-Receiver Configuration and a 1:1:4:4 Ratio (Receiver 3) 81

30. Improvement Due to Arraying With a Four-Receiver Configuration and a 1:4:4:4 Ratio (Receiver 1) 82

31. Improvement Due to Arraying With a Four-Receiver Configuration and a 1:1:1:4 Ratio (Receiver 4) 83

32. Improvement Due to Arraying With a Four-Receiver Configuration and a 1:4:4:16 Ratio (Receiver 4) 84

33. Decision-Directed Carrier Recovery Loop 85

34. Decision-Directed and Coupled Receiver Configuration 86

1. INTRODUCTION

Recently, there has been some interest in a carrier arraying system to combine the received carrier signals at geographically separated antennas with different carrier phases to improve the overall carrier tracking performance [1-3]. The expected improvement occurs both in terms of the rms phase jitter and radio loss or the carrier-to-noise power spectral density ratio (CNR) margin.

The scheme of [1-3] treats one of the receivers as "master" receiver that tracks its received phase noise process by a comparatively large bandwidth loop. It is aided by other loops in combining the signals received from other receivers at an intermediate frequency (IF). In turn, the "master" receiver broadcasts its voltage-controlled oscillator (VCO) output signal to other receivers so as to aid their tracking processes. Thus, the coupling among various receivers in this configuration occurs at both RF and IF stages. If the phase processes among various receivers are strongly correlated, so that the loop noise bandwidth of all receivers other than the "master" can be reduced enough to achieve negligible tracking errors, then the IF combining occurs almost coherently and the system (first receiver) is expected to perform optimally.

The above scheme, however, seems to have been arrived at intuitively and it is not clear if the performance is optimal. In fact, for the case of equal antenna size and receiver noise temperatures, one would expect some symmetry in the receivers' coupling that is absent in this scheme. Moreover, as will be shown in this publication, if the phase processes are not very strongly correlated, then signal combining in this manner can result in a very significant loss of optimality, in terms of both CNR margin and data detection performance. In an alternative scheme presented in [4], individual

carrier signals are tracked by independent PLLs and the (linear) signal combining takes place at the baseband (subcarrier) level or at the symbol stream level just prior to the data detection.

In this publication, we formulate the problem of parameter estimation for an antenna array as an optimal estimation problem in a way similar to the case of a single antenna [5-9]. The proposed configurations arrived at in this manner consist of two distinct stages as shown in Figures 1a and 1b, wherein the first stage provides mutual coupling among the loops for joint estimation of various phase processes, while the second stage performs signal alignment and combining. While the two configurations are identical in terms of the first stage, they differ markedly with respect to the second stage. Whereas the second stage of the configuration I of Figure 1a involves linear combining of various signals, the configuration of Figure 1b achieves both an explicit phase alignment and the signal combining. The optimization technique also yields the actual coefficients of coupling for these configurations.

In practice, one could of course use the proposed structure, but the actual coefficients may then be related to more intuitive parameters such as the loop noise bandwidths of various loops. Another advantage of the proposed scheme is that under relatively strong correlation among various phase processes, the mutual coupling among receivers is at baseband only as against at IF and RF levels in the previous scheme. In the proposed scheme, the coupling among receivers is via baseband error signals, and in the absence of coupling (simply by disabling the interconnections among various receivers), the system reduces to a decoupled configuration, i.e., individual receivers track their respective phase processes. This may be a desirable feature and is not

common to the scheme of [1-3]. Moreover, a consequence of this approach is that the system explicitly takes into account any correlation among various receiver parameters as noise temperatures. The scheme of [1-3] does not suggest any mechanism for this. A decision-directed version of the proposed scheme can be used for signals with relatively high E_S/N_0. It consists of the simple addition of the quadrature-phase components of the mixers from various receivers for the purpose of data detection. Such signal combining, as expected, requires the transmission of high information rate (related to data rate) baseband signals from all the receivers to one of the selected receivers.

It is also to be noted that for the case of weak correlations among the phase processes, the scheme of [1-3] would not be satisfactory in that the phases of the IF signals at the input to the combiner are uncorrelated. Adding such signals would result in a drastic performance loss compared to the case of strong coupling. For this case, the proposed configuration II effectively averages out the phase errors at various receivers, thus performing an explicit phase alignment in addition to the implicit alignment achieved via mutual coupling and resulting in the same performance as for the strong coupling case. The scheme is applicable to the cases of both the residual carrier and the decision-directed (suppressed carrier) loops. Thus, the scheme provides a novel method for optimum signal combining under considerable phase jitters among estimated phase processes.

In this technique, the high information rate (related to data rate) signals are transmitted at some IF frequency for the purpose of optimum nonlinear combining at one of the selected receivers. Alternatively, these signals may be transmitted at baseband and modulated at the central receiver by an IF frequency for the purpose of

phase aligment. Figures 1a and 1b may be of help in the conceptual understanding of the two proposed schemes. In the next section, we derive these structures by the application of optimal estimation theory; we also present their more detailed schematic.

Detailed performance evaluations of the proposed schemes are presented in the following sections of this publication. These results show that for the case of very high correlation among various phase processes and equal CNR among the N receivers, there is an improvement of $10\log_{10} N$ dB in terms of effective CNR due to arraying, as is intuitively expected. However, the more important and perhaps surprising aspect of the presented results is that with the proposed arraying scheme, the same improvement can be obtained for the complete range of correlation coefficients.

The decision-directed versions of the proposed coupled-receiver configurations incorporate a transition detection scheme in the loop so as to provide a near-optimum estimation/detection performance even under the conditions of relatively high phase errors that may be encountered during acquisition.

2. SIGNAL MODEL AND RECEIVER STRUCTURE

We consider the problem of estimating the phase processes $\theta_i(k), i = 1, 2, \ldots N$ from the sampled version of the received carrier signals $y^i(k)$, i.e.,

$$y^i(k) = A\sqrt{2}\,\mathrm{Sin}(\omega_c t_k + \theta^i(k)) + \overline{v}^i(k); \quad i = 1, 2, \ldots, N \tag{1}$$

where t_k is the kth sampling time, ω_c is the known carrier frequency and $\overline{v}^i(k)$, the observation noise, is the sampled version of a narrow-band, zero-mean, white-Gaussian noise process $\overline{v}^i(t)$. In (1), without loss of any generality, we have assumed that the carrier amplitude is equal for all the receivers, while the additive noise variance may differ for various receivers. This is in view of the fact that the performance of the estimation algorithm depends only on the signal-to-noise ratio and not individually on the signal and noise powers. However, with minor variations, the following estimation algorithm includes the case where A is replaced by A^i; $i = 1, 2, \ldots N$ in signal model (1). The phase processes $\theta^i(k)$ at various receivers are assumed, in general, to be partially correlated processes (in the limit these may be completely uncorrelated or in the other extreme may be identical) and are modeled as

$$\theta^i(k) = \ell' x^i(k); \;\; \ell' = [1 \;\; 0 \ldots 0]; \quad i = 1, 2, \ldots, N \tag{2}$$

In (2) above, $x^i(k)$ denotes the state vector of dimension n_s associated with the ith phase process. For the case of a single receiver configuration, the state vector $x^i(k)$ is modeled as [8]:

$$x^i(k+1) = \Phi_s x^i(k) + w^i(k) \tag{3}$$

where Φ_s is an $n_s \times n_s$ matrix and $w^i(k)$ is a zero-mean, white-Gaussian noise process independent of $\overline{v}^i(k)$.

For the multireceiver configuration considered here, we model the state dynamics as follows:

$$\begin{bmatrix} x^1(k+1) \\ x^2(k+1) \\ \vdots \\ x^N(k+1) \end{bmatrix} = (\Phi_s \otimes F) \begin{bmatrix} x^1(k) \\ x^2(k) \\ \vdots \\ x^N(k) \end{bmatrix} + \begin{bmatrix} w^1(k) \\ w^2(k) \\ \vdots \\ w^N(k) \end{bmatrix} \tag{4}$$

where $\otimes$ denotes the Kronecker matrix product (the definition is included in Appendix A), F is an $(N \times N)$ matrix, and the dynamic noise processes, $w^i(k)$, are in general mutually correlated. Thus, the processes $x^i(k)$ may be coupled both via the matrix F and via the cross covariances of $w^i(k)$, $i = 1, 2, \ldots, N$. In a simpler model, F may be taken to be an identity matrix, and an appropriate structure may be imposed on the covariance Q of $w(k)$. The latter denotes the Nn_s dimensional noise vector in (4). Denoting by $x(k)$ the composite state vector for the multireceiver configuration, one may write (4) in the following compact form:

$$x(k+1) = \Phi\, x(k) + w(k) \tag{5}$$

with $\Phi \triangleq \Phi_s \otimes F$. We assume that $w(k)$ is a zero-mean, white-Gaussian process independent of $\overline{v}(k) \triangleq [\{\overline{v}^1(k)\}^T \ldots \{\overline{v}^N(k)\}^T]^T$, where T denotes the matrix transpose. Thus,

$$\begin{aligned} &E[\overline{v}(k)] = 0, \quad E[w(k)] = 0 \\ &E[\overline{v}(k)\overline{v}^T(k)] = \overline{R}, \quad E[w(k)w^T(k)] = Q; \quad E[\overline{v}(k)w^T(j)] = 0 \quad ; j, k = 1, 2, \ldots \end{aligned} \tag{6}$$

The measurement equation (1) may also be written in the following vector-matrix form:

$$y(k) = h(x(k), k) + \overline{v}(k) \tag{7}$$

where

$$y(k) \triangleq [y^1(k) \ldots y^N(k)]^T, \quad \overline{v}(k) \triangleq [\overline{v}^1(k) \ldots \overline{v}^N(k)]^T$$

$$h(x(k),k) \triangleq [h^1(x,k) \ldots h^N(x,k)]^T$$

$$h^i(x,k) = A\sqrt{2}\,\mathrm{Sin}(\omega_c t_k + \theta^i(k)) \tag{8}$$

$$= A\sqrt{2}\,\mathrm{Sin}(\omega_c t_k + \ell^T x^i(k)) \quad ; \; i = 1,2,\ldots,N$$

As shown in Appendix A, the extended Kalman filter equations for the signal model (5-8) are given by (A1), (A15-A17), (A5), and (A14).Under the assumption of a small estimation error, $\tilde{x}(k+1/k) = x(k+1) - \hat{x}(k+1/k)$, the filter equations may be simplified as follows: Representing the bandpass additive noise $\overline{v}^i(k)$ in terms of its baseband quadrature components $\overline{v}_i^i(k)$ and $\overline{v}_q^i(k)$ as

$$\overline{v}^i(k) = \overline{v}_i^i(k)\,\mathrm{Sin}\,(\omega_c t_k + \ell' x^i(k)) + \overline{v}_q^i(k)\,\mathrm{Cos}\,(\omega_c t_k + \ell' x^i(k))$$

the prediction error $\eta^i(k+1)$ given by (A17) may be approximated by

$$\eta^i(k+1) = A\ell^T \tilde{x}^i(k+1/k) + \frac{1}{\sqrt{2}}\,\overline{v}_i^i(k+1); \quad i = 1,2,\ldots,N \tag{9}$$

We note that $\eta(k+1) \triangleq [\eta^1(k+1) \ldots \eta^N(k+1)]^T$ of (9) is also the one-step-ahead prediction error for the following model:

$$y(k+1) = A\,H\,x(k+1) + \frac{1}{\sqrt{2}}\,\overline{v}_i(k+1) \tag{10}$$

where

$$H \triangleq \begin{bmatrix} \ell^T & 0 & \ldots & \ldots & 0 \\ 0 & \ell^T & \ldots & \ldots & 0 \\ \ldots & \ldots & \ldots & \ldots & \ldots \\ 0 & \ldots & \ldots & \ldots & \ell^T \end{bmatrix} \quad ; \quad \ell^T = [1 \;\; 0 \ldots 0]$$

and $\overline{v}_i(k+1)$ is the vector consisting of $\overline{v}_i^j$ as its jth elements. It is also clear that under the assumption of small estimation error, the filter equations of Appendix A reduce to the following standard linear Kalman filter equations:

$$\hat{x}(k+1/k+1) = \Phi\,\hat{x}(k/k) + K(k+1)\eta(k+1) \tag{11a}$$

$$\eta^i(k+1) = \sqrt{2}y^i(k+1)\,\mathrm{Cos}\,(\hat{\Theta}^i(k+1)) \tag{11b}$$

$$\hat{\Theta}^i(k+1) = \omega_c t_{k+1} + \ell^T\,\hat{x}^i\,(k+1/k) \tag{11c}$$

$$K(k+1) = A\,P(k+1/k)H\,S^{-1}(k+1) \tag{11d}$$

$$P(k+1/k+1) = P(k+1/k) - A^2\,P(k+1/k)H^T S^{-1}(k+1)H\,P(k+1/k) \tag{11e}$$

$$P(k+1/k) = \Phi P(k/k)\Phi^T + Q \tag{11f}$$

$$S(k+1) = H\,P(k+1/k)H^T + R \tag{11g}$$

where R is the covariance of the measurement noise vector $\overline{v}_i(k+1)/\sqrt{2}$ appearing in (10) and is equal to $\overline{R}/2$. Note that in the derivation of the filter equations in Appendix A, the measurement noise covariance matrix $\overline{R}$ is assumed to be diagonal. However, in view of equations (9-10), the recursions (11) are applicable to the case of nondiagonal R as well.

3. OPTIMUM ESTIMATION VIA COUPLED, PHASE-LOCKED LOOPS

The various antennas may be geographically separated in most situations, including space exploration. Therefore, for the purposes of proposed implementation, we represent the solution (11) as a set of interacting phase-locked loops with various PLLs associated with their respective receivers and the interaction among them occurring over low data rate communication links. Such an arrangement is illustrated in Figure 2a for the case of two receivers. The receiver configuration of the figure may be simplified by replacing the components of the Kalman gain matrix by its steady-state value, which may be precomputed. In addition, the feedback gain vectors K^{12} and K^{21} (superscripts refer to the specific block in the partition of the Kalman gain matrix) may equivalently be replaced by scalars to bring the organization of the figure into a more conventional form.

Considering first the case when $F_{12} = F_{21} = 0$, and denoting by $\hat{\Theta}^1(z)$ the Z transform of the input $\hat{\theta}^1(k)$ to the phase modulator in Figure 2a (in actual implementation, the phase modulator is replaced by NCO, whose input is the difference signal $(\hat{\theta}^1(k) - \hat{\theta}^1(k-1))(K_v \Delta t)^{-1}$ with Δt being the lead time and K_v equal to the NCO sensitivity), then $\hat{\Theta}^1(z)$ is given by

$$\hat{\Theta}^1(z) = \ell^T F_{11} \Phi_s [z\, I - F_{11} \Phi_s]^{-1} K^{11} \eta^1(z) + \ell^T F_{11} \Phi_s [z\, I - F_{11} \Phi_s]^{-1} K^{12} \eta^2(z) \quad (12)$$

It may also be expressed in the following more convenient form:

$$\hat{\Theta}^1(z) = G^{11}(z) \eta^1(z) + G^{12} \eta^2(z)$$

$$G^{11}(z) = \ell^T F_{11} \Phi_s [z\, I - F_{11} \Phi_s]^{-1} K^{11}, \quad G^{12}(z) = \ell^T F_{11} \Phi_s [z\, I - F_{11} \Phi_s]^{-1} K^{12} \quad (13)$$

For the case of $n_s = 2$ and with

$$\Phi_s = \begin{bmatrix} 1 & T \\ 0 & 1 \end{bmatrix}$$

the filter transfer function $G^{11}(z)$ may be obtained as

$$G^{11}(z) = \frac{F_{11}(K_1^{11} + K_2^{11}T)z - F_{11}^2 K_1^{11}}{(z - F_{11})^2} \tag{14}$$

Similarly, $G^{12}(z)$ is obtained by replacing K^{11} by K^{12} in (14).

This formulation ignores the internal state of the filter related to the initial condition $\hat{x}^1(0/0)$. However, by selecting the initial states of the two filters $G^{11}(z)$, $G^{12}(z)$, such that their sum is equal to $\hat{x}^1(0/0)$, and with the proper implementation of the filter, this problem is eliminated. Figure 2b shows an equivalent implementation of the receiver coupling for the case of $F_{12} = F_{21} = 0$. The filter transfer functions $G^{21}(z)$ and $G^{22}(z)$ have a form similar to (14) for the case of $n = 2$. Figure 3 shows a digital filter implementation wherein the filter states are related to $\hat{x}(0/0)$ as discussed above.

For the case of F_{12}, $F_{21} \neq 0$, it is required that the filter states of the second receiver also be fed back to receiver 1. In this case, the implementation of a two-receiver configuration is depicted in Figure 4 wherein S_1 and S_2 are multivariable digital filters. A detailed schematic diagram for filter S_1 is shown in Figure 5. The implementation of filter S_2 is very similar.

4. AN EVALUATION OF THE PROPOSED CONFIGURATION

Under the assumption that the estimation errors are relatively small, as is the case under high CNR, the phase detector may be approximated by linear characteristics and the performance of the system is given by $P(k+1/k)$ of equation (11). As $k \rightarrow \infty$, the matrix $P(k+1/k)$ approaches a steady-state value denoted by $\overline{P}$, which is the solution of the following algebraic matrix Riccati equation:

$$\overline{P} = \Phi\left[\overline{P} - A^2\overline{P}\, H^T\, S^{-1}\, H\, \overline{P}\right]\Phi^T + Q \tag{15}$$

As shown in [10], the solution $\overline{P}$ is given in terms of the eigenvectors of the following $2n$ dimensional matrix H_f:

$$H_f = \begin{bmatrix} \Phi^{-T} & \Phi^{-T}H^TR^{-1}H \\ Q\,\Phi^{-T} & \Phi + Q\,\Phi^{-T}H^TR^{-1}H \end{bmatrix} \tag{16}$$

Moreover, the eigenvalues of H_f are such that the reciprocal of an eigenvalue is also an eigenvalue. Assuming that the eigenvalues are distinct, then H_f may be factorized as

$$H_f = W\, D\, W^{-1} \tag{17}$$

where D is a diagonal matrix consisting of the eigenvalues of H_f along its main diagonal, with the first half (n) entries having their magnitude greater than one, and W being a nonsingular, eigenvector matrix. With the matrix W partitioned into $n \times n$ blocks as below,

$$W = \begin{bmatrix} W_{11} & W_{12} \\ W_{21} & W_{22} \end{bmatrix} \tag{18}$$

then the steady-state solution $\overline{P}$ is given by

$$\overline{P} = W_{21}W_{12}^{-1} \tag{19}$$

The steady-state filter error covariance matrix is then obtained by substituting $\overline{P}$ for $P(k+1/k)$ on the right hand side of (11e), as

$$\overline{P}_F = \overline{P} - A^2 \overline{P}\, H^T S^{-1} H\, \overline{P} \tag{20}$$

Substitution of $\overline{P}$ for $P(k+1/k)$ also yields the Kalman gain matrix K from (11d, g). Knowledge of K then permits the implementation of the (time-invariant) digital filters in Figures 1-5.

In Appendix B, we consider coupled, dual-receiver, configuration-employing type I and type II loops in more detail. For type II loops, which are of more interest here, equations (B15)-(B22) present an analytical solution in a convenient form for the matrix W of (18) as a function of the various parameters, r_1, r_2, T, q_{11}, etc., related to the joint phase processes model (B11). The filter error covariance matrix $\overline{P}$ for a two-receiver configuration, with each receiver employing a second-order loop, is then evaluated on the basis of equations (B15)-(B22), (19), and (20) for various values of these parameters. One of the most important quantities of interest is the ratio of the phase error variance of a receiver operating under coupled configuration to that obtained without any coupling while keeping the statistics of various processes the same. To keep the presentation simple (where only a relatively small number of parameters vary), we assume that the process noise in each receiver has equal variance $q_{11} = q_{22}$ in (A1). This is an appropriate assumption for the present application. Denoting by $\overline{P}_{Fk}$ the steady-state filter error covariance matrix for the kth receiver operating independently, this performance measure for the kth receiver is simply equal to 10 $\log_{10}\{\overline{P}_{F1}(1,1)/\overline{P}_F(1,1)\}$ and 10 $\log_{10}\{\overline{P}_{F2}(1,1)/\overline{P}_F(3,3)\}$ respectively for $k =$

1, 2, and is evaluated for various values of the parameters T, $\rho = q_{12}/q_{11}$ and $\sigma_a^2/\sigma_v^2 \triangleq (q_{11}/T^2 r_k)$ with r_k equal to the observation noise variance for receiver k. The notations σ_a^2 and σ_v^2 have been used in [7,8] and have been introduced here for the purpose of referring to the results obtained in [7,8] for the case of a single receiver. As shown in [8] for the case of a single receiver, the parameter σ_a^2/σ_v^2 is decisive in determining the optimal loop-noise bandwidth of the phase-locked loop.

A more effective performance measure is the required increase in the received signal-to-noise power ratio for a single receiver, in order to achieve the same phase error as obtained by the dual receiver. The performance of a single receiver has been analyzed in some detail in [8] and some of those results are reproduced here in Figures 6-8. Figure 10 plots the normalized, two-sided bandwidth $2B_p$ of the optimum phase-locked loop as a function of σ_a^2/σ_v^2, where $B_p = B_L T$, with B_L denoting the actual loop-noise bandwidth in Hz. From these figures, it is observed that for a fixed σ_a^2, reduction in σ_v^2 results in increased bandwidth, and thus some of the advantage of reduced σ_v^2 is offset by increased B_L as far as the phase error variance is concerned. Thus, whereas in the absence of the process noise ($\sigma_a^2 = 0$) and a fixed loop bandwidth, the phase error variance is inversely related to the input SNR, this is not so for the case of $\sigma_a^2 \neq 0$. As shown in [8] for the case of $\sigma_a^2 \neq 0$, the optimum loop performance may be approximated by

$$P_{F1}(1,1)/\sigma_v^2 T \cong \begin{cases} 1.32(\sigma_a^2/\sigma_v^2)^{.22}, & T = 0.1\,s \\ 1.4(\sigma_a^2/\sigma_v^2)^{.25} & T = 0.01\,s \end{cases}$$

In general, for any value of T, the performance for an appropriate range of (σ_a^2/σ_v^2)

may be approximated by

$$P_{F1}(1,1)/\sigma_v^2 T \cong a(\sigma_a^2/\sigma_v^2)^b$$

for some constants a, b. With p_1, p_2 representing the values of $P_{F1}(1,1)$ for σ_v^2 equal to $\sigma_{v_1}^2$, $\sigma_{v_2}^2$ respectively with σ_a^2 constant, then

$$(\sigma_{v_1}^2/\sigma_{v_2}^2) = (p_1/p_2)^{(\frac{1}{1-b})}$$

or

$$10\ log_{10}(\sigma_{v_1}^2/\sigma_{v_2}^2) = 10\ \log_{10}(p_1/p_2)\ \times (1-b)^{-1}$$

Thus, the improvement in terms of the signal-to-noise ratio is $(1-b)^{-1}$ times the improvement in phase error variance. For b equal to .25, this additional factor is about 1.33. For a constant signal amplitude, $A = 1$, corresponding to the received signal power $P_0 = 1$, $A^2/\sigma_v^2 = 2P_0T/N_0$, and thus the improvement in σ_v^2 is also equal to the improvement in terms of the carrier power to noise power spectral density ratio (CNR).

The curves labeled "precombining" in Figures 9 and 10 depict the performance improvement as defined above for the case of $T = 0.1s, r_1 = r_2 = 1.0$, and for ρ = .995 and .999 respectively. Note that as the system is assumed to be linear, the phase variances can be normalized by the additive noise variances; the performance improvement depends only upon the ratio r_1/r_2, and not on the individual values of r_1, r_2. Figure 11 plots the corresponding result for the case of $T = 0.5s$. As may be inferred from these figures, an improvement of about 1.7 dB in terms of phase error variance σ_ϕ^2 is obtained for the case of $\rho = 0.999$. Similar results are obtained for different sampling rates. Note that this information is adequate for ascertaining

the actual phase error variance for the coupled loops, with the performance for the single loop available in [7,8] and reproduced here for reference. Figure 12 plots the performance improvement as a function of σ_a^2/σ_v^2 for a fixed value of $\rho = -.999$ and $T = 0.5s$. As may be observed from Figure 12, when $\sigma_a^2/\sigma_v^2 = 0.1$, the improvement due to arraying in terms of σ_ϕ^2 is 1.7 dB, while the effective improvement in terms of CNR is 2.1 dB. Performance when $T = 0.1s$ or $.01s$ is not significantly different. All the results presented in this section refer to the "precombining" results in Figures 6-32 and pertain to the proposed scheme 1 (ignoring the effect of a linear signal combiner) in contrast to the "post-combining" results also depicted in these figures. The latter performance curves, which pertain to the proposed scheme 2 (involving an explicit phase alignment) are discussed in a subsequent section.

With the performance improvement (due to arraying) curves in Figures 9-12, along with the actual performance curves for a single receiver presented in Figures 6-8, one may determine the actual phase error variance for the arrayed system. For example, with (σ_a^2/σ_v^2) equal to 1.0 and $T = 0.1s$, the phase error variance is equal to $1.28(N_0/2P_0)$ without arraying, while with a dual receiver it is equal to $.79(N_0/2P_0)$.

5. PERFORMANCE COMPUTATION VIA RECURSIVE SOLUTION

The closed-form solution (16-19) of the algebraic Riccati equation, while of general nature, is cumbersome to compute for higher system dimensions. For a system dimension higher than 4 (matrix H_f dimension greater than 8), it is no longer feasible to come up with simple scalar equations as described in Appendix B for the case of a dual-receiver configuration, and thus one has to compute the eigenvalues and eigenvectors of H_f by some numerical algorithms. As such computations are numerically sensitive, we instead evaluate the performance by a recursive solution approach. In this approach, one simply solves the recursions (11e, f) for $k = 0, 1, 2, \ldots M$ with M selected such that the Euclidean norm $\|\Delta P\|$ of the matrix $P(k+M/k+M-1)-P(k+M-1/k+M-2)$, normalized by the norm of $P(k+M-1/k+M-2)$, is smaller than some specified value ϵ. In these recursions, ϵ is selected equal to 10^{-5}. The initial value $P(0/-1)$ is taken to be a diagonal matrix with its diagonal elements equal to 10^3. The recursions (11e, f) are performed for the first 50 iterations without the test, after which the recursion is terminated subject to the condition $\|\Delta P\|/\|P\| \leq \epsilon$. Figures 13-15 plot the results in terms of performance improvement as a function of σ_a^2/σ_v^2 and for three distinct values of T. Comparison of Figures 12 and 13 shows that both methods yield the same result, thus cross-verifying the computations.

Figures 16-19 plot the performance of a three-receiver configuration for the case of equal CNR for each receiver. Several values of the sampling period and σ_a^2/σ_v^2 have been considered. A few representative cases corresponding to $T = 0.1,\ .5,\ .01$ and (σ_a^2/σ_v^2) equal to .1 and 10 are presented here (these correspond to a loop bandwidth in the range of 0.2 Hz to a few Hz). For all of these cases, the performance improvement

over a single receiver is about 2.6 dB in terms of phase error variance and approximately 3.4 dB in terms of CNR.

It is also of interest to consider the case of unequal CNRs at various receivers. As a representative case, we consider the situation in which some of the receivers have 6 dB lower CNR compared to the others. Such is the case within a good approximation, for example, with the NASA Deep Space Network with 70/70/34 or 70/34/34-meter antenna receiver stations. The performance for this case, with $T = .01\,s$ and $\sigma_a^2/\sigma_v^2 = 1.0$, is presented in Figures 20-24. As is apparent from Figure 20, which depicts the first case, there is an improvement (for $\rho = 0.999$) of about 2.6 dB for receiver 1 in terms of effective CNR. When compared to the improvement obtained by a two-receiver system with equal CNRs, this represents an additional improvement of 0.5 dB attributed to the third, smaller antenna station. We also note here that as for the case of a two-receiver configuration, the performance improvement is not sensitive to σ_a^2/σ_v^2 or T. For comparison, we plot the performance improvement for the above case, but with $\sigma_a^2/\sigma_v^2 = 0.1$ and $T = 0.1$ in Figure 25. Comparisons of the results in Figures 20 and 25 show insignificant differences in the two cases. For the case of unequal CNRs, the parameter σ_a^2/σ_v^2 is measured with reference to the receiver having the highest CNR.

The performance improvement in the receivers with lower CNRs is even more spectacular when compared to the receiver with the highest CNR. As shown in Figure 22, for the above case (70/34/34-meter antenna stations), the improvement for the 34-meter antenna receiver is about 5 dB in terms of effective CNR. For the case of 1:1:4 ratio among noise variances (70/70/34-meter configuration), the performance improvement for the smaller station is 5.8 dB, as shown in Figure 23. Figure 24 presents the result

for the 1:4:16 ratio, in which case the improvement for the smallest station is 7.1 dB. Note that all these improvements are at $\rho = .999$ and may be a little higher or lower depending upon the actual value of ρ.

Figures 26-32 plot the performance for the case of various four-receiver configurations. For the convenience of presentation, we fix the values of parameters T and σ_a^2/σ_v^2 at .01 s and 1.0 respectively. Similar performance curves are obtained for different values of these parameters. As depicted in Figure 26, for the case of equal receiver noise variances for all the receivers, and for $\rho = .999$, one obtains an improvement of about 3.1 dB in terms of phase error variance and 4.1 dB in terms of effective CNR. Figures 27 and 28 plot the performance improvement for receiver 1 for two different cases of unequal CNRs among various receivers. The effective improvement for the case of a 1:1:1:4 ratio among various receiver noise variances is 3.6 dB, while for the case of a 1:1:4:4 ratio, the improvement is about 2.9 dB. As is also true for the case of a three-receiver configuration, the CNR improvement is spectacular for smaller antenna receivers. As is apparent from Figure 29, in a 1:1:4:4 ratio situation, the receiver with the smaller antenna achieves an improvement of about 6.1 dB. The corresponding improvement for the case of a 1:4:4:4 configuration is about 5.4 dB. Figures 31 and 32 plot the results on the performance improvements for the receiver with the smallest CNR for two more configurations with 1:1:1:4 and 1:4:4:16 ratios respectively. These improvements are about 6.5 dB and 7.5 dB respectively.

It may be noted that while for the case when the same information (data) is carried by all of the links, the performance of only the largest antenna receiver (or actually the aggregate performance of all the receivers) would be of importance, there

are other interesting situations where the performance of all individual receivers is significant. This is the case, for example, with the frequency reuse (and/or polarization reuse) telecommunication satellites with spot beams, wherein different information is transmitted to different receivers but over the same carrier frequency. In this case, a smaller earth terminal can dramatically improve its performance (in terms of carrier recovery) by proper coordination with a larger terminal. The coordination can be done via inexpensive, low-capacity, terrestrial links. These links need to carry only very low rate information representing the loop correction signals.

6. A NOVEL SIGNAL-COMBINING CONFIGURATION FOR COUPLED RECEIVERS

For the case of most interest in this publication, wherein the carrier signals received at various receivers are data modulated by the same information, the system performance can be further improved by post-loop combining of the signals. For the case of a data-modulated signal, a decision-directed approach is used and the data detector becomes an integral part of the loop. Figure 33 depicts the schematic of such a loop for the case of a single receiver for reference. Note that the superscripts on various signals have been removed in that figure, and the phase detector outputs (baseband) are given by

$$\begin{aligned} \eta(k) &= A\ \mathrm{Sin}(\tilde{\theta}(k) + \pi\ D(k)) + \frac{1}{\sqrt{2}}\ \overline{v}_i(k) \\ \xi(k) &= A\ \mathrm{Cos}(\tilde{\theta}(k) + \pi\ D(k)) + \frac{1}{\sqrt{2}}\ \overline{v}_q(k) \end{aligned} \tag{21}$$

where $\tilde{\theta} = \theta(k) - \hat{\theta}(k)$ represents the phase estimation error and $\{D(k)\}$ represents the sampled version of the data signal, i.e.,

$$D(k) = b_j \ ; \quad (j-1)M \leq k \leq jM - 1 \tag{22}$$

In equation (22), b_j represents the jth data bit and M is the number of samples within one data-bit period. For the purposes of carrier phase estimation, the data detection could be based upon a differential approach, even for the case of coherent modulation. This approach has the advantage of better acquisition and tracking than is feasible with coherent detection. This is in view of the fact that if there is a considerable frequency drift in the loop (as in acquisition mode), then the coherent detector in the loop will provide a very high probability of error. Due to this fact, the loop may not

lock. However, the differential approach would provide estimates of data transitions with a low probability of error, provided that the phase drift (resulting due to a nonzero differential frequency component in the loop error) is smaller compared to the minimum phase separation among various symbols. For the case of BPSK modulation, the signals corresponding to "1" and "0" differ in their phase by π rad. For a more detailed and elaborate implementation of this concept, one may refer to [11], where the acquisition and tracking of a very high dynamic signal are considered.

For the case of binary modulation, one may apply the following decision rule for the data transition detection: With

$$\eta_a(j) = \frac{1}{M} \sum_{k=(j-1)M}^{jM-1} \eta(k) \;\; ; \quad \xi_a(k) = \frac{1}{M} \sum_{k=(j-1)M}^{jM-1} \xi(k)$$
$$s(j) = \left\{ (\eta_a(j) - \eta_a(j-1))^2 + (\xi_a(j) - \xi_a(j-1))^2 \right\}^{\frac{1}{2}} \tag{23}$$

the decision rule is

$$\hat{b}_j = \hat{b}_{j-1} \qquad \text{if } s(j) < V_T$$
$$\tag{24}$$
$$\neq \hat{b}_{j-1} \qquad \text{if } s(j) > V_T$$

In (24), V_T represents some appropriate threshold. Note that in the absence of noise, $s(j) = 0$ or $2A$ depending upon whether b_j is equal to b_{j-1} or not, irrespective of phase error $\tilde{\theta}$, such that the average phase error in the two consecutive bit periods is equal. Thus, V_T may be set to A in the presence of noise. Alternatively, one could compare $|\xi_a(j) - \xi_a(j-1)|$ against some threshold to detect a transition.

Note that if the data are coherently modulated, then a separate post-loop detection may be applied to obtain $\hat{b}_j$ coherently as shown in Figure 33. The output of this

detector would be meaningful only if the loop has acquired and the phase error $\tilde{\theta}$ is small.

It is clear that in the above detection scheme, there would be some signal loss due to nonzero $\tilde{\theta}(k)$. In a multiple-receiver configuration, such a possible loss can be minimized by averaging the phase errors before a decision is made. As the phase errors $\tilde{\theta}^i(k)$ in various receivers corresponding to $i = 1, 2, \ldots, N$ are only partially correlated, the average error would have a smaller variance than the individual errors $\tilde{\theta}^i(k)$. Figure 34 shows a detailed schematic diagram for the scheme that achieves the desired objective for the case of two receivers. This has been referred to earlier as scheme 2 (Figure 1b). In the first instance, we assume that the two receivers have equal CNR. Figure 34 depicts the schematic diagram of an implementation that effectively averages out the phase estimation error $\tilde{\theta}(k)$ and the noise associated with the two receivers for the purpose of optimal estimation. In the figure, ω_d represents some appropriate frequency introduced for implementing the frequency (and phase) division. Representing the receiver input noise $\overline{v}^i(k)$ (after being averaged over one symbol period) in terms of its baseband components $\tilde{v}_i^i(k)$ and $\tilde{v}_q^i(k)$ as

$$\begin{aligned} \overline{v}^i = \tilde{v}_i^i(k)\ \mathrm{Sin}\ [\omega_c t_k + \tilde{\theta}^1(k) + \pi\ D(k)] \\ + \tilde{v}_q^i(k)\ \mathrm{Cos}\ [\omega_c t_k + \tilde{\theta}^2(k) + \pi\ D(k)] \end{aligned} \tag{25}$$

then the output of the rf mixer 1 in Figure 34 is given by

$$\begin{aligned} \eta_B^1(k) = \left[A + \frac{1}{\sqrt{2}}\ \tilde{v}_i^1(k)\right]\ \mathrm{Sin}\ [\omega_d t_k + \tilde{\theta}^1(k) + \pi\ D(k)] \\ + \frac{1}{\sqrt{2}}\ \tilde{v}_q^1(k)\ \mathrm{Cos}\ [\omega_d t_k + \tilde{\theta}^1(k) + \pi\ D(k)] \end{aligned} \tag{26}$$

For the case of medium-to-high E_s/N_0 ratio, the output of the limiter/frequency divider

1 denoted $\eta_D(k)$ is approximated as

$$\eta_D^1(k) \cong A \text{ Sin } \left\{ \frac{1}{2}(\omega_d t_k + \tilde{\theta}^1(k) + \pi\ D(k) + \tilde{\theta}_n^1(k)) \right\}$$
$$\tilde{\theta}_n^1(k) = \tan^{-1} \left\{ \frac{\tilde{v}_q^1(k)/\sqrt{2}}{A + \tilde{v}_i^1(k)/\sqrt{2}} \right\} \tag{27}$$

Similarly, the output of the lower frequency divider in Figure 34 is given by

$$\xi_D^1(k) \cong A\text{Cos}\{\frac{1}{2}(\omega_d t_k + \tilde{\theta}(k) + \pi\ D(k) + \tilde{\theta}_n^1(k)\} \tag{28}$$

For the approximation (27) to be valid, the signal-to-noise ratio $2A^2/E[\tilde{v}_i^1]^2 = 2E_S/N_0$ (E_S denotes data-symbol energy) must be much higher compared to 1. In general, for the case of MPSK signaling with M distinct phases, this ratio is given by $(2E_b/N_0)\log_2 M$. Thus, for $M = 4$ (corresponding to QPSK signal) and $E_b/N_0 = 0$ dB, the signal-to-noise ratio $2A^2/E[\tilde{v}_i^1]^2$ is equal to 6 dB and may be adequate. Higher values of M, of course, lead to even higher SNR. For those cases where $2E_S/N_0$ is not sufficient, the scheme may be suitably modified by extending the observation period to more than one symbol. The signal combiner combines the $\{\eta_D,\ \xi_D\}$ signals from the two receivers according to the following trigonometric identities:

$$\eta_I(k) = \eta_D^1(k)\xi_D^2(k) + \eta_D^2(k)\xi_D^1(k)$$

$$= A\text{Sin}\{\omega_d t_k + \tilde{\theta}(k) + \pi\ D(k) + \tilde{\theta}_n(k)\} \tag{29}$$

$$\xi_I(k) = \xi_D^1(k)\xi_D^2 - \eta_D^1(k)\eta_D^2(k)$$

$$= A\text{Cos}\{\omega_d t_k + \tilde{\theta}(k) + \pi\ D(k) + \tilde{\theta}_n(k)\}$$

with

$$\tilde{\theta}(k) = \frac{1}{2}\big(\tilde{\theta}^1(k) + \tilde{\theta}^2(k)\big) \quad ; \qquad \tilde{\theta}_n(k) = \frac{1}{2}\big(\tilde{\theta}_n^1(k) + \tilde{\theta}_n^2(k)\big)$$

When ω_d is an IF frequency, one may equivalently generate $\eta_I(k)$ and $\xi_I(k)$ by mixers and bandpass filters. Finally, the complex-mixer in Figure 34 down-converts the signals η_I, ξ_I to baseband, resulting in its outputs given by

$$\eta(k) = A\mathrm{Sin}\{\tilde{\theta}(k) + \pi\ D(k) + \tilde{\theta}_n(k)\}$$

$$\xi(k) = A\mathrm{Cos}\{\tilde{\theta}(k) + \pi\ D(k) + \tilde{\theta}_n(k)\} \tag{30}$$

For a high CNR case, $\tilde{\theta}_n(k)$ may be approximated by

$$\tilde{\theta}_n(k) = \tan^{-1}(\tilde{v}_q(k)/\sqrt{2}A) \quad ; \qquad \tilde{v}_q(k) = \frac{1}{2}\big(\tilde{v}_q^1(k) + \tilde{v}_q^2(k)\big)$$

Since $\{\tilde{v}_q^1(k)\}$ and $\{\tilde{v}_q^2(k)\}$ are independent noise sequences, the variance of $\tilde{v}_q(k)$ is only one-half of the variance of either of these noise components. Thus, in addition to averaging out the phase errors $\tilde{\theta}^1(k)$, $\tilde{\theta}^2(k)$, the scheme also effectively averages out the measurement noise (as an optimal detector should). Data transitions are then detected by substituting $\eta(k)$, $\xi(k)$ of (30) into equations (23, 24).

The above scheme can be generalized to the case when the two receivers have unequal CNRs at their inputs. As shown in the following, the optimum weighting of the two phase error terms $\tilde{\theta}^1(k)$ and $\tilde{\theta}^2(k)$ would be α and $(1-\alpha)$ respectively for some $0 < \alpha < 1$, where in general α would be different than 0.5. This is achieved by using the frequency division by α^{-1} and $(1-\alpha)^{-1}$ in the upper and lower limiter/frequency divider respectively. If necessary, α may be approximated by a rational number for the purpose of implementation. Note that this scheme affords the same weighting to the

measurement noise v_i^1 and v_i^2. If α is close to $r_2/(r_1+r_2)$, then this is also optimum from the viewpoint of minimizing the noise. In a more general case, the optimal weighting may be derived so as to minimize the probability of error, or equivalently, the ratio $E[\mathrm{Cos}^2\tilde{\theta}(k)]/E[\tilde{v}_q^2]$. For the case of equal CNRs, the optimum solution is $\alpha = 0.5$. This "post-loop" combining can be generalized to a multiple-receiver configuration in a straightforward manner.

With the phase errors $\tilde{\theta}_1$ and $\tilde{\theta}_2$ having zero means and covariance matrix P, the weighted average phase error $\tilde{\theta} = \alpha\tilde{\theta}_1 + (1-\alpha)\tilde{\theta}_2$ has the following variance:

$$E[\tilde{\theta}]^2 = \alpha^2 P_{11} + (1-\alpha)^2 P_{22} + 2\alpha(1-\alpha)P_{12} \tag{31}$$

In (31), P_{11}, etc., denote the elements of the matrix, P. Setting the derivative of $E[\tilde{\theta}^2]$ with respect to α equal to zero, the optimum weight α is given by

$$\alpha = \left(\frac{P_{22} - P_{12}}{P_{11} + P_{22} - 2P_{12}}\right)$$

For the more general case of N receivers, let

$$\tilde{\theta} = \alpha_1\tilde{\theta}^1 + \cdots + \alpha_N\tilde{\theta}^N \tag{32}$$

Then, the minimization problem consists of minimization of

$$E[\tilde{\theta}]^2 = \alpha_v^T P\ \alpha_v \ ; \quad \alpha_v \stackrel{\Delta}{=} [\alpha_1\ \ \alpha_2 \ldots \alpha_N]^T \tag{33}$$

subject to the constraint

$$\alpha_v^T u = 1 \ ; \ \ u \stackrel{\Delta}{=} [1\ 1 \ldots 1]^T \tag{34}$$

Using the Lagrangian method of minimization, we obtain the following optimum solution for α_v:

$$\alpha_v = (u^T P^{-1} u)^{-1} P^{-1} u \tag{35}$$

Recall that the constraint (33) is necessary so as to ensure that the data-phase modulation in the combined signal remains equal to $\pi D(k)$.

In the more general case, where it is required to maximize the signal-to-noise ratio $E[\mathrm{Cos}\tilde{\theta}]^2/E[\tilde{v}_q^2]$, the optimization problem is more complex. However, the following approximate procedure is proposed for the solution. We first minimize the weighted sum $E[\tilde{\theta}]^2 + \gamma E[\tilde{v}_q^2]$ with respect to α_v for any specified γ: i.e., minimize

$$\alpha_v^T P\, \alpha_v + \gamma\, \alpha_v^T\, R\, \alpha_v \tag{36}$$

subject to the constraint (33). The solution as a function of γ is then given by

$$\alpha_v = \left\{u^T (P + \gamma\, R)^{-1} u\right\}^{-1} (P + \gamma\, R)^{-1} \tag{37}$$

With the expansion of $\mathrm{Cos}\tilde{\theta}$ in terms of its Taylor series,

$$E[\mathrm{Cos}^2\tilde{\theta}] = 1 - m_2 + \frac{1}{3} m_4 - + \cdots$$

where m_j denotes the jth moment of $\tilde{\theta}$, $E[\tilde{\theta}]^j$ for $j = 1, 2, \ldots$. In the general case, it is difficult to evaluate these moments precisely. For the purposes of this approximation, we may assume $\tilde{\theta}$ to be Gaussian (following from a linearized approximation of the phase detector), and thus the optimization index may be approximated by (retaining only the first three terms)

$$\left\{1 - \alpha_v^T P\, \alpha_v + (\alpha_v^T P\, \alpha_v)^2\right\} / (\alpha_v^T R\, \alpha_v) \tag{38}$$

and can be minimized with respect to γ by an appropriate numerical technique.

Figures 6-32 also plot the "post-combining" improvement in the phase error variance at the input to the coherent detector (see Figure 34). This is defined as

$10\log_{10}\{\overline{P}_{Fk}(1,1)/E[\tilde{\theta}]^2\}$, where $\overline{P}_{Fk}$ is the phase error variance for the kth receiver operating by itself, and $\tilde{\theta}$ is the averaged phase error given by (32). This represents the overall improvement in the phase error variance for the proposed decision-directed multireceiver configuration 2, and for brevity is termed the "post-combining" improvement (in Figures 6-32). In these figures, we also plot the "post-combining" CNR improvement, defined as the required increase in the CNR for the single receiver, so as to reduce its phase error variance by the improvement factor $\{\overline{P}_{Fk}(1,1)/E[\tilde{\theta}]^2\}$ defined above. For the case of equal CNRs, the effective noise variance at the input to the coherent detector is 1/N times the noise variance for the case of a single receiver. Based on this information, for a given CNR, the total improvement in the (E_b/N_0) ratio is given by

$$(E_b/N_0)_I = 10\log_{10} N + 10\log_{10}\{E[\mathrm{Cos}\tilde{\theta}^k]^2/E[\mathrm{Cos}\tilde{\theta}]^2\} \tag{39}$$

For illustration, with $E[\tilde{\theta}^k]^2 = .5(\mathrm{rad})^2$, $T = .01s$, $\sigma_a^2/\sigma_v^2 = 1.0$, and a four-receiver configuration, Figure 26 shows an improvement in the phase error variance of 4.5-5.7 dB, depending upon ρ (corresponding to an effective CNR improvement of 6-7 dB). With the approximation (based on Gaussian assumption on $\tilde{\theta}$) that

$$\begin{aligned} E[\mathrm{Cos}\tilde{\theta}]^2 &\cong 1-\sigma^2+\sigma^4 \;\; ; \quad \sigma^2 = E[\tilde{\theta}^2] \\ E[\mathrm{Cos}\tilde{\theta}] &\cong 1-\frac{\sigma^2}{2}+\frac{\sigma^4}{8} \end{aligned} \tag{40}$$

we have

$$E[\tilde{\theta}^2] = .13 \; ; \; E[\mathrm{Cos}\tilde{\theta}^k]^2 = .75 \; ; \quad E[\mathrm{Cos}\tilde{\theta}]^2 \cong .883$$

$$(E_b/N_0)_I \cong 6.8\mathrm{dB} \quad \text{for} \quad \rho \quad \text{small},$$

and

$$E[\tilde{\theta}^2] = .177 \; ; \quad E[\mathrm{Cos}\tilde{\theta}]^2 \cong .854 \; ; \quad (E_b/N_0)_I \cong 6.6\mathrm{dB} \quad \text{for} \;\; \rho \;\; \text{large}.$$

We note that an alternative simpler scheme 1, with the signals $\xi(k)$ (see Figures 33 and 34) simply averaged out, may result in a considerable signal loss compared to the proposed post-loop combining method of this publication. To illustrate the point, let us consider the case when ρ is relatively small, say 0.5, so that $\tilde{\theta}^k$ from various receivers (even under coupled mode) are nearly uncorrelated. For example, with $T = .01$s, $\sigma_a^2/\sigma_v^2 = 1.0$, and with a received signal-to-noise ratio yielding the phase error variance of 0.5 $(\text{rad})^2$, without coupling in a four-receiver configuration, there is an improvement of only 0.24 dB (see Figure 26) and the individual receiver phase error variance (under coupled mode) is thus $E[\tilde{\theta}^k]^2 = .466$ $(\text{rad})^2$. The correlation coefficient between various phase errors $\tilde{\theta}^k$ is computed to be only .11, and thus even after "precombining," various $\tilde{\theta}^k$ are almost independent. For simplicity, we assume that $\tilde{\theta}^k$ and hence $\text{Cos}\tilde{\theta}^k$ for $k = 1, \ldots 4$ are in fact independent random variables. With the approximation (40), we have

$$E[\text{Cos}\tilde{\theta}^k]^2 \cong .751$$

$$E\Big[\frac{1}{4}\sum_{k=1}^{4}\text{Cos}\tilde{\theta}^k\Big]^2 \cong .66$$

Thus, there is a loss of $10\log_{10}.19 = -1.8$ dB relative to the ideal case. Essentially, the spread on phase error variance partly offsets the improvement due to noise reduction. Ignoring the nonlinearities in the phase-locked loops, the improvement in terms of (E_b/N_0) compared to one receiver system is given by

$$(E_b/N_0)_I \cong 6 + 10\log_{10}(.66/.751) = 5.4 \text{ dB}$$

By the proposed method of post-dectection combining, however, $E[\tilde{\theta}^2] \cong .1165$ $(\text{rad})^2$ with $E[\text{Cos}\tilde{\theta}]^2 \cong .897$, thus resulting in an (E_b/N_0) improvement of 6.8 dB. Thus,

in this case, the additional gain resulting from the proposed post-detection nonlinear combining is 1.4 dB over the simpler linear combining method 1. As in arriving at this simple result, we have ignored nonlinearities (worse at higher variances) and made a Gaussian assumption on $\tilde{\theta}$ in arriving at (40), the actual difference may be even higher than 1.4 dB. For higher values of ρ , the improvement in the phase error variance is attributed to both the "precombining" and "post-combining" processes, as is apparent from Figures 6-32. Taking into account the phase detector nonlinearities under relatively low SNR conditions, it is clear that the combined gain due to both predetection and post-detection would be actually much higher than 6.8 dB, especially at high values of ρ. This is so because the loop operating with $E[\tilde{\theta}^2] = 0.5$ (rad)^2 (predicted on the basis of linear theory and without arraying) is expected to involve much higher degradation due to nonlinearities compared to a loop with $E[\tilde{\theta}^2] = .177$ (rad)^2 (obtained with arraying), in view of the simulation results of [7,8] for the case of a single loop with phase detector nonlinearity. In fact, when the problems of cycle slipping associated with nonlinear behavior are also considered, it may not even be feasible to operate the loop at such high values of $E[\tilde{\theta}^2]$. Thus, an additional gain of 1.5-3 dB is expected over systems which involve only baseband signal combining (no carrier arraying) for a four-receiver configuration with a net gain in terms of (E_b/N_0) in the range of 3-4 dB. Similar results would hold for other receiver configurations.

7. CONCLUSIONS

We have presented two novel estimation/detection schemes for multireceiver communication systems for the coordinated estimation of the phase and frequency of data-modulated carrier signals. These should reduce the radio loss to a negligible value and thus effectively minimize the probability of data detection.

Considering first the case of no data modulation (residual carrier) and formulating the problem in a state-space description, we have derived an estimator structure on the basis of optimal estimation theory. This configuration consists of coupled phase-locked loops with individual PLLs tracking the carrier signals associated with various receivers and aided by other loops on a mutual basis. Detailed results of analysis and computation have been presented to illustrate the improvement obtained due to such a coupling over that achieved for the case of independently operating PLLs.

Various receiver configurations, including 2-4 receivers, have been considered for the cases of both equal and unequal CNRs at the receivers. We have considered a wide range of values for the ratio of process noise to additive noise variance (a dominant parameter in controlling the loop bandwidth) and a wide range of correlation coefficient ρ among the phase processes at the input to various receivers. The improvement has been measured both in terms of the reduction in the phase error variance (phase jitter) and also in terms of the extension of the CNR margin (reduction in the required CNR).

It is apparent from the results presented in this publication, that for a relatively high value of ρ, loop arraying provides an effective CNR improvement of about 2-4.5 dB, depending upon the number of receivers in the configuration, for the receiver with the highest CNR at its input. This improvement is applicable over a very wide

range of loop noise bandwidths (process noise variances). For receivers with smaller input CNR (smaller antenna aperture), the improvement is more dramatic. For the case considered in this publication, wherein each receiver can have one of two possible CNRs (corresponding, for instance, to either a 34-meter or a 70-meter antenna), the maximum CNR improvement can be as high as 7 dB.

For the case of relatively high ρ, the above scheme can be extended to the data-modulated case (suppressed carrier or data-aided residual carrier loop), by replacing the individual PLL by a decision-directed version. The data detection is achieved on the basis of a signal obtained by combining the appropriate baseband signals (quadrature components of the mixer) from all the loops. For relatively high values of ρ, it turns out from the analysis (as is also intuitively expected) that the residual phase errors from various loops are also highly correlated and thus simple combining of the baseband signals does not result in a significant loss of optimality. In the decision-directed version of the loop, we have removed the data modulation within the loop on the basis of differential detection or transition detection [9], as this provides a better acquisition performance than the usual matched filter detection.

Apart from being an optimum configuration, a major advantage of the proposed scheme with respect to an earlier scheme in the literature is that here the coupling among loops is only via low frequency baseband signals (loop error signals) as against coupling at the IF and RF levels required in the previous scheme. This feature is especially attractive when the various receivers are geographically separated by large distances as in the case with the Deep Space Network. However, it may be emphasized that the scheme is of a general nature and also has various other applications as well.

For example, in the case of frequency or polarization-reuse satellite configurations, the scheme can be applied for coordinated and thus improved phase estimation even though different carriers (channels) carry different data.

For the case of relatively low values of ρ, both the above scheme and the scheme of [1-3] are of little use. As seen from the results presented in this publication, loop coupling by itself, in this case, provides very small improvement even though the estimation configuration is optimum. Thus, for $\rho = 0.5$ and a four-receiver configuration, one obtains less than a 1-dB improvement through coupling. In this case, it is essential to recognize at the outset that the overall objective is to minimize the probability of error or minimize the phase jitter in the combined baseband signal. An equivalent way to achieve this is to estimate individual phases with errors $\tilde{\theta}_k$ as before to obtain the baseband signals $D\text{Cos}\tilde{\theta}_k$ (D denotes data) and from these signals obtain a composite signal $D\text{Cos}\tilde{\theta}$ where $\tilde{\theta}$ is an optimal average of various error signals $\tilde{\theta}_k$. The second scheme in this publication does indeed achieve such combining. From the analysis, it turns out that for low values of ρ, $\tilde{\theta}_k$s are essentially uncorrelated and it is essential to average out $\tilde{\theta}_k$ in this manner. For the purposes of data detection, the proposed scheme also automatically averages out the additive noise.

The proposed configuration II requires inputting the data signal at an intermediate frequency to a selected master receiver from all the remaining receivers. The mutual (two-way) coupling is the same as for configuration I, i.e., it involves only low frequency loop error signals. The performance of the proposed configuration II has also been evaluated under appropriate simplifying assumptions and has been presented in this publication. From these results, it is apparent that this scheme can provide a CNR

improvement of about 8 dB for a four-receiver, equal CNR configuration over the complete range of ρ. An interesting observation is that for the second scheme, the performance is better for lower values of ρ than for the higher range of ρ. This is directly opposite to the result for configuration I and may at first sight seem to be counter-intuitive. However, the result is easily explained on the basis of a fundamental averaging principle.

Thus, the variance of the average of N random variables χ_k, $k = 1, \ldots, N$ (assumed to be identically distributed for simplicity) depends directly on the correlation coefficients among the variables χ_k and achieves a minimum for zero cross-correlations. Replacing χ_k by θ_k then justifies the results presented in this publication on an intuitive basis also. It should further be noted that there is no known scheme for this case of low ρ in the published literature.

One could, of course, use the more sophisticated configuration II even for relatively high values of ρ. At the cost of some complexity, this results in marginal improvement over the first, simpler scheme.

8. SUGGESTIONS FOR FUTURE RESEARCH

As is generally the case with such estimators, the parameters of the proposed optimal estimators, e.g., noise bandwidths of various PLLs, are based on the knowledge of certain statistics of the received signal model as the ratio σ_a^2/σ_v^2 and the correlation coefficient ρ. In practice, the unknown statistical parameters may be replaced by some appropriate bounds or estimates of these. This may result in some possible loss of optimality, which is dependent on the accuracy of these estimates. The estimates of σ_a^2, σ_v^2 and ρ may be obtained either on an offline or on a real-time basis, the latter procedure resulting in an adaptive optimal system. Development of such adaptive procedures is an important part of the suggested future research in this area.

The performance results presented in this publication were derived on the basis of linear estimating theory and are applicable for a relatively high CNR case. Under relatively high CNR and tracking mode, the phase estimation errors are relatively small and the phase detectors in various PLLs may be approximated by linear characteristics, resulting in a linear model for the complete coupled system. However, for relatively low CNRs, a linear approximation may not be valid and the results presented here may represent only an approximation of the actual performance. For relatively low CNR, and/or in the acquisition mode, it is necessary to obtain results on the basis of nonlinear theory or by computer simulations. This forms another part of the proposed future research. Also, as indicated in Section 6, the proposed nonlinear phase alignment and combining technique is applicable when $2E_s/N_0$ is much higher compared to 1. Investigation of a scheme that overcomes this limitation by extending the combination to a multisymbol period is also part of such a proposal.

REFERENCES

[1] Divsalar, D. and Yuen, J.H., "Improved Carrier Tracking Performance with Coupled Phase-locked Loops," TDA Progress Report 42-66, pp. 148-171, Jet Propulsion Laboratory, California Institute of Technology, Pasadena, CA, September 1981.

[2] Brockman, M.H., "Enhanced Radio Frequency Carrier Margin Improvement for an Array of Receiving Systems with Unequal Predetection Signal-to-Noise Ratios," TDA Progress Report 42-76, pp. 170-188, Jet Propulsion Laboratory, California Institute of Technology, Pasadena, CA, October 1983.

[3] Brockman, M.H., "Performance Characteristics for an Array of Two Receiving Systems with Unequal Predetection Signal-to-Noise Ratios and Enhanced Radio Frequency Carrier Margin Improvement," TDA Progress Report 42-84, pp, 101-111, Jet Propulsion Laboratory, California Institute of Technolgy, Pasadena, CA, October 1985.

[4] Divsalar, D., "Symbol Stream Combining Versus Baseband Combining for Telemetery Arraying," TDA Progress Report 42-74, pp. 13-28, Jet Propulsion Laboratory, California Institute of Technology, Pasadena, CA, August 1983.

[5] Kumar, R. and Hurd, W. J., "A Class of Optimum Digital Phase-locked Loops," Proceedings of the 25th IEEE Conference on Decision and Control, Athens, Greece, December 1986.

[6] Polak, D.R. and Gupta, S.C., "Quasi Optimum Digital Phase-locked Loops,"IEEE Transactions on Communications, Vol. 21, pp. 75-82, January 1973.

[7] Kumar, R. and Hurd, W.J., "Fixed Lag Smoothers for Carrier Phase and Frequency Tracking," Proceedings of the IASTED International Symposium on Applied Control and Identification, pp. 160-166, December 1986.

[8] Kumar, R., "Optimum Filters and Smoothers Design for Carrier Phase and Frequency Tracking," JPL Publication 87-10, Jet Propulsion Laboratory, CA, May 1, 1987.

[9] Aguire, S., Hurd W.J., Kumar, R. and Statman, J., "A Comparison of Methods for DPLL Loop Filter Design," TDA Progress Report 42-87, pp. 114-124, Jet Propulsion Laboratory, California Institute of Technology, Pasadena, CA, November 1986.

[10] Vaughan, D.R., "A Nonrecursive Algebraic Solution for the Discrete Riccati Equation," IEEE Transactions on Automatic Control, pp. 597-598, October 1970.

[11] Kumar, R., "Efficient Detection and Signal Parameter Estimation with Applications to High Dynamic GPS Receivers," JPL Publication 88-42, Jet Propulsion Laboratory, California Institute of Technology, Pasadena, CA, December 15, 1988. (See also, Proceedings of SuperComm/International Communications Conference '90, April 1990.)

[12] Kelly, C.N. and Gupta, S.C., "Discrete-Time Demodulation of Continuous-Time Signals," IEEE Transactions on Information Theory, Vol. IT-18, pp. 488-493, July 1972.

[13] Fortmann, T.E., "A Matrix Inversion Identity," IEEE Transactions on Automatic Control, p. 599, October 1970.

[14] Kumar, R., "A Fast Algorithm for Solving a Teoplitz System of Equations," IEEE Transactions on Acoustics, Speech and Signal Processing, Vol. ASSP-33, No. 1, pp. 254-267, February 1985.

APPENDIX A: Extended Kalman Filter Equations for the Signal Model (5-8)

In the following, the extended Kalman filter equations are obtained by expanding the nonlinear vector measurement function $h(x,k)$ into a Taylor series around the predicted estimate of $x(k)$ and retaining only the linear and quadratic terms. These equations are then simplified by ignoring $2\omega_c t$ and the higher harmonic terms present in the recursions as in [8, 12]. In fact, the development here is not much different than in [8]. With $\hat{x}(k+1/k)$ denoting the one-step ahead prediction of $x(k+1)$, then the extended Kalman filter equations for the model (5-8) are given by the following filter state equations:

$$\hat{x}(k+1/k+1) = \Phi\hat{x}(k/k) + M(k+1)\nu(k+1) \tag{A1}$$

$$\nu(k+1) = y(k+1) - h(\hat{x}(k+1/k), k+1) \tag{A2}$$

and filter gain:

$$M(k+1) = P(k+1/k)h_x^T\sigma^{-1}(k+1) \tag{A3}$$

In (A3), $P(k+1/)$ denotes $E\big[\{x(k+1) - \hat{x}(k+1/k)\}\{x(k+1) - \hat{x}(k+1/k)\}^T\big]$ and has the following recursion:

$$P(k+1/k) = P(k+1/k) - P(k+1/k)h_x^T\sigma^{-1}(k+1)h_x\,P(k+1/k) \tag{A4}$$

$$P(k+1/k) = \Phi\,P(k/k)\Phi^T + Q \tag{A5}$$

$$\sigma(k) = h_x\,P(k/k-1)h_x^T + \overline{R}(k) + \frac{1}{2}\frac{\partial^2 h}{\partial x^2} :\ P(k/k-1).\ \Big[\frac{\partial^2 h}{\partial x^2} :\ P(k/k-1)\Big]^T \tag{A6}$$

where h_x denotes the $(N \times n)$ gradient matrix and

$$\frac{\partial^2 h}{\partial x^2} : P(k/k-1) = \sum_{i,j=1}^{n} \frac{\partial^2 h}{\partial x_i \partial x_j} \left(P(k/k-1)\right)_{ij} \qquad (A7)$$

is an N vector.

To simplify the recursions (A1)-(A7), the gradients h_x and h^i_{xx} are evaluated as follows: The $N \times n$ gradient matrix h_x is given by

$$h_x = A\sqrt{2} \begin{bmatrix} \mathrm{Cos}\hat{\Theta}^1(k) & 0 & \cdots & 0 \\ 0 & \mathrm{Cos}\hat{\Theta}^2(k) & \cdots & 0 \\ \cdots & \cdots & \cdots & \cdots \\ 0 & 0 & 0 & \mathrm{Cos}\hat{\Theta}^N(k) \end{bmatrix} \otimes \ell^T \qquad (A8)$$

where $\otimes$ denotes the Kronecker matrix product and $\ell^T = [1\ 0 \ldots 0]$ is a row vector of dimension n_s. Similarly $\frac{\partial^2 h}{\partial x^2} : P(k/k-1)$ is the following diagonal matrix:

$$\frac{\partial^2 h}{\partial x^2} : P(k/k-1) =$$

$$-A\sqrt{2} \begin{bmatrix} \{\mathrm{Sin}\hat{\Theta}^1(k) P^{11}_{\phi}\} & 0 & \cdots & 0 & 0 \\ 0 & \{\mathrm{Sin}\hat{\Theta}^2(k) P^{22}_{\phi}\} & 0 & \cdots & 0 \\ \cdots & \cdots & \cdots & \cdots & \cdots \\ 0 & 0 & 0 & \cdots & \{\mathrm{Sin}\hat{\Theta}^N(k) P^{NN}_{\phi}\} \end{bmatrix} \qquad (A9)$$

where P^{ii}_{ϕ} denotes the ith diagonal term of the matrix P_{ϕ}, and P_{ϕ} is the diagonal version of the phase error covariance matrix, i.e., it is a submatrix of $P(k/k-1)$, consisting of elements with 1, (n_s+1), $(2n_s+1), \ldots ((N-1)n_s+1)$ as their row and column indices. Substitution of (A8) and (A9) in (A6) shows that

$$\sigma(k) = B(k) + \overline{R}(k) \qquad (A10)$$

where $B(k)$ is a diagonal matrix with its ith diagonal element given by

$$B^{ii}(k) = 2P^{ii}_{\phi} A^2 \mathrm{Cos}^2\hat{\Theta}^i(k) + (P^{ii}_{\phi})^2 A^2 \mathrm{Sin}^2\hat{\Theta}^i(k)$$

Denoting by $P_{\phi S}$ the diagonal matrix with its ith diagonal element equal to $(P_\phi^{ii})^2$

$$\sigma(k) = A^2\left[P_\phi + \frac{1}{2}P_{\phi S} + \tilde{R}(k)\right] + A^2\left[P_\phi - \frac{1}{2}P_{\phi S}\right]C_M$$

where C_M is a diagonal matrix with ith element equal to $\mathrm{Cos}2\hat{\Theta}^i(k)$.

Thus

$$\sigma^{-1}(k) = A^{-2}\left[I + D(k)C_M\right]^{-1}\left[P_\phi + \frac{1}{2}P_{\phi S} + \tilde{R}(k)\right]^{-1} \qquad (A11)$$

$$D(k) = \left[P_\phi + \frac{1}{2}P_{\phi S} + \tilde{R}(k)\right]^{-1}\left[P_\phi - \frac{1}{2}P_{\phi S}\right]; \quad \tilde{R}(k) = \overline{R}(k)/A^2 \qquad (A12)$$

Assuming $\tilde{R}(k)$ to be a diagonal matrix, then all the matrices above are diagonal and each of the diagonal terms of the matrix $\left[I+D(k)C_M\right]^{-1}$ may be individually expanded into a Fourier series. Thus

$$\sigma^{-1}(k) = A^{-2}\left[P_\phi + \frac{1}{2}P_{\phi S} + \tilde{R}(k)\right]^{-1}\{\mathcal{A}_0 + \mathcal{A}_1 C_M + \cdots\} \qquad (A13)$$

The ith elements of the diagonal matrices $\mathcal{A}_0$ and $\mathcal{A}_1$ are given by

$$\mathcal{A}_0^{ii} = \frac{1}{\sqrt{1-[D^{ii}(k)]^2}}$$

$$\mathcal{A}_{11}^{ii} = \frac{2}{D^{ii}(k)}\left\{1 = \frac{1}{\sqrt{1-[D^{ii}(k)]^2}}\right\}$$

with C_1 a diagonal matrix and its ith diagonal element given by

$$C^{ii} = \frac{1}{D^{ii}(k)}\left\{1 - \left[\frac{1-D^{ii}(k)}{1+D^{ii}(k)}\right]^{\frac{1}{2}}\right\}$$

then as in [6, 10], ignoring the high frequency terms, the recursion for $P(k+1/k+1)$ is given by

$$\begin{aligned} P(k+1/k+1) = {} & P(k+1/k) - P(k+1/k)H^T A^2 \\ & \left[A^2 P_\phi + \frac{1}{2}A^2 P_{\phi S} + \overline{R}(k+1)\right]^{-1} C\, H\, P(k+1/k) \end{aligned} \qquad (A14)$$

with

$$H = \begin{bmatrix} \ell' & 0 & \cdots & \cdots & 0 \\ 0 & \ell' & 0 & \cdots & 0 \\ 0 & \cdots & \cdots & \cdots & \ell' \end{bmatrix}; \quad \ell' = [1\,0 \ldots 0]$$

Moreover, the filter error correction term is given by

$$M(k+1)\nu(k+1) = K(k+1)\eta(k+1) \tag{A15}$$

$$K(k+1) = A\,P(k+1/k)H^T C\left[A^2 P_\phi + \frac{1}{2}A^2 P_{\phi S} + \overline{R}(k+1)\right]^{-1} \tag{A16}$$

and the ith component of the vector $\eta(k+1)$ is given by

$$\eta^i(k+1) = \sqrt{2}\, y^i(k+1)\mathrm{Cos}(\hat{\Theta}^i(k+1)); \quad i = 1, 2, \ldots, N \tag{A17}$$

The Kronecker matrix product of any two matrices A and B is by definition the following $(mp \times nr)$ matrix, given in a block partitioned form:

$$A \otimes B = \begin{bmatrix} a_{11}B & . & . & . & a_{1n}B \\ a_{21}B & . & . & . & a_{2n}B \\ . & . & . & . & . \\ a_{m1}B & . & . & . & a_{mn}B \end{bmatrix}$$

where A is an $(m \times n)$ matrix with a_{ij} denoting its ijth element for $i = 1, \ldots, m$; $j = 1, 2, \ldots, n$, and B is any $(p \times r)$ matrix.

APPENDIX B: Steady State Performance Equations for a Dual-Receiver Communications System

In the following, we present a closed-form expression for the performance of a two-receiver configuration for the two cases of first-order and second-order loop filters.

In the first-order loop filter case, $\Phi = H = I$ where I is a 2×2 identity matrix, and

$$R = \begin{bmatrix} r_1 & 0 \\ 0 & r_2 \end{bmatrix}; \quad Q = \begin{bmatrix} q_{11} & q_{12} \\ q_{12} & q_{22} \end{bmatrix} \tag{B1}$$

The matrix H_f of (16) is given by

$$H_f = \begin{bmatrix} 1 & 0 & 1/r_1 & 0 \\ 0 & 1 & 0 & 1/r_2 \\ q_{11} & q_{12} & (1+q_{11}/r_1) & q_{12}/r_2 \\ q_{12} & q_{22} & q_{12}/r_1 & (1+q_{22}/r_2) \end{bmatrix} \tag{B2}$$

With a few manipulations, the characteristic polynomial of the matrix H_f is given by

$$|\lambda I - H_f| = \lambda^4 - (4+t)\lambda^3 + (6+2t+\Delta)\lambda^2 - (4+t)\lambda + 1 \tag{B3}$$

where $|\ |$ denotes the determinant of the matrix, and

$$\Delta = \frac{q_{11}q_{22} - q_{12}^2}{r_1 r_2} = \frac{|Q|}{r_1 r_2}; \quad t = \frac{q_{11}}{r_1} + \frac{q_{22}}{r_2} \tag{B4}$$

From the symmetry of (B3), it is apparent that if λ_1 is an eigenvalue of H_f, then so is λ_1^{-1}. In fact, $|\lambda I - H_f|$ may be factorized as

$$|\lambda I - H_f| = (\lambda^2 - c_1\lambda + 1)(\lambda^2 - c_2\lambda + 1) \tag{B5}$$

for some c_1, c_2 such that each quadratic form has its roots with their product equal to 1. Comparison of (B3) and (B5) shows that c_1, c_2 are solutions of the following

equation:

$$c^2 - (4+t)c + (4+2t+\Delta) = 0$$

or

$$c_{1,2} = \frac{1}{2}[(4+t) \pm \sqrt{(t^2 - 4\Delta}] \qquad (B6)$$

To compute the eigenvectors of H_f, we obtain the matrix

$$C = \text{Cofact}[\lambda I - H_f]$$

It is actually sufficient to evaluate the elements of the first row of C as functions of λ. With some manipulations, these are given by

$$C_{11} = (\lambda-1)^3 - t(\lambda-1)^2 + \left(\Delta - \frac{q_{22}}{r_2}\right)(\lambda-1) + \Delta$$

$$C_{12} = \frac{q_{12}}{r_2}(\lambda-1) \qquad (B7)$$

$$C_{13} = q_{11}(\lambda-1)^2 - \frac{|Q|}{r_2}(\lambda-1) - \frac{|Q|}{r_2}$$

$$C_{14} = q_{12}(\lambda-1)^2$$

With λ_1 and λ_2 denoting the roots with magnitude greater than 1 of the quadratic forms in (B5), we have the following desired eigenvectors:

$$\begin{bmatrix} W_{11} \\ W_{21} \\ W_{31} \\ W_{41} \end{bmatrix} = \begin{bmatrix} C_{11} \\ C_{12} \\ C_{13} \\ C_{14} \end{bmatrix}_{\lambda=\lambda_1} \quad ; \quad \begin{bmatrix} W_{12} \\ W_{22} \\ W_{32} \\ W_{42} \end{bmatrix} = \begin{bmatrix} C_{11} \\ C_{12} \\ C_{13} \\ C_{14} \end{bmatrix}_{\lambda=\lambda_2} \qquad (B8)$$

The steady-state error covariance matrix is then given by

$$\overline{P} = \begin{bmatrix} W_{31} & W_{32} \\ W_{41} & W_{42} \end{bmatrix} \begin{bmatrix} W_{11} & W_{12} \\ W_{21} & W_{22} \end{bmatrix}^{-1} \qquad (B9)$$

Thus, the order of computations is the solution of (B6), followed by the solution of the roots of quadratic forms in (B5), and then the computations (B8) and (B9). The steady-state filter error covariance matrix is obtained by the substitution of $\overline{P}$ in (20) with A assumed to be 1, without any loss of generality. Alternatively, one may replace (B9) by the elements of the third row of C given below:

$$C_{31} = \left\{(\lambda-1)^2 - \frac{q_{22}}{r_2}(\lambda-1) - \frac{q_{22}}{r_2}\right\}/r_1$$

$$C_{32} = \left\{q_{12}(\lambda-1) + q_{12}\right\}/r_1 r_2 \qquad (B10)$$

$$C_{33} = \left\{(\lambda-1)^3 - \frac{q_{22}}{r_2}(\lambda-1)^2 - \frac{q_{22}}{r_2}(\lambda-1)\right\}$$

$$C_{34} = \left\{q_{12}(\lambda-1)^2 + q_{12}(\lambda-1)\right\}/r_1$$

Numerical Example:

Let

$$r_1 = r_2 = 1; \quad q_{11} = q_{22} = q_{12} = 0.5$$

Thus, from (B4), (B6)

$$\Delta = 0,\ t = 1,\ C_1 = 3,\ C_2 = 2$$

The root (of magnitude > 1) of $(\lambda^2 - c_1\lambda + 1)$ is equal to 2.62 and that of $(\lambda^2 - c_2 + 1)$ is 1.0. (This is the limiting case as Q is a singular matrix.) From (B10), the corresponding

eigenvectors (after possible scaling) are given by

$$[1 \quad 1 \quad 1.62 \quad 1.62]^T; \qquad [1 \quad -1 \quad 0 \quad 0]^T$$

From (B9), the steady-state covariance matrix $\overline{P}$ is computed as

$$\overline{P} = \begin{bmatrix} 0 & 1.62 \\ 0 & 1.62 \end{bmatrix} \begin{bmatrix} 1 & 1 \\ -1 & 1 \end{bmatrix}^{-1} = \begin{bmatrix} .81 & .81 \\ .81 & .81 \end{bmatrix}$$

The filter error covariance matrix $\overline{P}_F$ computed from (20) has all its entries equal to .31. Without arraying, the corresponding value is computed from (15), (20) and is equal to 0.5. Thus, arraying results in an improvement of about 2 dB in the phase error variance.

In the second-order loop filter case, the various matrices are given by

$$\phi = \begin{bmatrix} \Phi_s & 0 \\ 0 & \Phi_s \end{bmatrix}; \quad \Phi_s = \begin{bmatrix} 1 & T \\ 0 & 1 \end{bmatrix}$$

$$H = \begin{bmatrix} 1 & 0 & 0 & 0 \\ 0 & 0 & 1 & 0 \end{bmatrix}; \quad R = \begin{bmatrix} r_1 & 0 \\ 0 & r_2 \end{bmatrix}$$

$$Q = \begin{bmatrix} q_{11}Q_s & q_{12}Q_s \\ q_{12}Q_s & q_{22}Q_s \end{bmatrix}; \quad Q_s = \begin{bmatrix} T^2/3 & T/2 \\ T/2 & 1 \end{bmatrix} \qquad (B11)$$

Substitution of these matrices into (16) yields H_f, which after simple row operations is modified into matrix H_{fm}. The modifications consist of adding $T \times \Re_1$ to $\Re_2$; $T \times \Re_3$ to $\Re_4$; $-\frac{T}{3} \times \Re_6$ to $\Re_5$ and $-\frac{T}{3} \times \Re_8$ to $\Re_7$ with $\Re_i$ denoting the ith row of H_f. The

corresponding matrix $(\lambda I - H_{fm})$ is given below.

$$\lambda I - H_{fm} =$$

$$\begin{bmatrix}
(\lambda-1) & 0 & 0 & 0 & -1/r_1 & 0 & 0 & 0 \\
\lambda T & (\lambda-1) & 0 & 0 & 0 & 0 & 0 & 0 \\
0 & 0 & (\lambda-1) & 0 & 0 & 0 & -1/r_2 & 0 \\
0 & 0 & \lambda T & (\lambda-1) & 0 & 0 & 0 & 0 \\
0 & -\frac{T}{6}q_{11} & 0 & -\frac{T}{6}q_{12} & (\lambda-1) & \overline{\lambda} & 0 & 0 \\
\frac{T}{2}q_{11} & -q_{11} & \frac{T}{2}q_{12} & -q_{12} & \frac{T}{2}\frac{q_{11}}{r_1} & (\lambda-1) & \frac{T}{2}\frac{q_{12}}{r_2} & 0 \\
0 & -\frac{T}{6}q_{12} & 0 & -\frac{T}{6}q_{22} & 0 & 0 & (\lambda-1) & \overline{\lambda} \\
\frac{T}{2}q_{12} & -q_{12} & \frac{T}{2}q_{22} & -q_{22} & \frac{T}{2}\frac{q_{12}}{r_1} & 0 & \frac{T}{2}\frac{q_{22}}{r_2} & (\lambda-1)
\end{bmatrix} \qquad (B12)$$

$$\overline{\lambda} \triangleq -\frac{T}{3}(\lambda-1) - T$$

With the application of the following matrix identity [13],

$$\begin{vmatrix} A & C \\ B & D \end{vmatrix} = |A| \cdot |D - CA^{-1}B| \qquad (B13)$$

and after a few tedious manipulations, one obtains the required characteristic polynomial in terms of $x = \lambda - 1$:

$$|\lambda I - H_f| = a(x+1)^2(x^2+6x+6)^2 + bx^4(x+1)(x^2+6x+6) + x^8$$
$$a = \frac{\Delta T^4}{36 r_1 r_2}; \quad \Delta = q_{11}q_{22} - q_{12}^2 \quad ; \quad b = \frac{T^2}{6}\left(\frac{q_{11}}{r_1} + \frac{q_{22}}{r_2}\right) \qquad (B14)$$

Alternatively, one may express $|\lambda I - H_f|$ in terms of λ as

$$P(\lambda) = \lambda^8 + (b-8)\lambda^7 + (a+28)\lambda^6 + (8a-9b-56)\lambda^5$$
$$+ (18a+16b+70)\lambda^4 + (8a-9b-56)\lambda^3 + (a+28)\lambda^2 + (b-8)\lambda + 1 \qquad (B15)$$

From the symmetry of the coefficients of the polynomial $P(\lambda)$, it is observed that if λ_1 is the root of $P(\lambda)$ then so is $1/\lambda_1$ for any λ_1. Thus

$$P(\lambda) = \prod_{i=1}^{4}(\lambda^2 + c_i\lambda + 1) \qquad (B16)$$

where $\prod$ denotes product. Comparison of (B15) and (B16) shows that

$$\begin{aligned} d_1 &\triangleq \sum_{i=1}^{4} c_i = b - 8 \\ d_2 &\triangleq \sum_{i=1}^{3} \sum_{j=i+1}^{4} c_i c_j = a + 24 \\ d_3 &\triangleq \sum_{i=1}^{2} \sum_{j=i+1}^{3} \sum_{k=j+1}^{4} c_i c_j c_k = 8a - 12b - 32 \\ d_4 &\triangleq c_1 c_2 c_3 c_4 \qquad\qquad = 16(a + b + 1) \end{aligned} \tag{B17}$$

and that c_1, c_2, c_3 and c_4 are negatives of the roots of the following equation:

$$y^4 + d_1\, y^3 + d_2\, y^2 + d_3\, y + d_4 = 0 \tag{B18}$$

The computation of the required eigenvalues (with magnitude > 1) of H_f proceeds as follows: Evaluate coefficients d_i's from (A14) and (A17), and factorize the polynomial (A18) into the product $\prod_{i=1}^{4}(y + c_i)$. For each value of $i = 1, 2, 3, 4$, obtain the roots of the quadratic equation, $\lambda^2 + c_i\lambda + 1 = 0$, among which only the one with its magnitude > 1 is retained.

With the application of Schur's identity [13, 14],

$$\begin{bmatrix} A & B \\ C & D \end{bmatrix}^{-1} = \begin{bmatrix} (A^{-1} + A^{-1}BHCA^{-1}) & -A^{-1}BH \\ -HCA^{-1} & (D - CA^{-1}B)^{-1} \end{bmatrix} \tag{B19}$$

and with some algebraic manipulations, the elements of the last column of the matrix $Adj(\lambda I - H_f)$ are obtained. In the computation of the $Adj(\lambda I - H_{f_m})$ from Schur's identity, we simply cancel out $|\lambda I - H_{f_m}|$ from the elements of $(\lambda I - H_{f_m})^{-1}$. Also, to obtain $Adj(\lambda I - H_f)$ from $Adj(\lambda I - H_{f_m})$, we post-multiply the latter by the following

matrix:

$$\begin{bmatrix} E_1 & 0 \\ 0 & E_2 \end{bmatrix}; \quad E_1 = \begin{bmatrix} 1 & 0 & 0 & 0 \\ -T & 1 & 0 & 0 \\ 0 & 0 & 1 & 0 \\ 0 & 0 & -T & 1 \end{bmatrix}; \quad E_2 = \begin{bmatrix} 1 & T/3 & 0 & 0 \\ 0 & 1 & 0 & 0 \\ 0 & 0 & 1 & T_3 \\ 0 & 0 & 0 & 1 \end{bmatrix} T/3$$

The elements of the last column of $Adj(\lambda I - H_f)$, (any other column could be selected as well) with C_j denoting the jth elements, have the following expressions in terms of $x \triangleq \lambda - 1$:

$$C_1 = -xB(x)\frac{q_{12}T^3}{18r_1r_2} \quad ; \qquad C_2 = (x+1)B(x)\frac{q_{12}T^4}{18r_1r_2}$$

$$C_3 = x(2x+3)U(x)\frac{T}{3r_2} \quad ; \qquad C_4 = -(2x^2+5x+3)U(x)\frac{T^2}{3r_2} \tag{B20}$$

$$C_5 = -x^2B(x)\frac{q_{12}T^3}{18r_2} \quad ; \qquad C_6 = -x^3\mathcal{C}(x)\frac{q_{12}T^3}{6r_2}$$

$$C_7 = x^2(2x+3)U(x)\frac{T}{3} \quad ; \qquad C_8 = x^3U(x) - (x+1)^2Y(x)\frac{q_{22}T^2}{6r_2}$$

where $B, \mathcal{C}, U, Y$ are the polynomials in x as follows.

$$B(x) = (2x^2+5x+3)(x^2+6+6) \quad ; \mathcal{C}(x) = (2x+3)(x^2+3x+2)$$

$$U(x) = x^4 + (x+1)(x^2+6x+6)\frac{q_{11}T^2}{6r_1} \quad ; Y(x) = x^4 + (x+1)(x^2+6x+6)\frac{\Delta T^2}{6r_1q_{22}} \tag{B21}$$

The eigenvectors W_i of the matrix H_f corresponding to λ_i, $i = 1, \ldots, 4$ are obtained by evaluating (B17), (B18) at $x = \lambda_i - 1$, i.e.,

$$W_i = [C_1 \quad C_2 \quad C_3 \ldots C_8]^T\big|_{x=\lambda_i-1} \tag{B22}$$

The steady-state error covariance matrices $\overline{P}$ and $\overline{P}_F$ are then evaluated from (18)-(20) as for the case of a first-order filter.

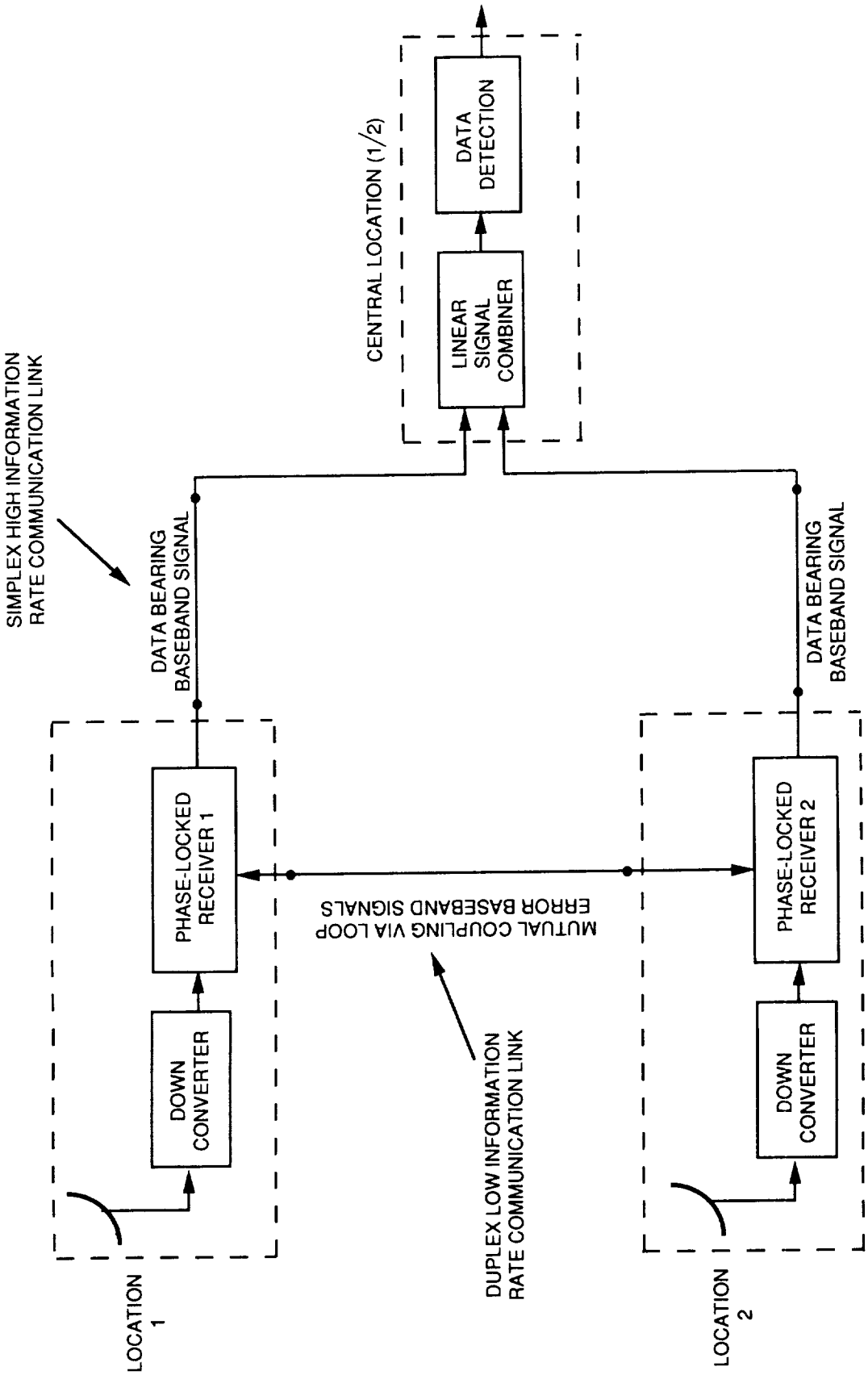

Fig. 1a. Proposed Estimation–Detection Scheme 1.

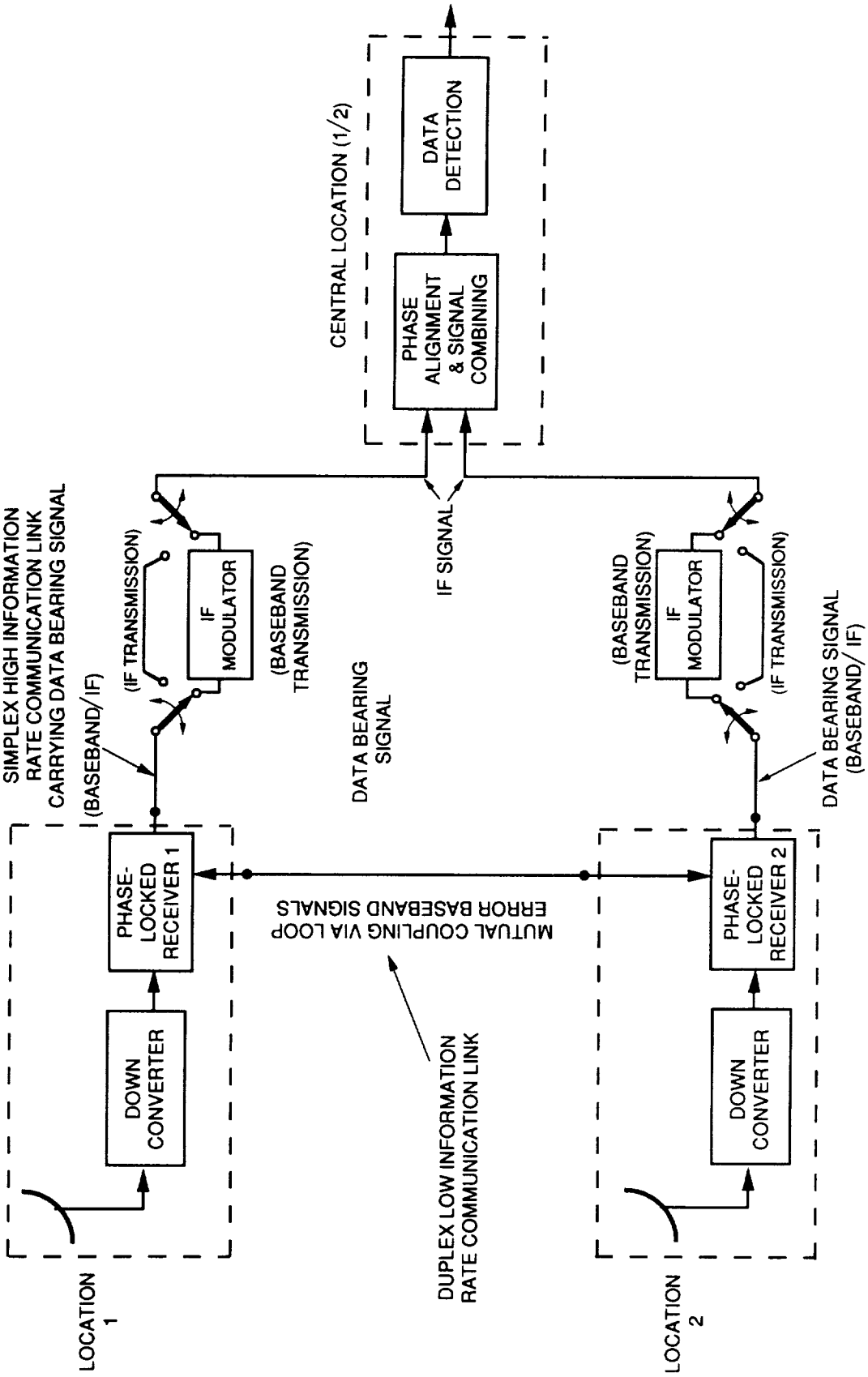

Fig. 1b. Proposed Estimation–Detection Scheme 2.

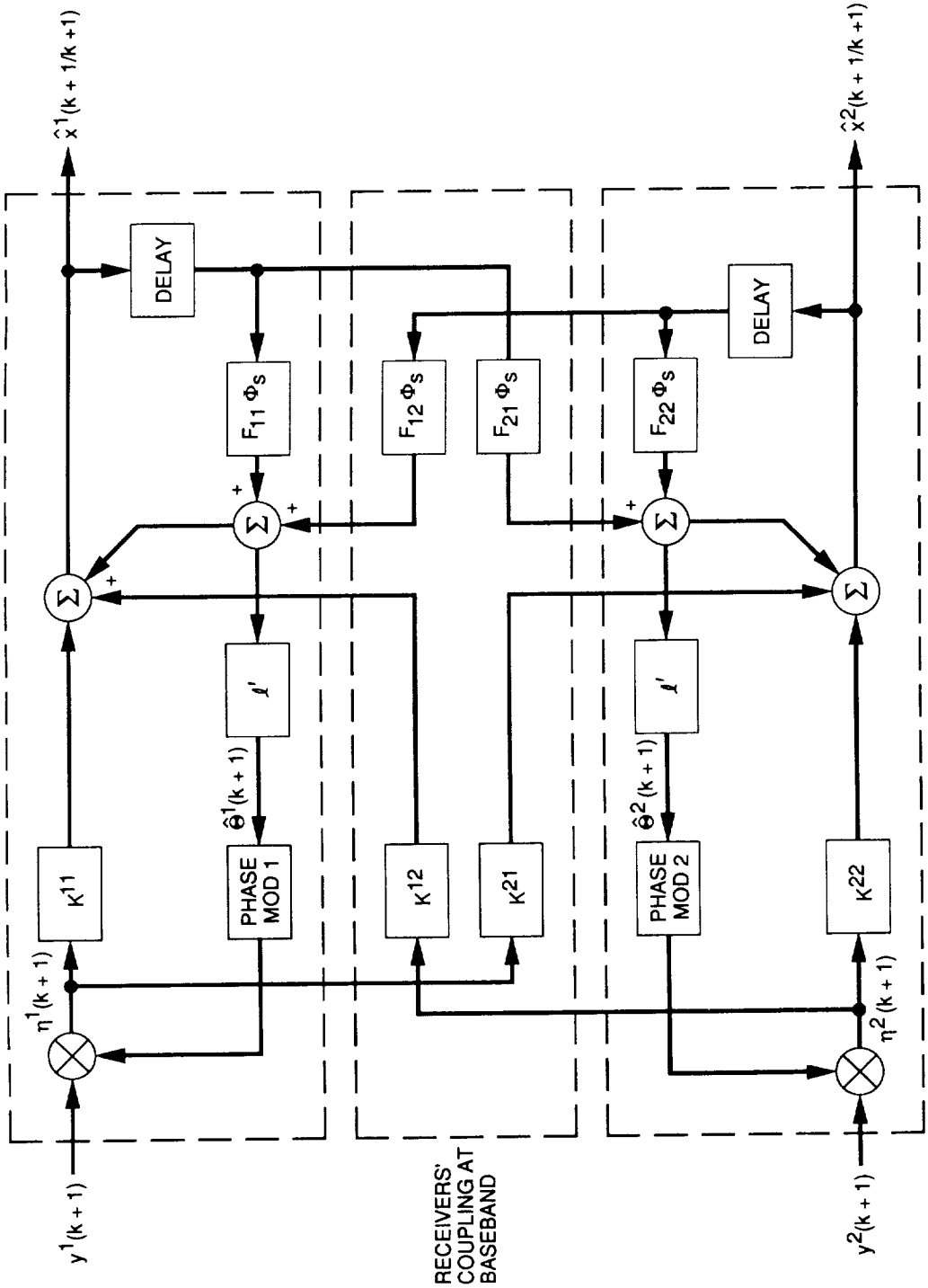

Fig. 2a. Multireceiver Configuration With N = 2 (Coupling Consists of Vector Baseband Signals).

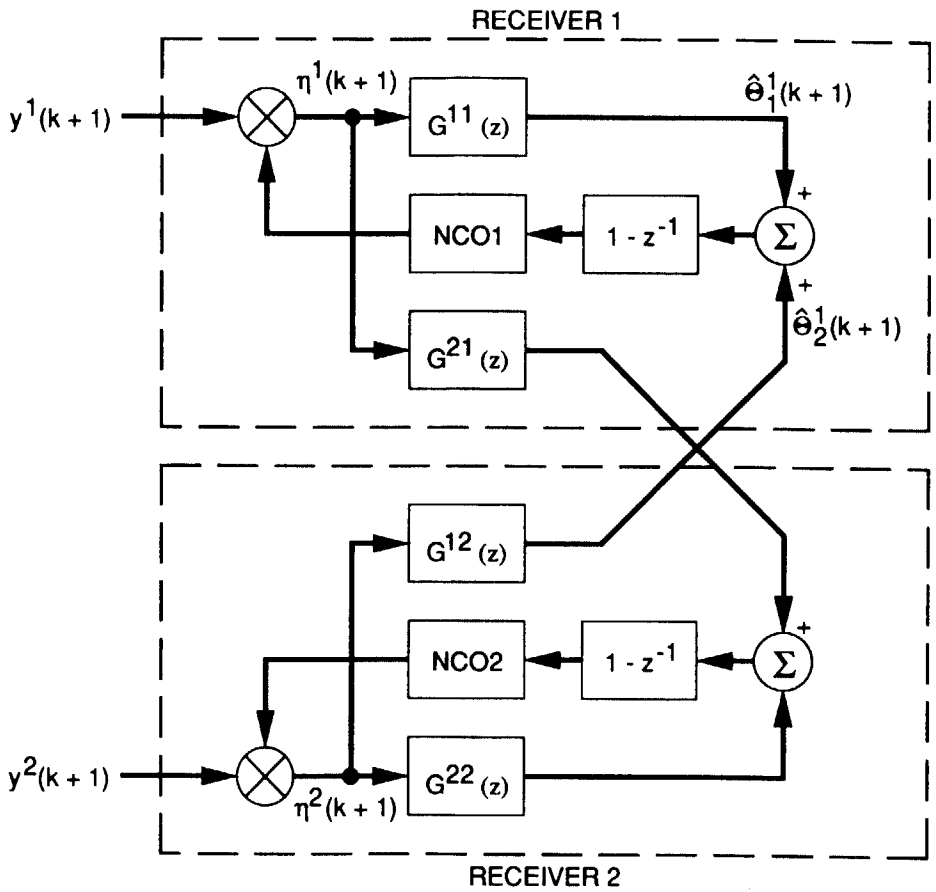

Fig. 2b. An Equivalent Implementation for the Case of Diagonal Matrix F and n = 2 (Coupling Consists of Baseband Scalar Signals).

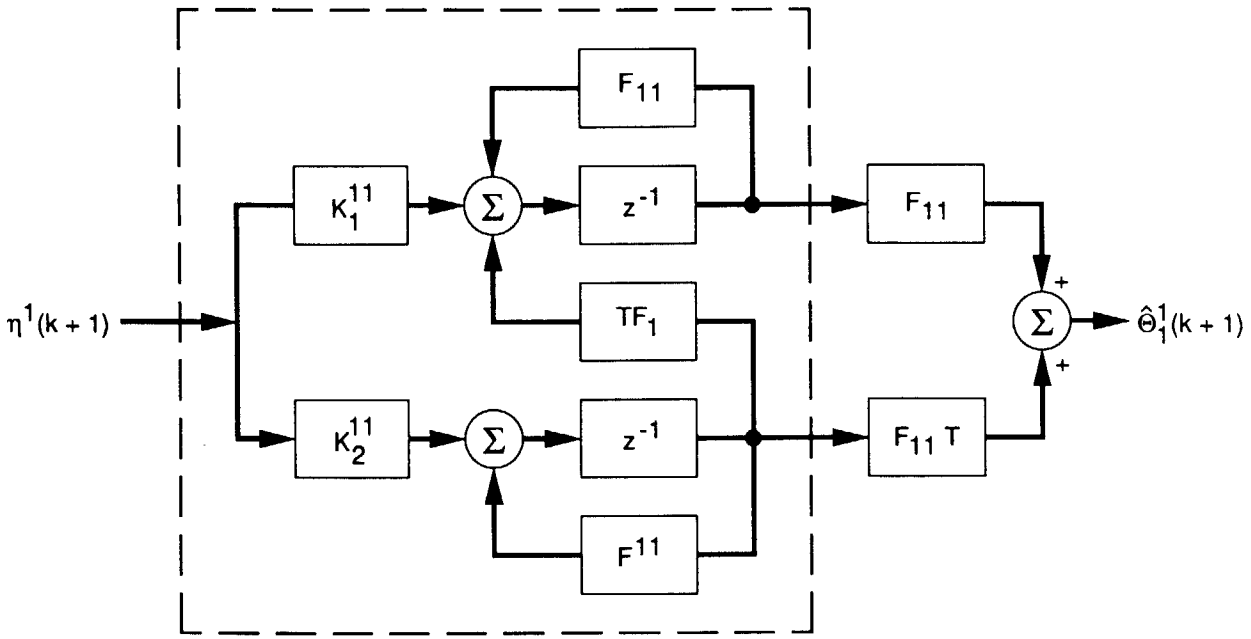

Fig. 3. Digital Filter Implementation of G^{11} (z); Filter States Correspond to $\hat{x}^1$ (k/k).

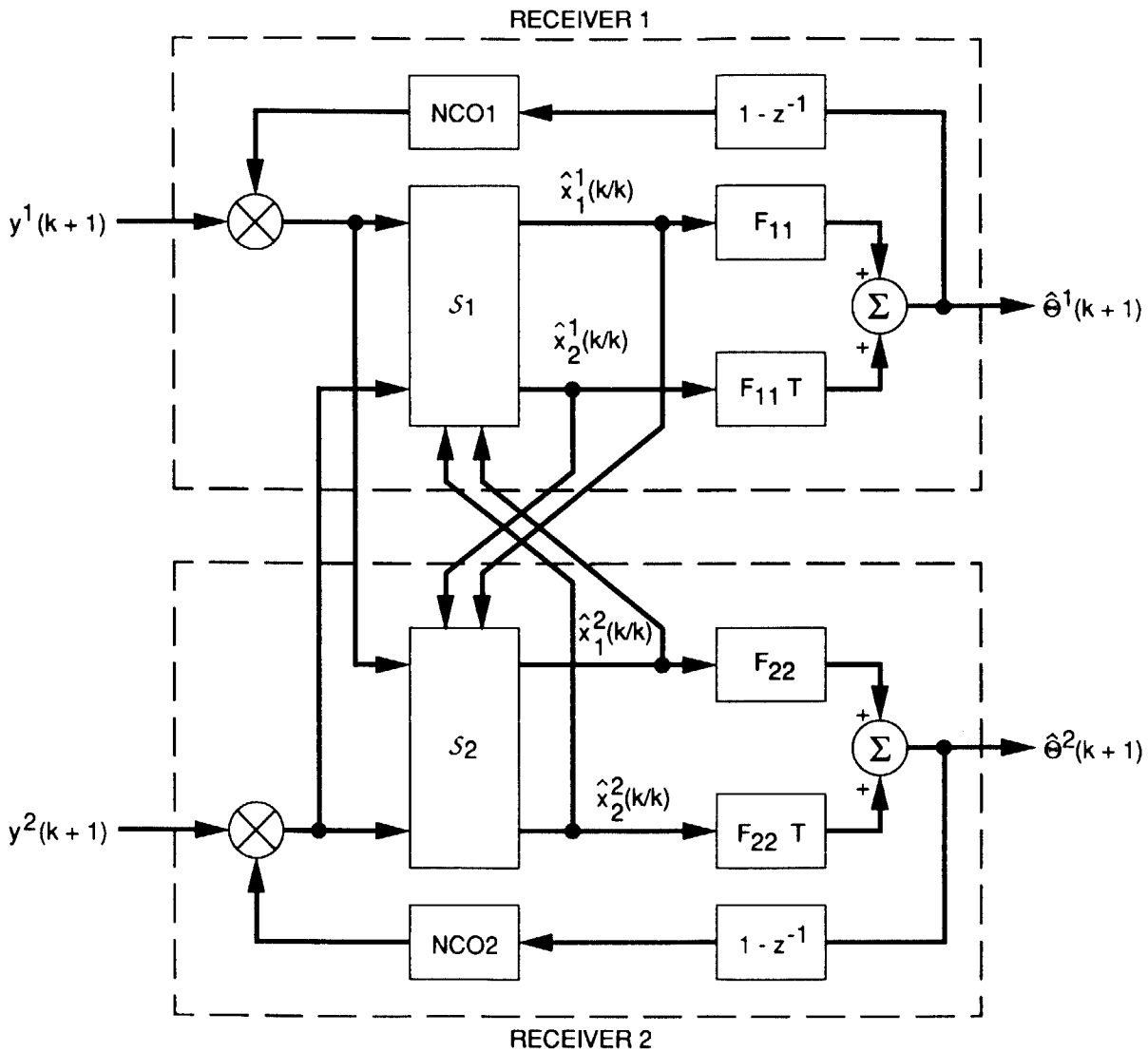

Fig. 4. An Equivalent Implementation of a Two-Receiver Configuration.

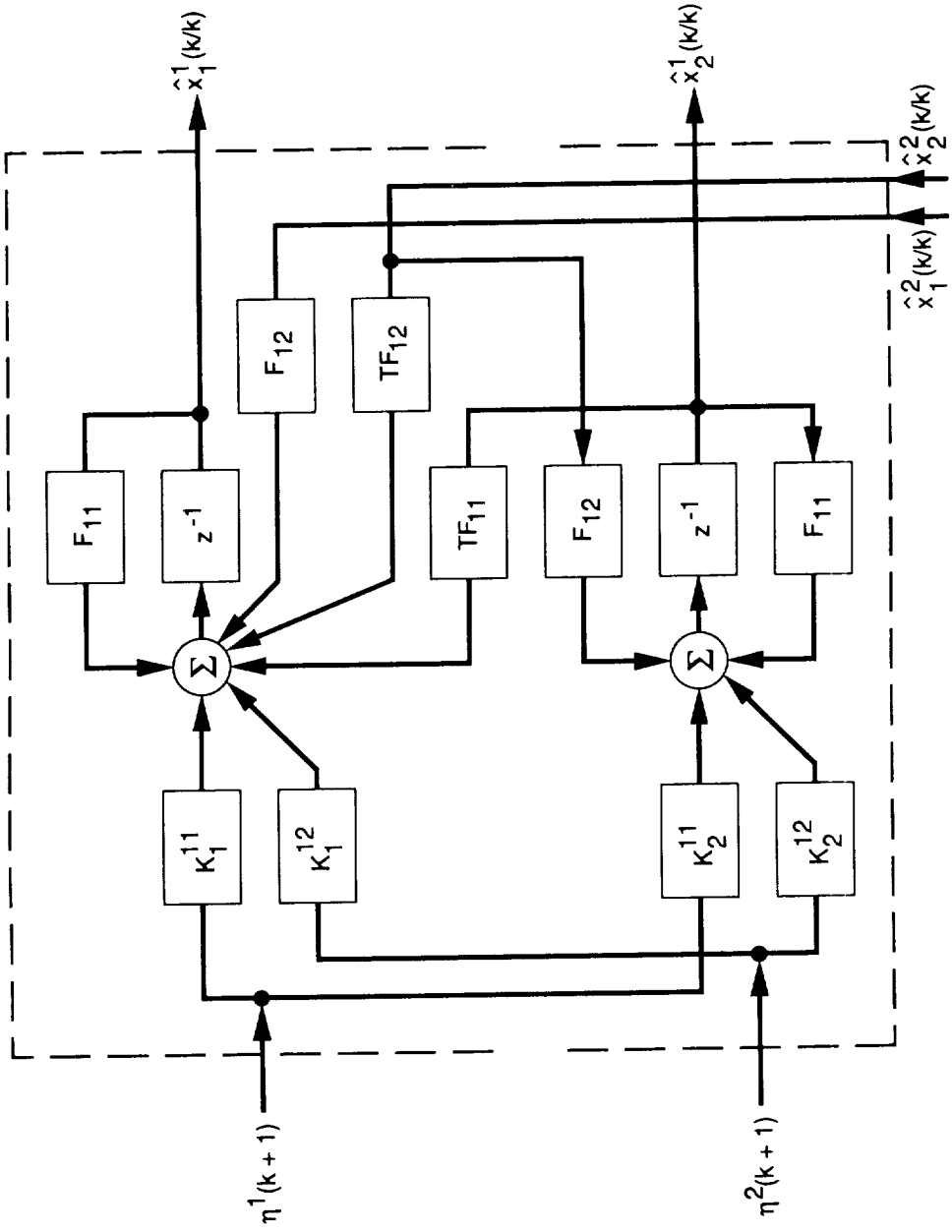

Fig. 5. Implementation of the Multivariable Digital Filter, S_1.

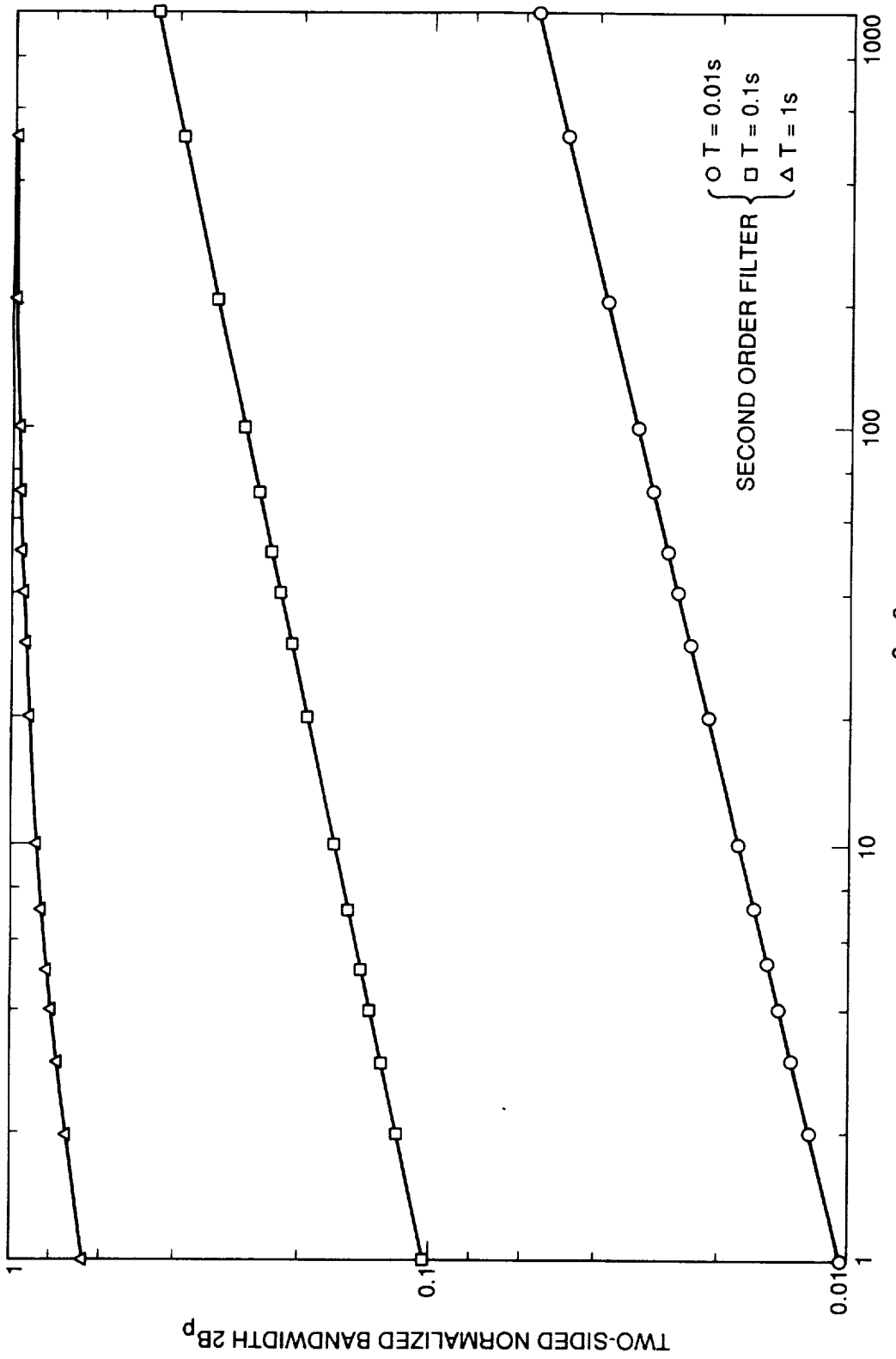

Fig. 6. Normalized Loop Noise Bandwidth of the Second-Order Filter vs. (σ_a^2/σ_v^2).

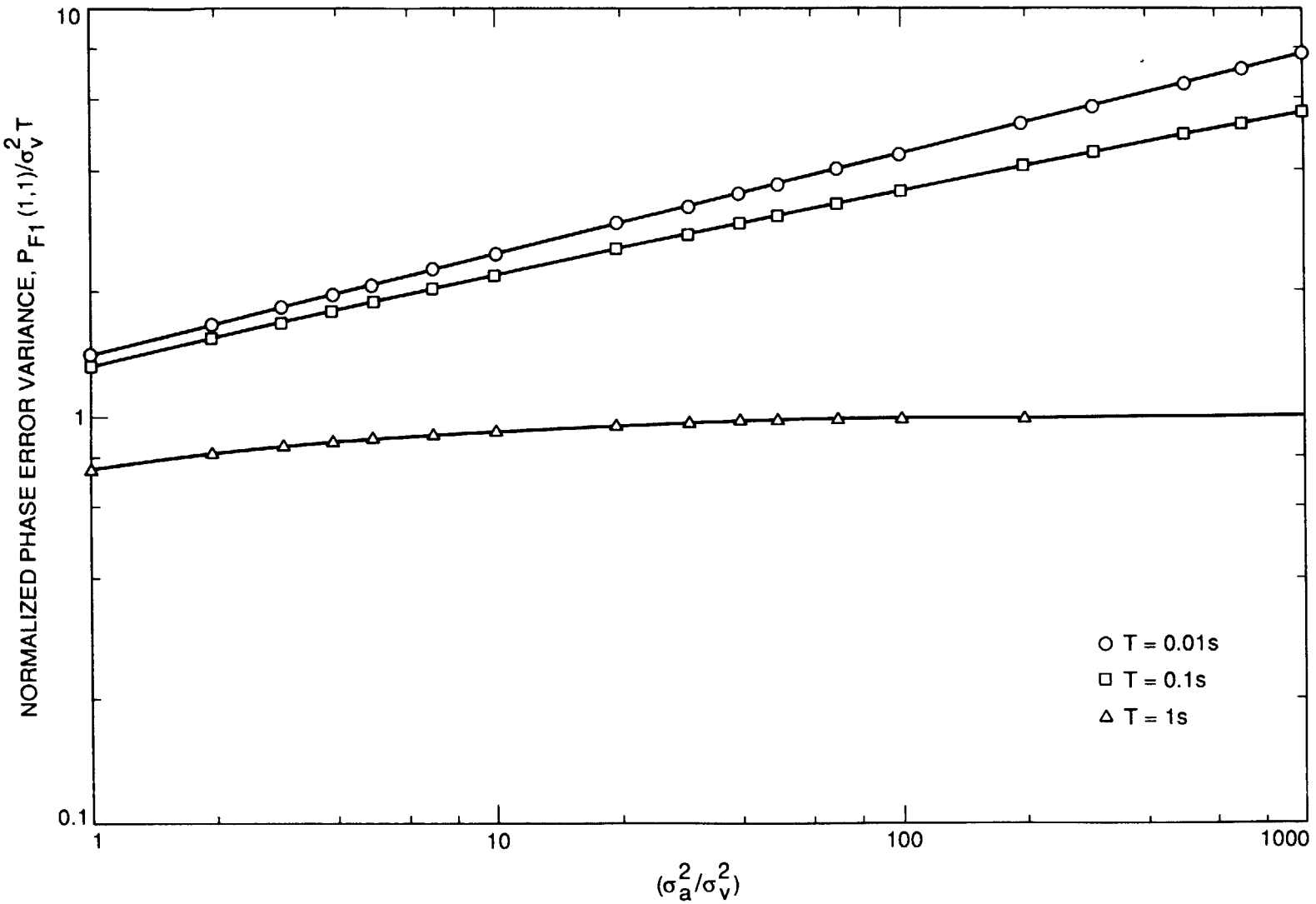

Fig. 7. Normalized Phase Error Variance vs. (σ_a^2/σ_v^2).

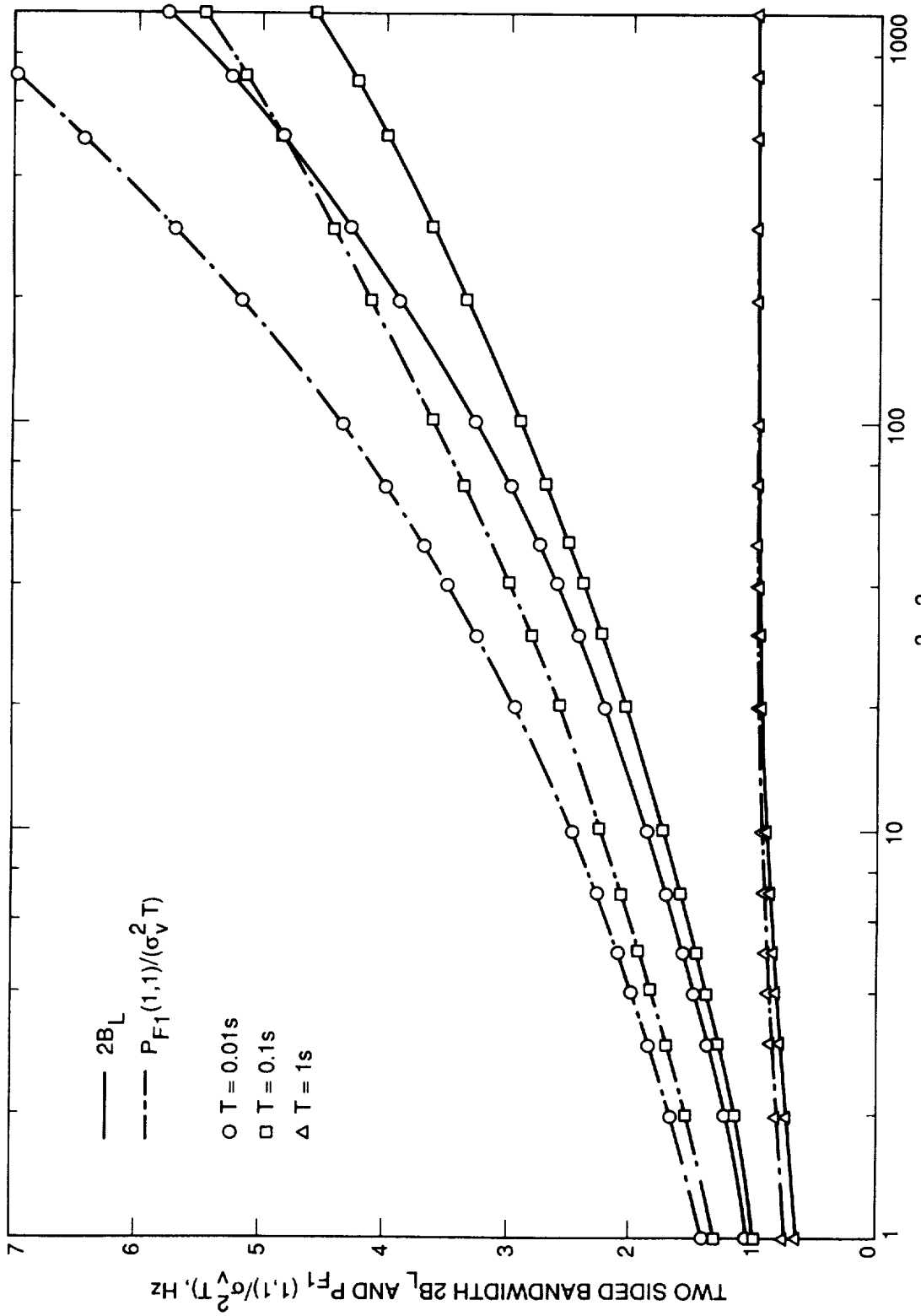

Fig. 8. Comparison of Filter Performance With and Without Process Noise.

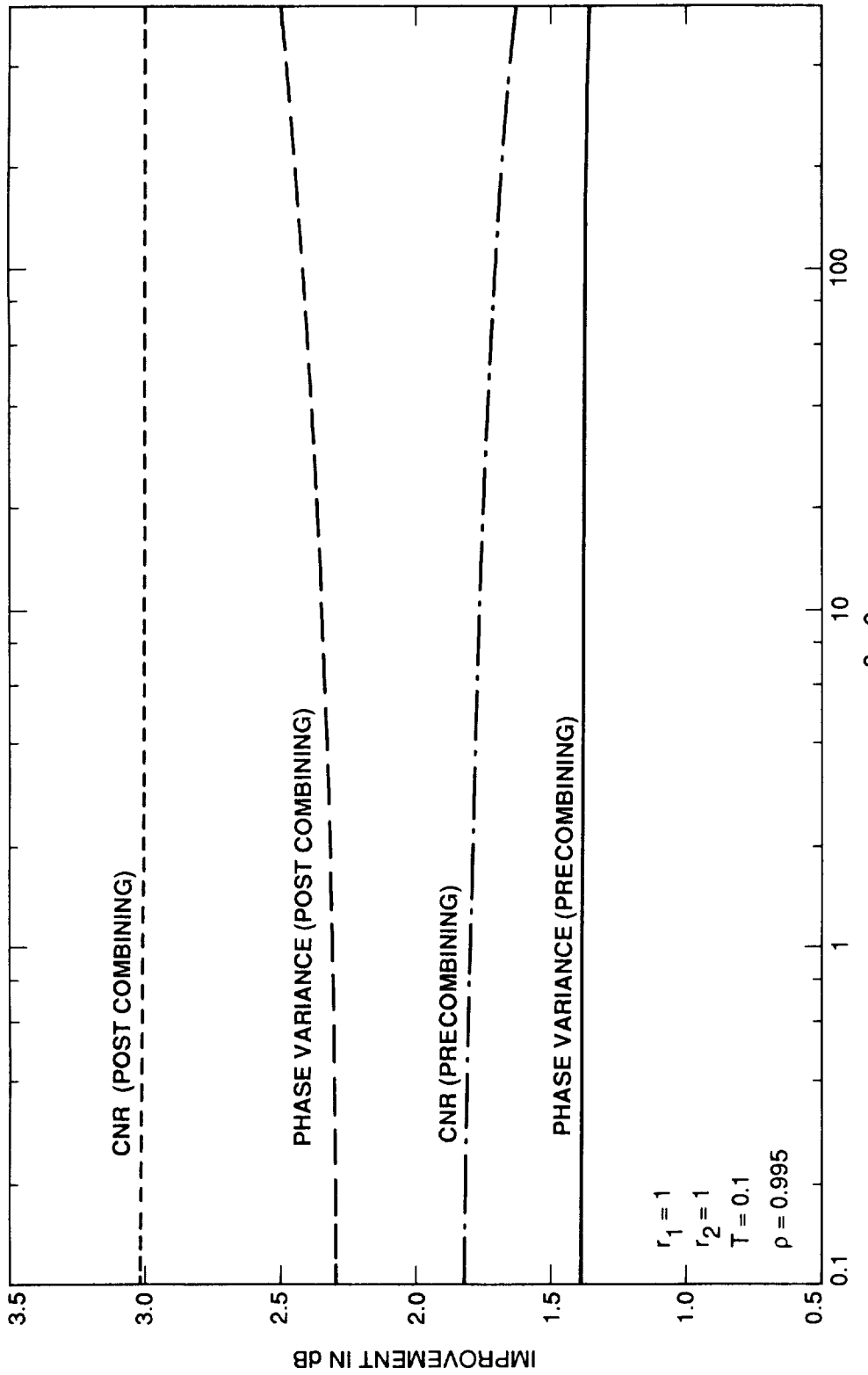

Fig. 9. Improvement Due to Arraying; $\rho = 0.995$ (Close-form Solution).

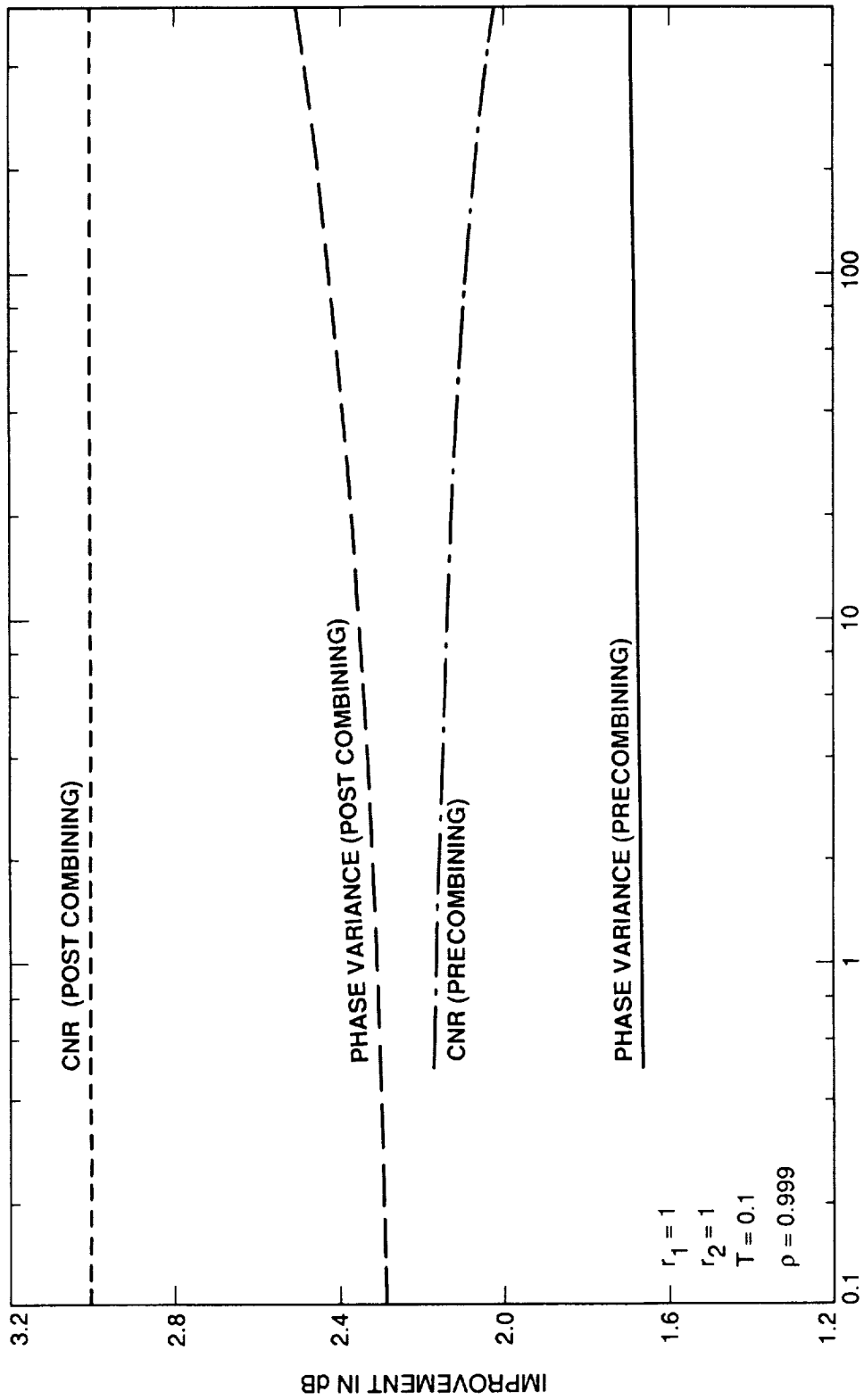

Fig. 10. Improvement Due to Arraying; $\rho = 0.999$ (Close-form Solution).

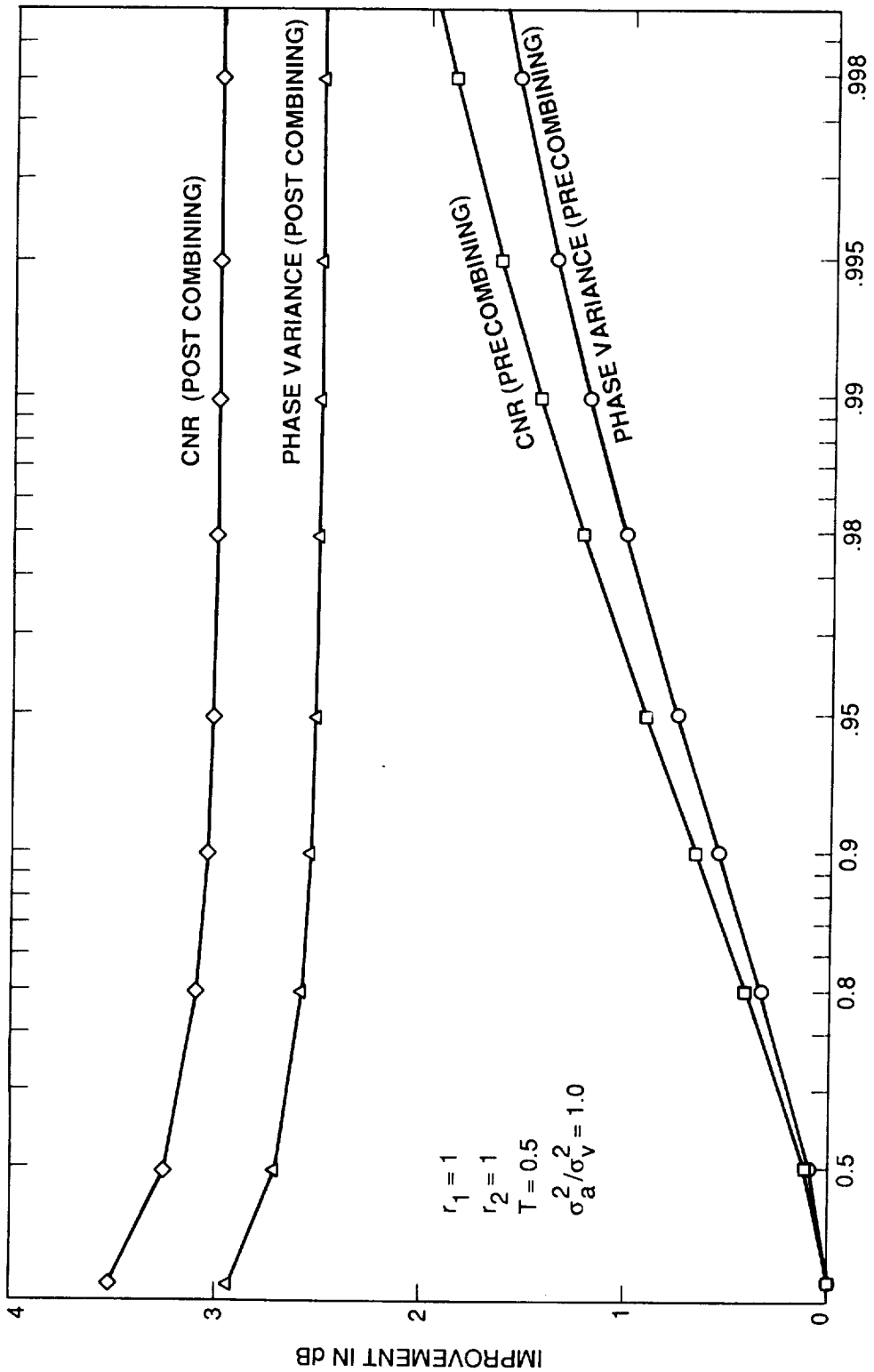

Fig. 11. Improvement Due to Arraying; $T = 0.5$, $\sigma_a^2/\sigma_v^2 = 1.0$ (Close-form Solution).

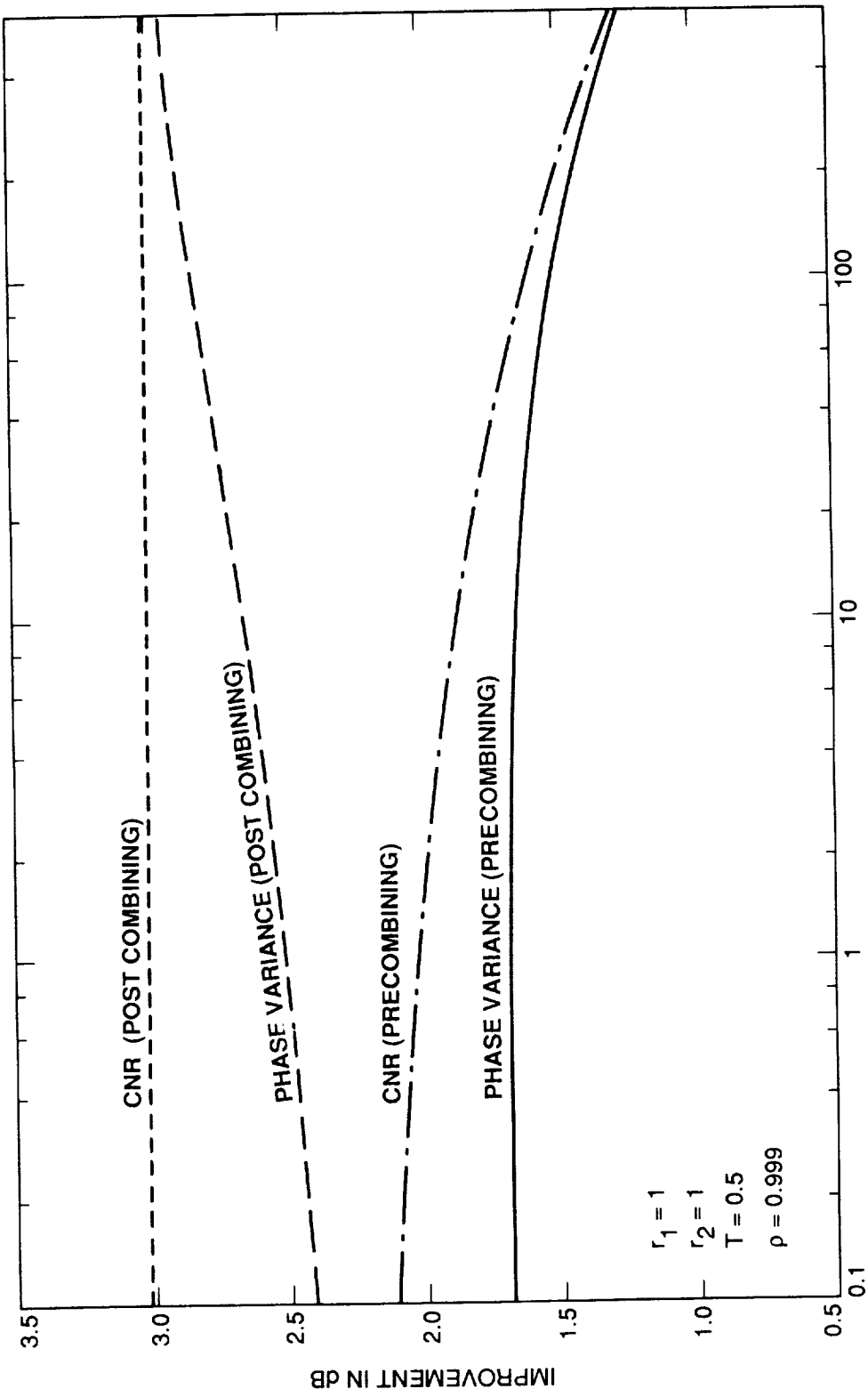

Fig. 12. Improvement Due to Arraying; $T = 0.5, \rho = 0.999$ (Close-form Solution).

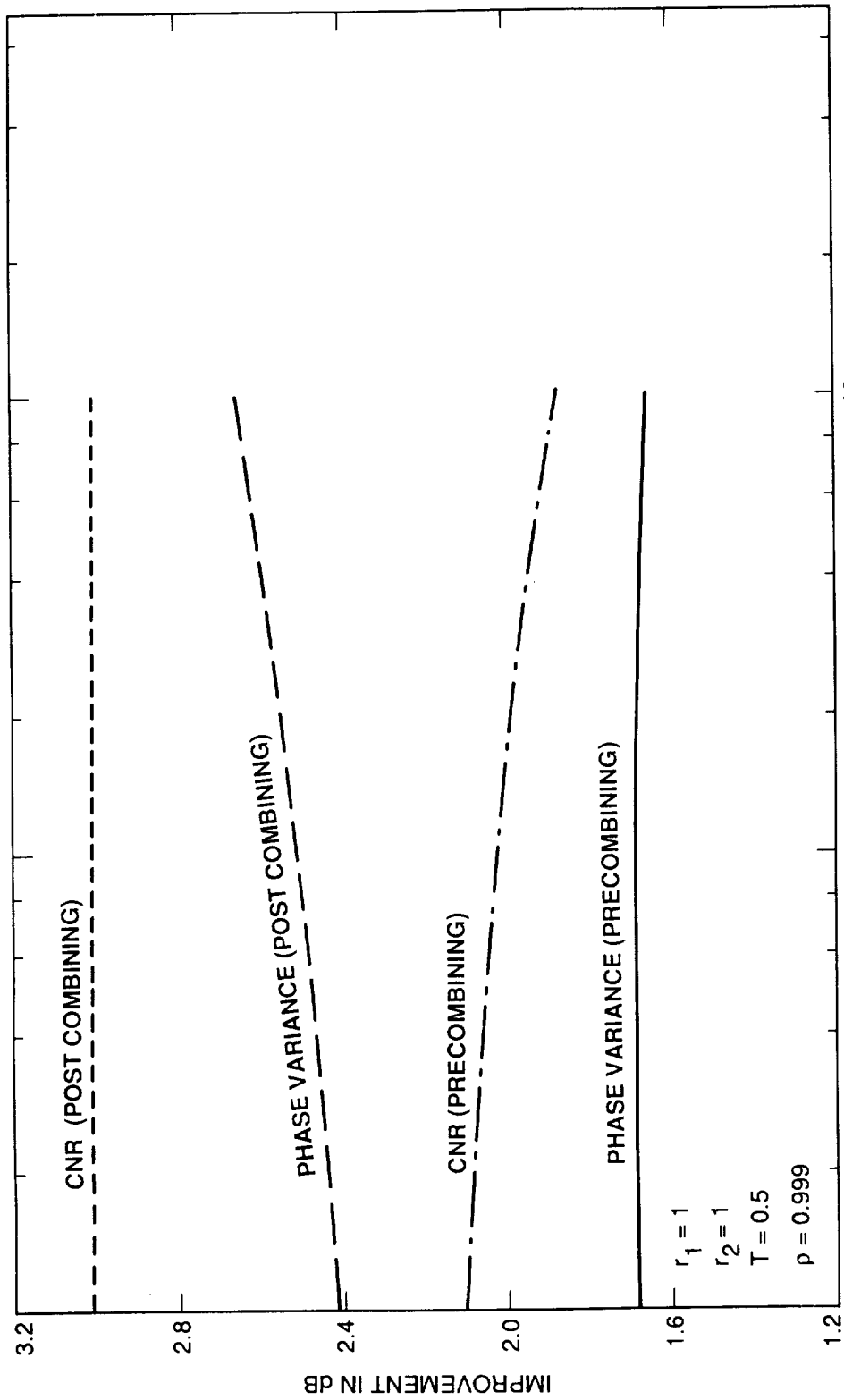

Fig. 13. Improvement Due to Arraying With a Two-Receiver Configuration; $T = 0.5$ (Recursive Solution).

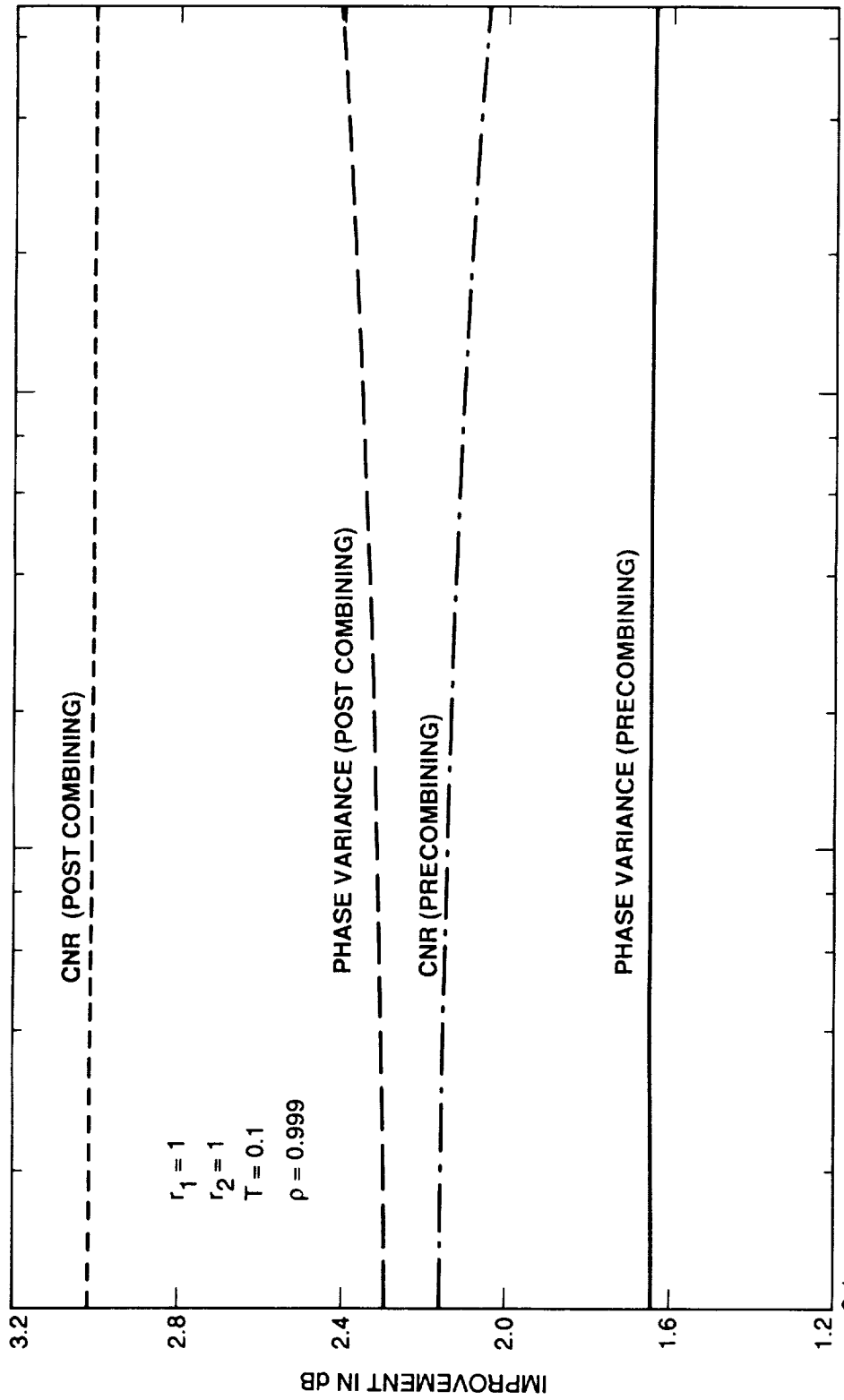

Fig. 14. Improvement Due to Arraying With a Two-Receiver Configuration; $T = 0.1$ (Recursive Solution).

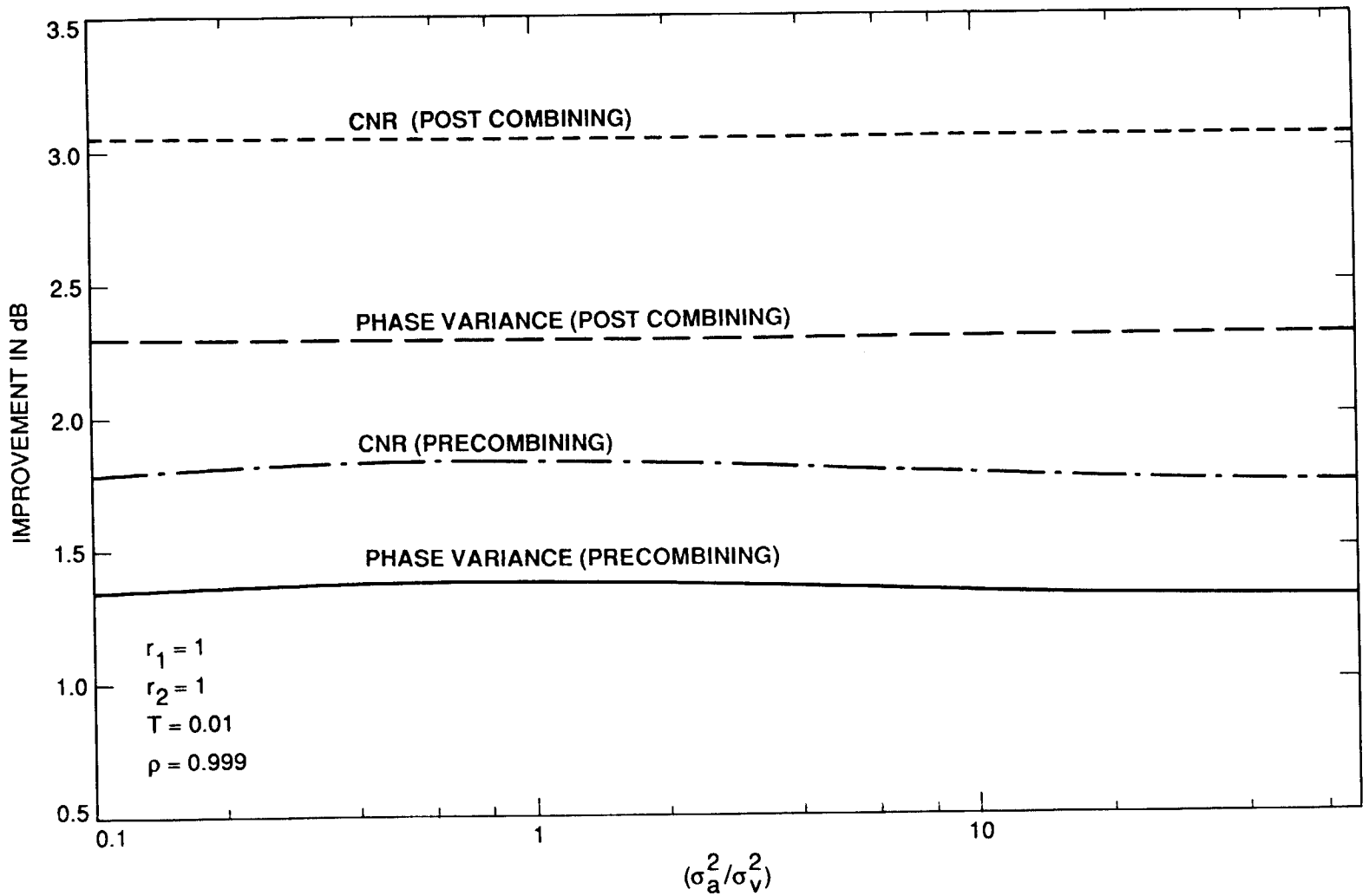

Fig. 15. Improvement Due to Arraying With a Two-Receiver Configuration; $T = 0.01$ (Recursive Solution).

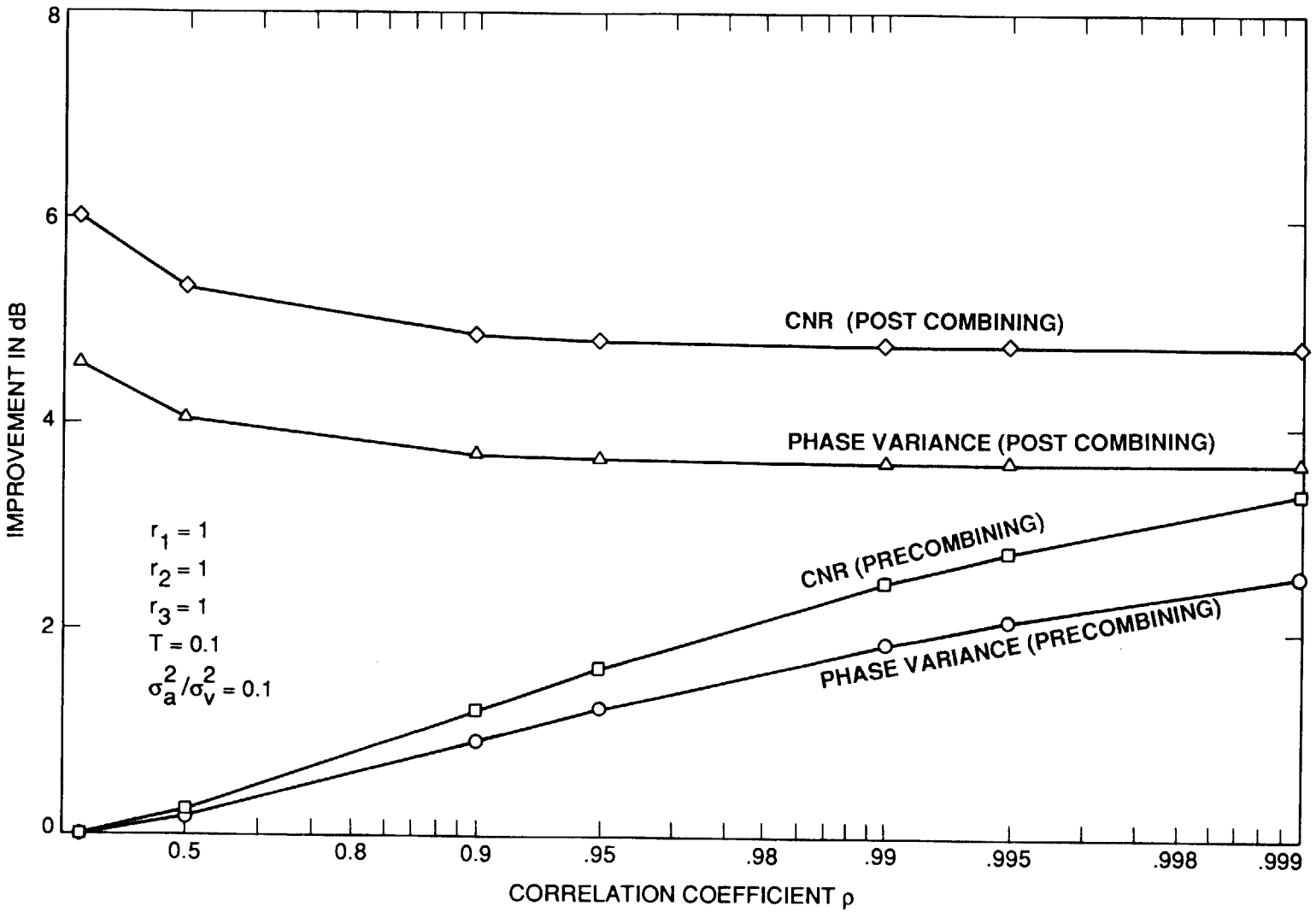

Fig. 16. Improvement Due to Arraying With a Three-Receiver Configuration (Equal CNR; $\sigma_a^2/\sigma_v^2 = 0.1$).

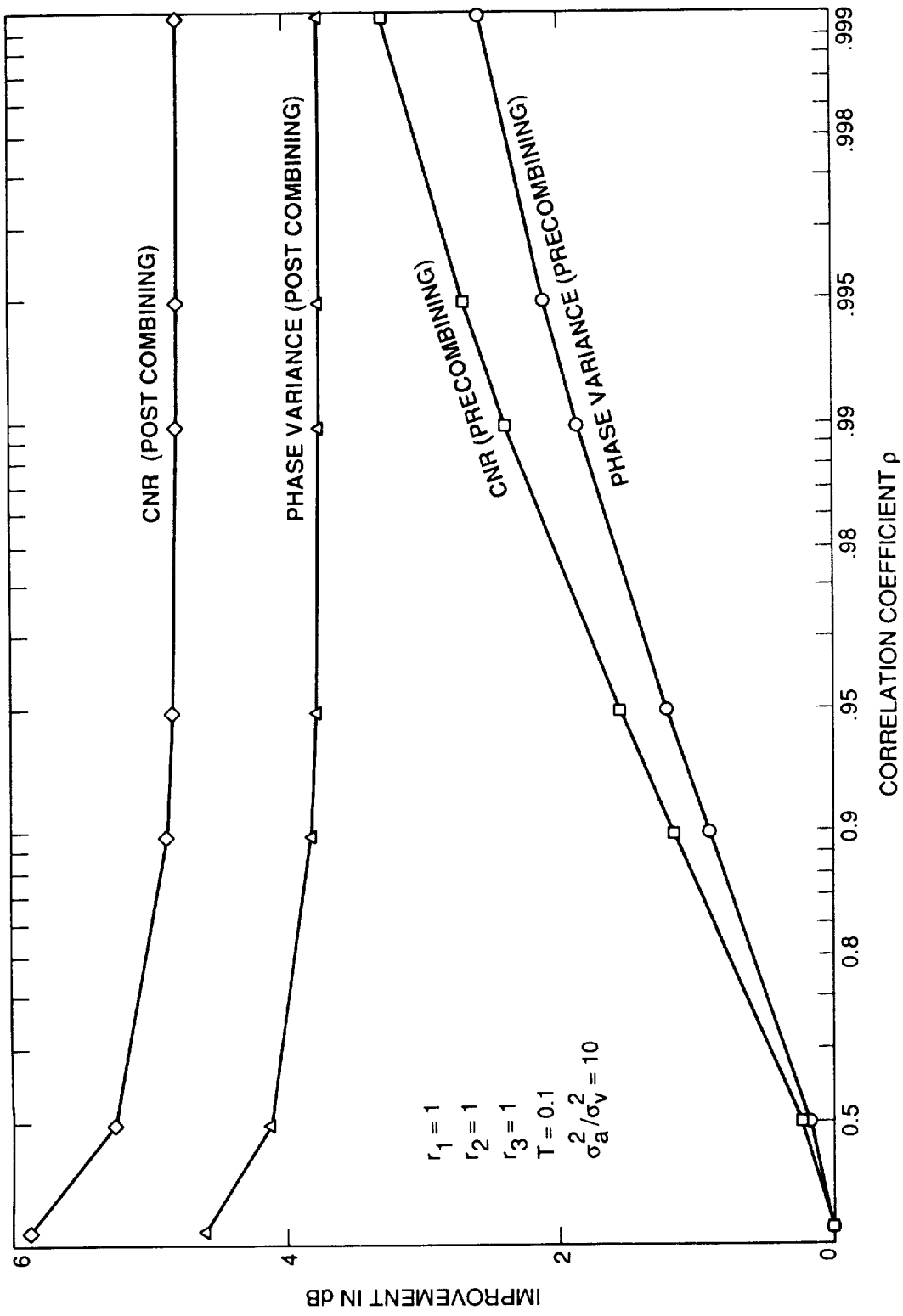

Fig. 17. Improvement Due to Arraying With a Three-Receiver Configuration (Equal CNR; $\sigma_a^2/\sigma_v^2 = 10$).

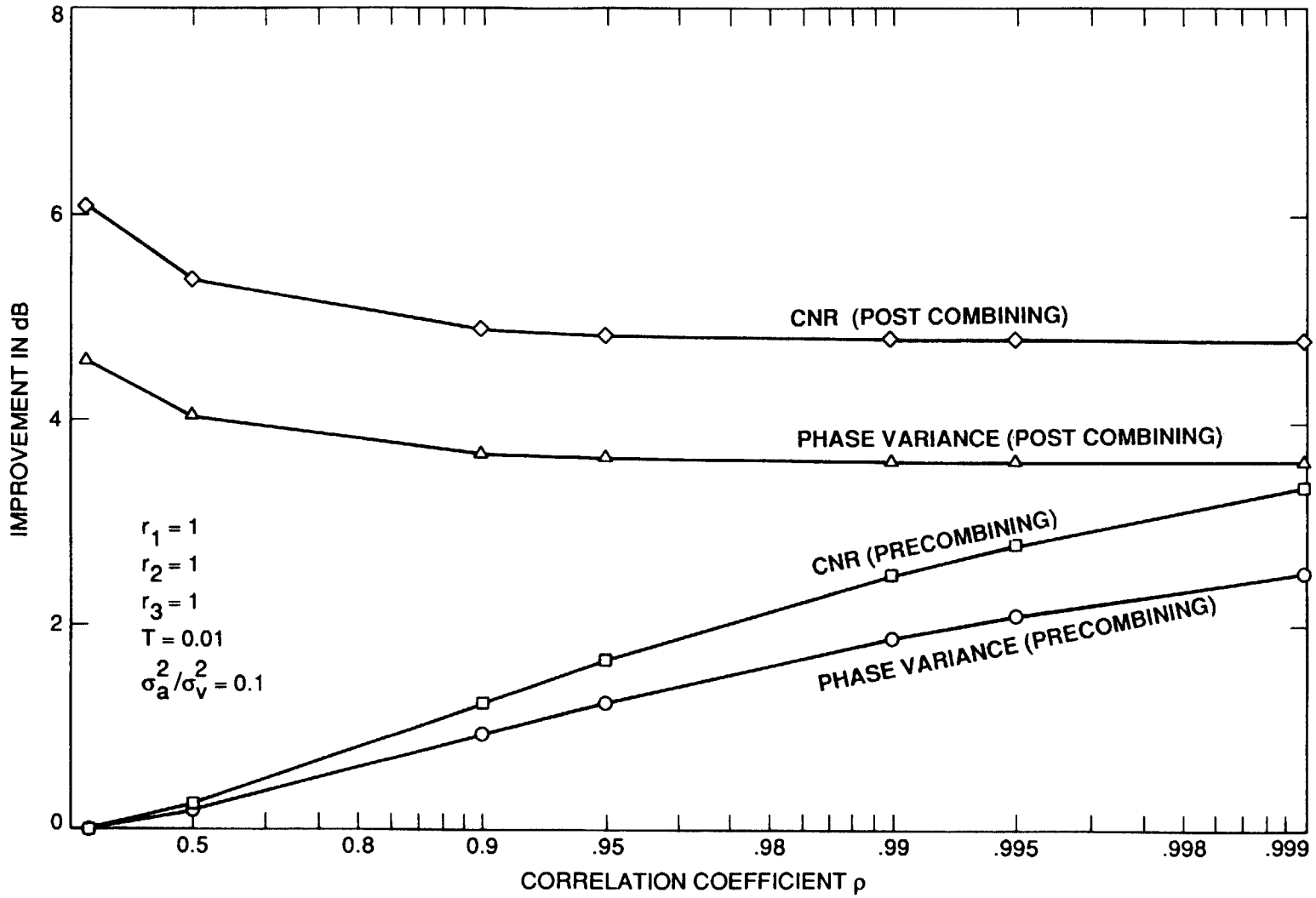

Fig. 18. Improvement Due to Arraying With a Three-Receiver Configuration (Equal CNR; $T = 0.01s$).

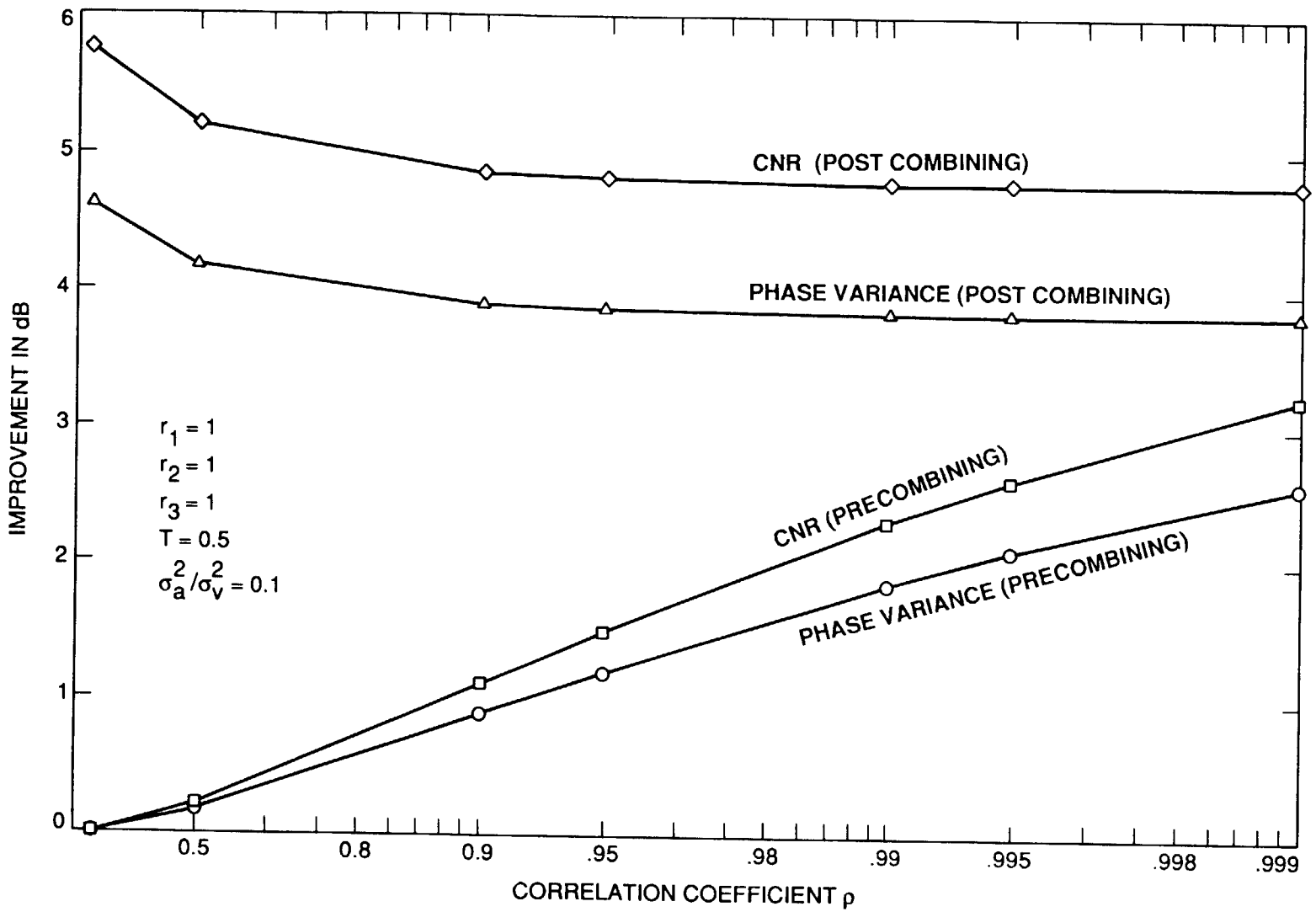

Fig. 19. Improvement Due to Arraying With a Three-Receiver Configuration (Equal CNR; $T = 0.5s$).

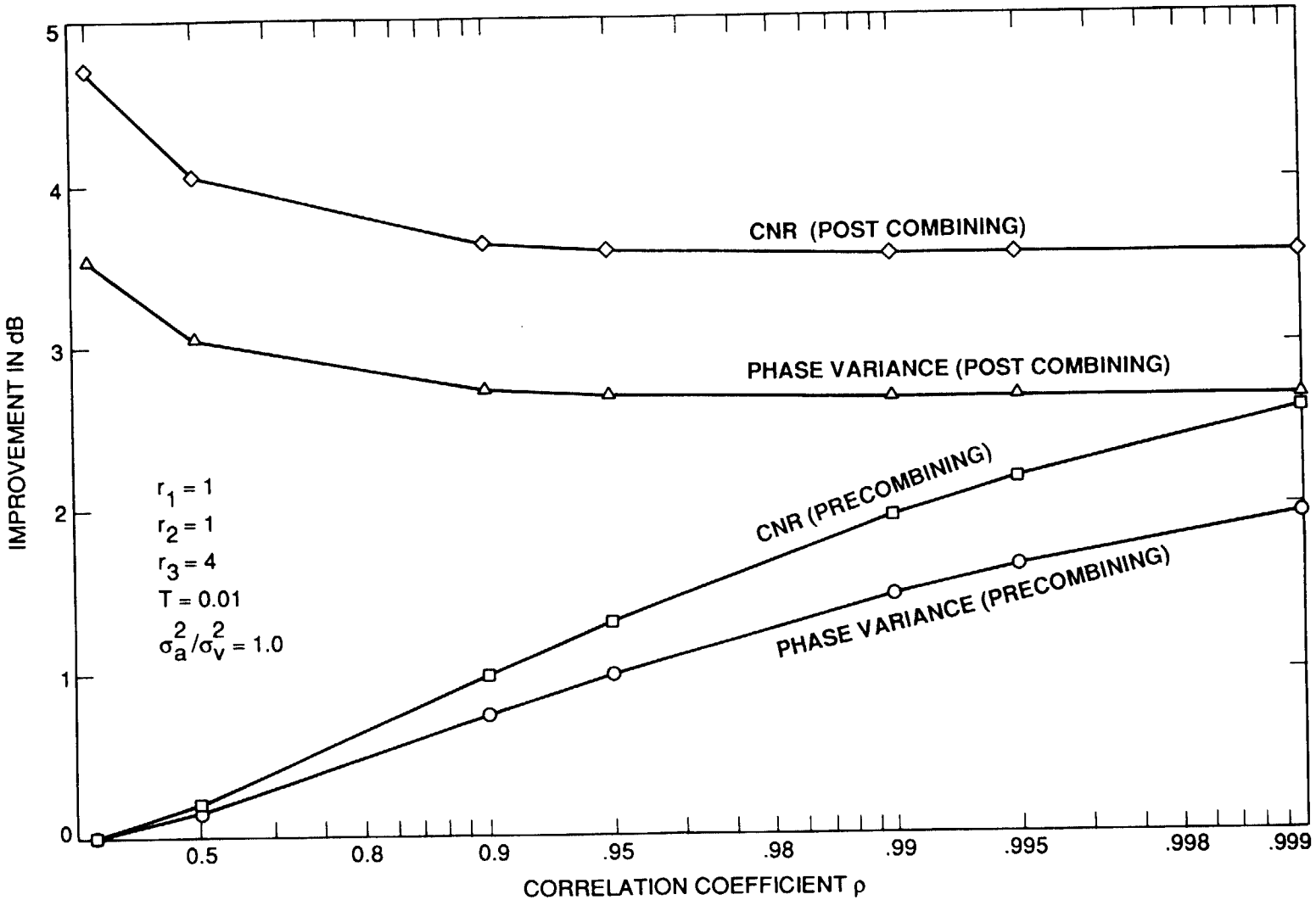

Fig. 20. Improvement Due to Arraying With a Three-Receiver Configuration and a 1:1:4 Ratio (Receiver 1).

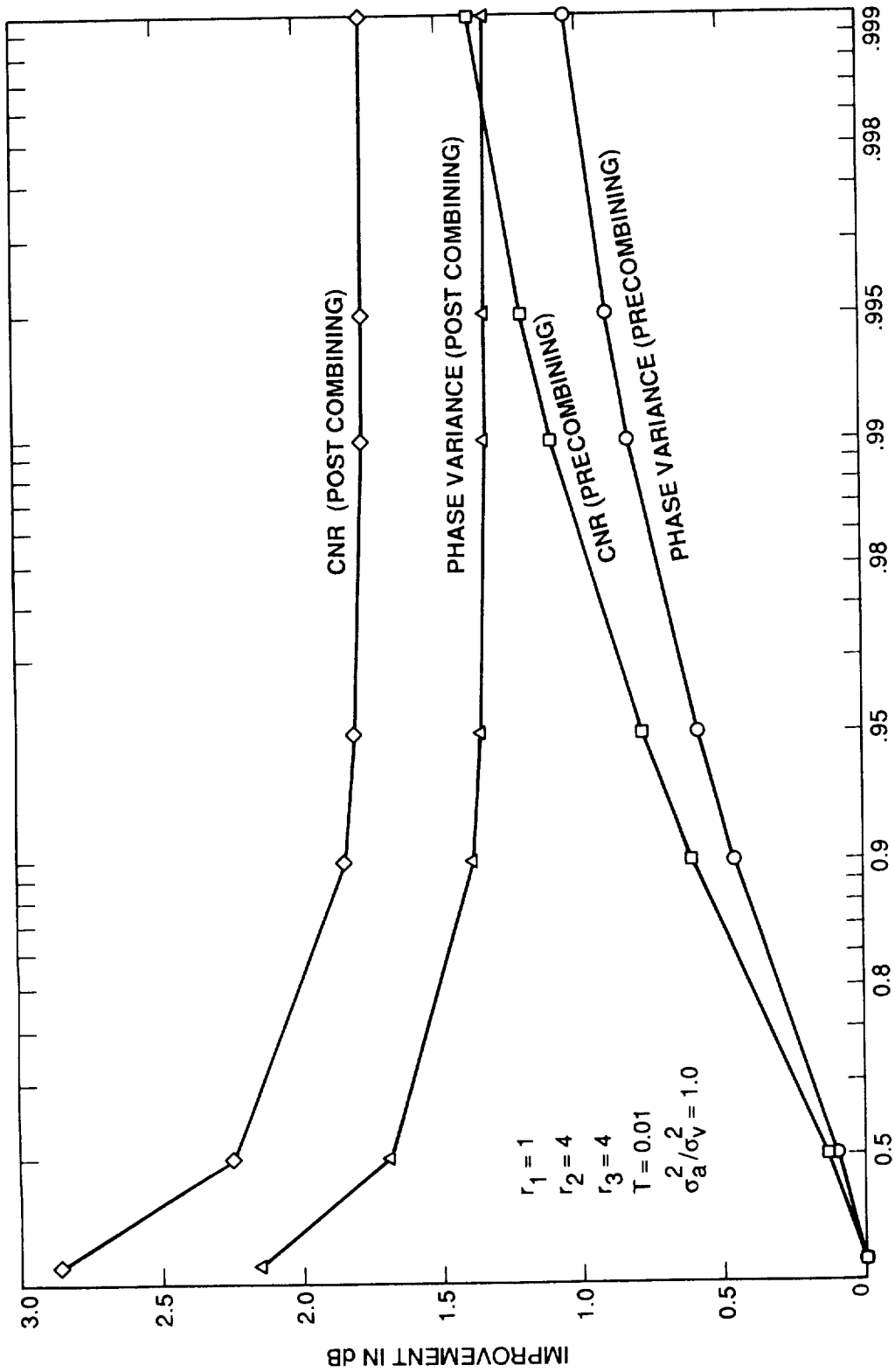

Fig. 21. Improvement Due to Arraying With a Three-Receiver Configuration and a 1:4:4 Ratio (Receiver 1).

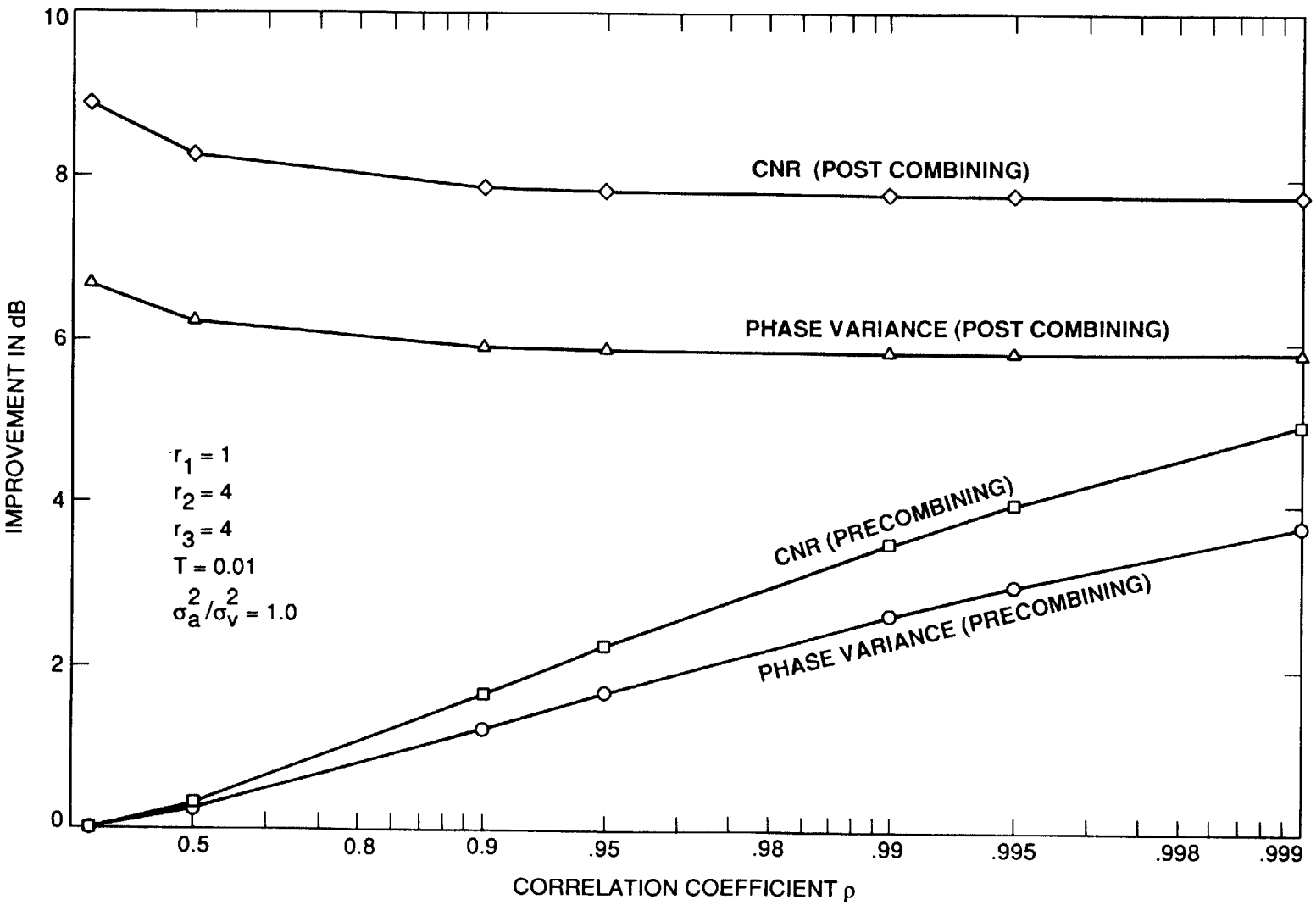

Fig. 22. Improvement Due to Arraying With a Three-Receiver Configuration and a 1:4:4 Ratio (Receiver 2).

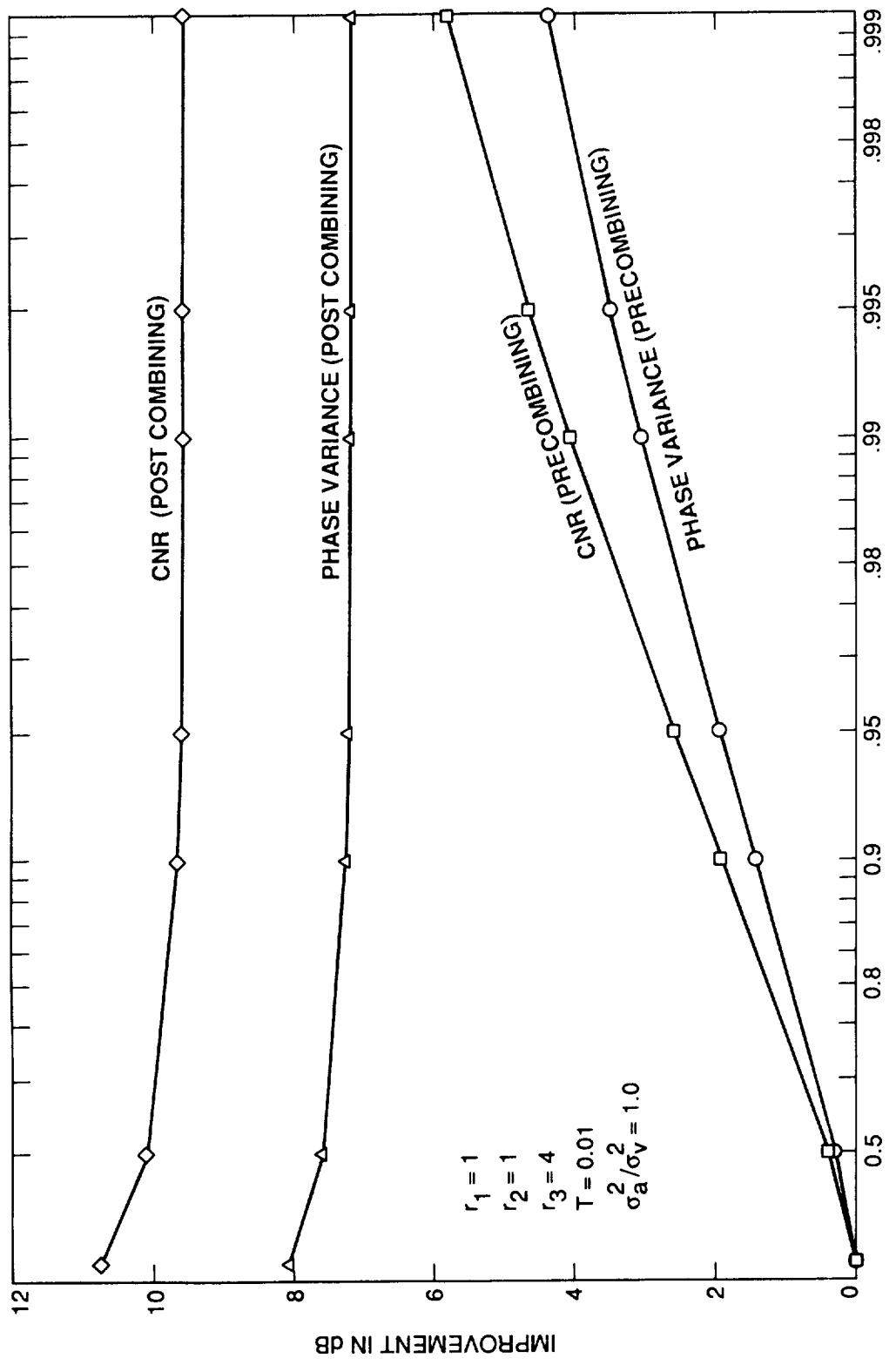

Fig. 23. Improvement Due to Arraying With a Three-Receiver Configuration and a 1:1:4 Ratio (Receiver 3).

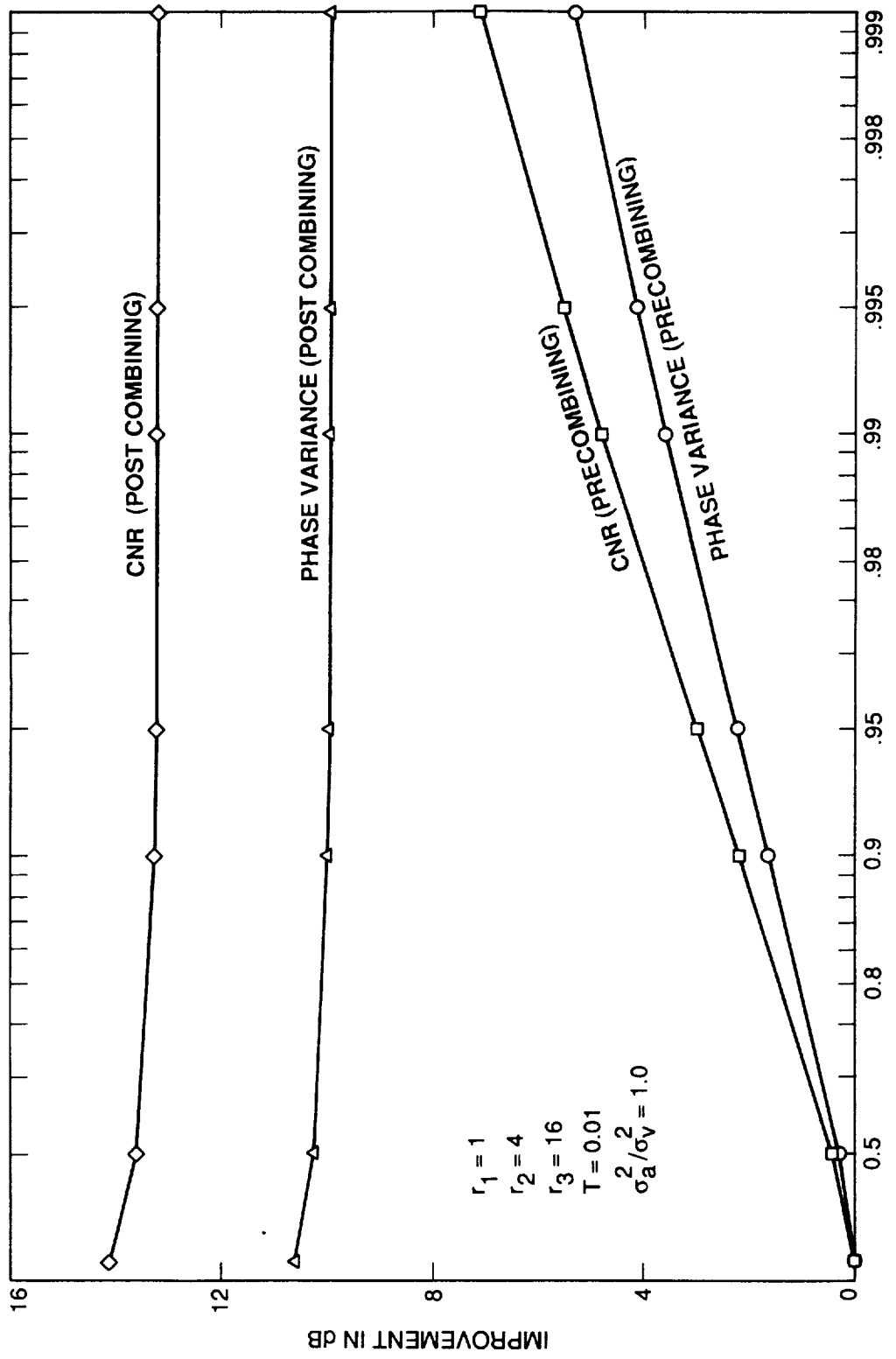

Fig. 24. Improvement Due to Arraying With a Three-Receiver Configuration and a 1:4:16 Ratio (Receiver 3).

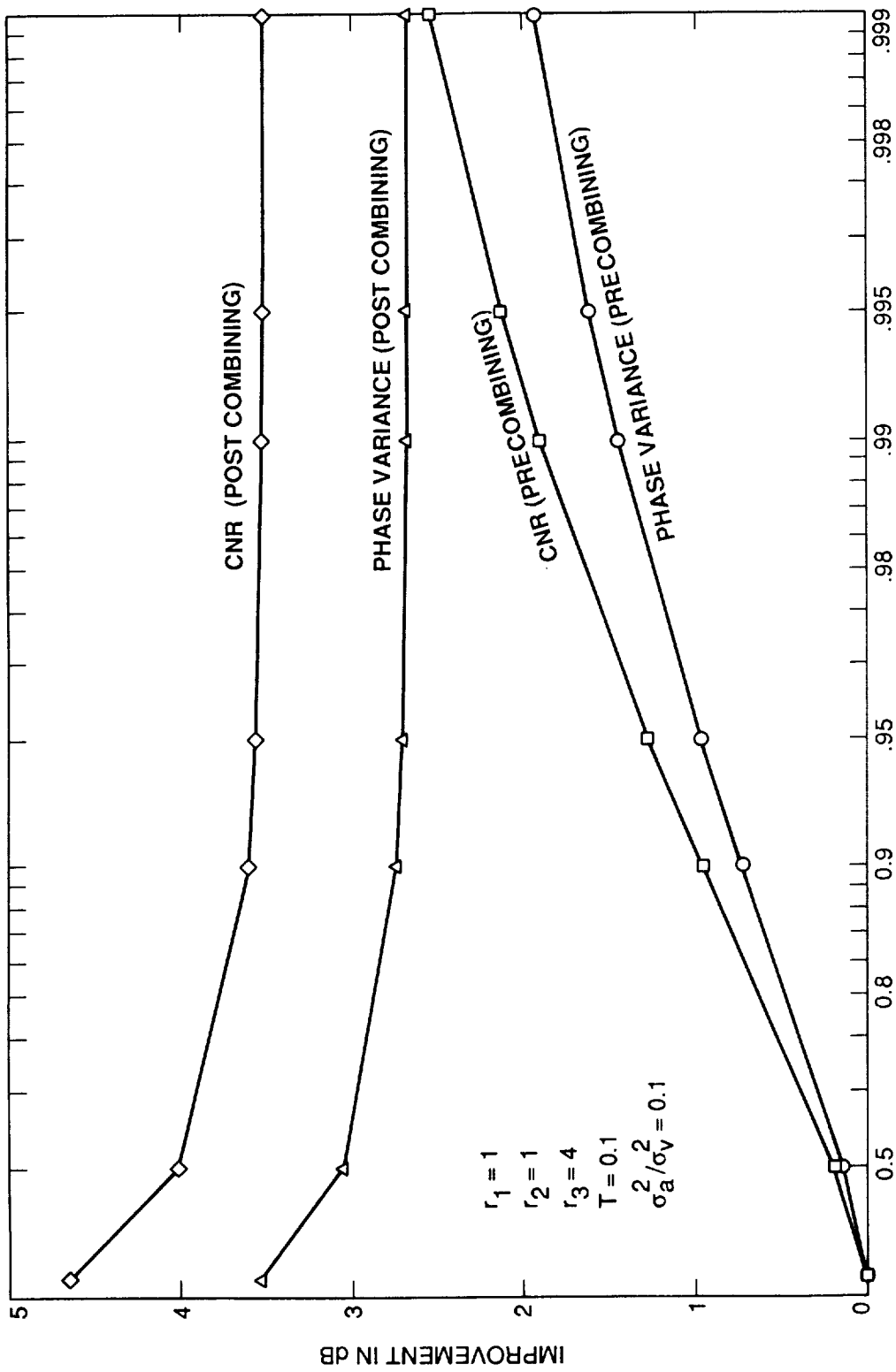

Fig. 25. Improvement Due to Arraying With a Three-Receiver Configuration and a 1:1:4 Ratio (Receiver 1).

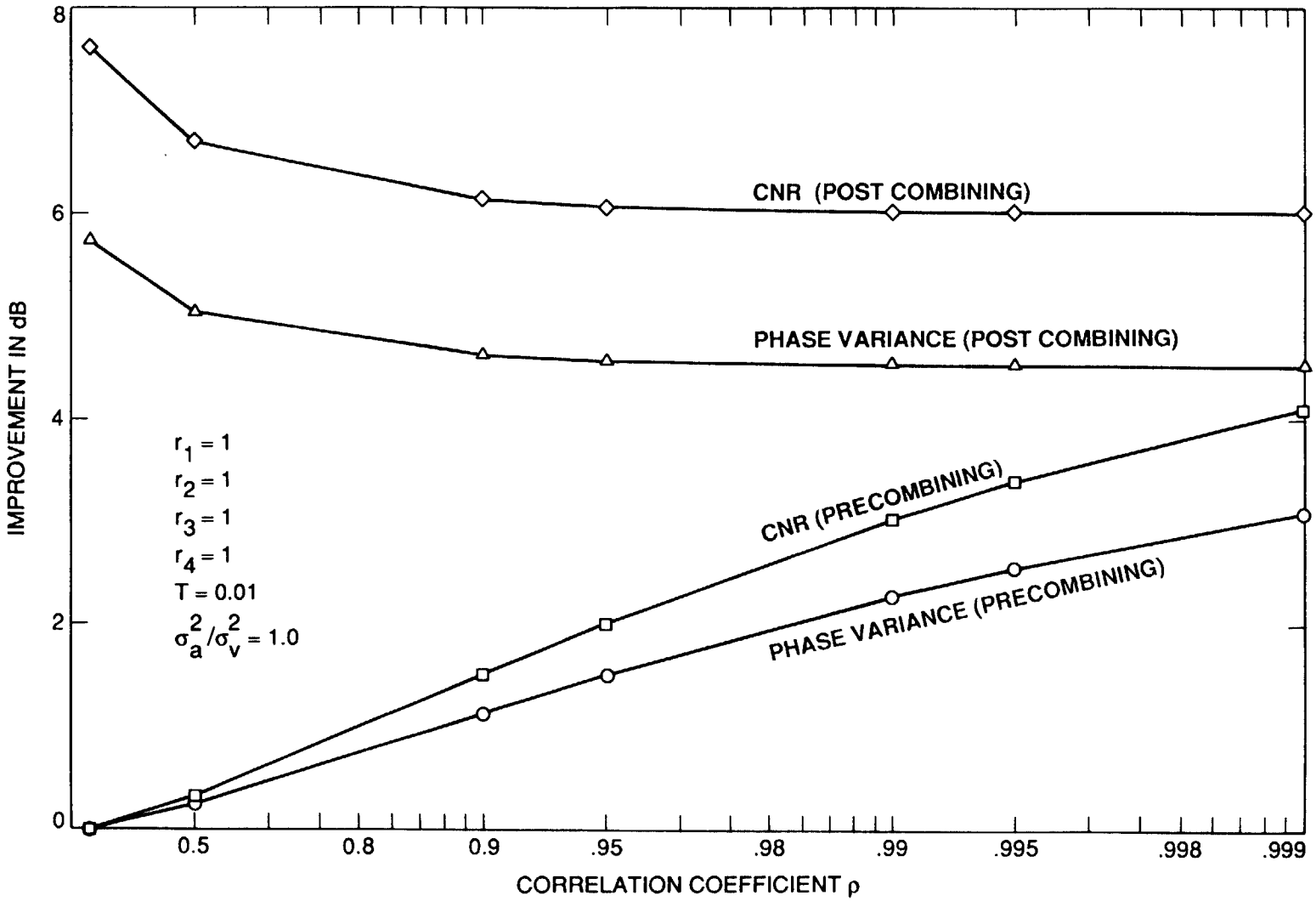

Fig. 26. Improvement Due to Arraying With a Four-Receiver Configuration; Equal CNR Case.

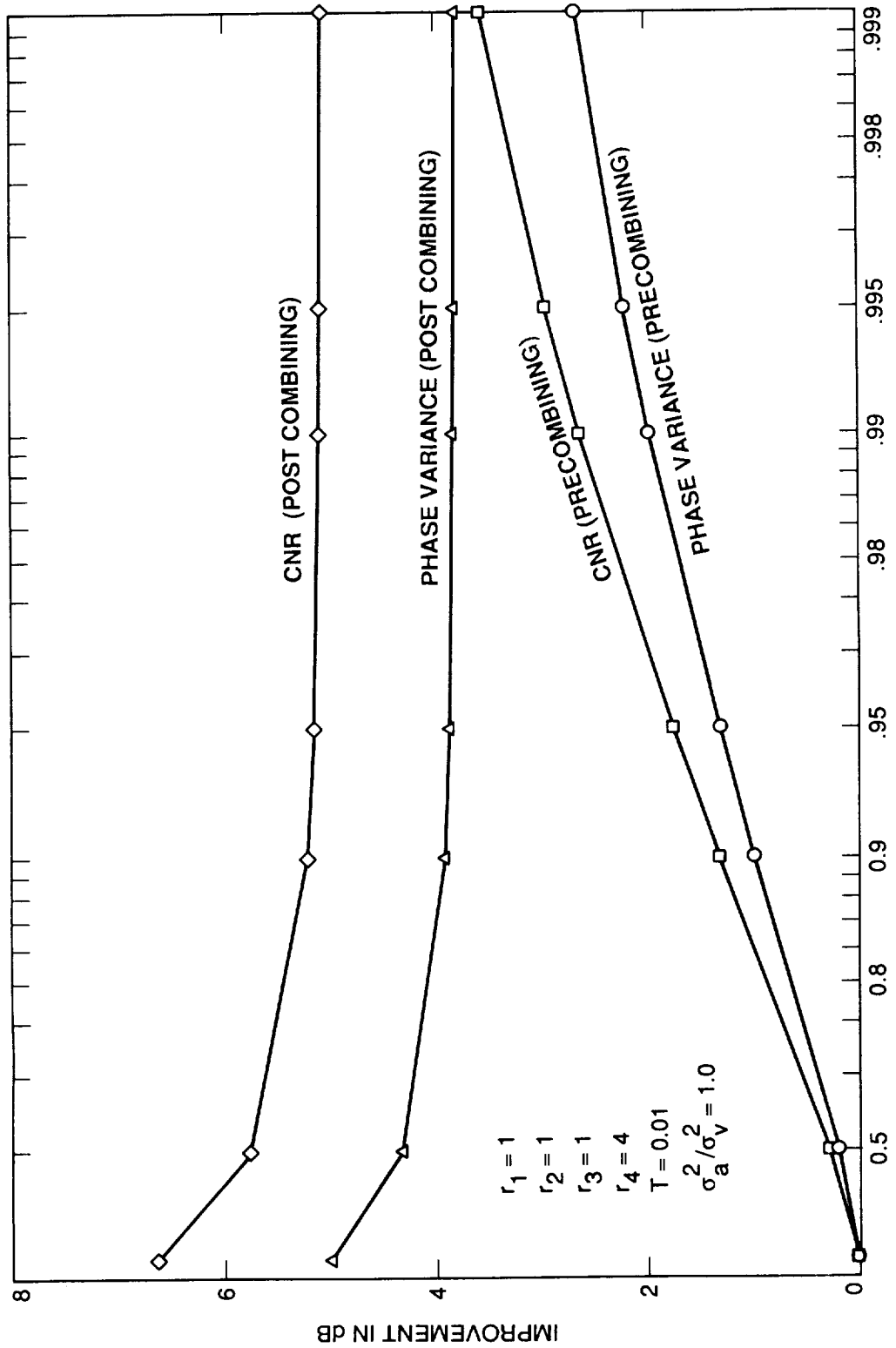

Fig. 27. Improvement Due to Arraying With a Four-Receiver Configuration and a 1:1:1:4 Ratio (Receiver 1).

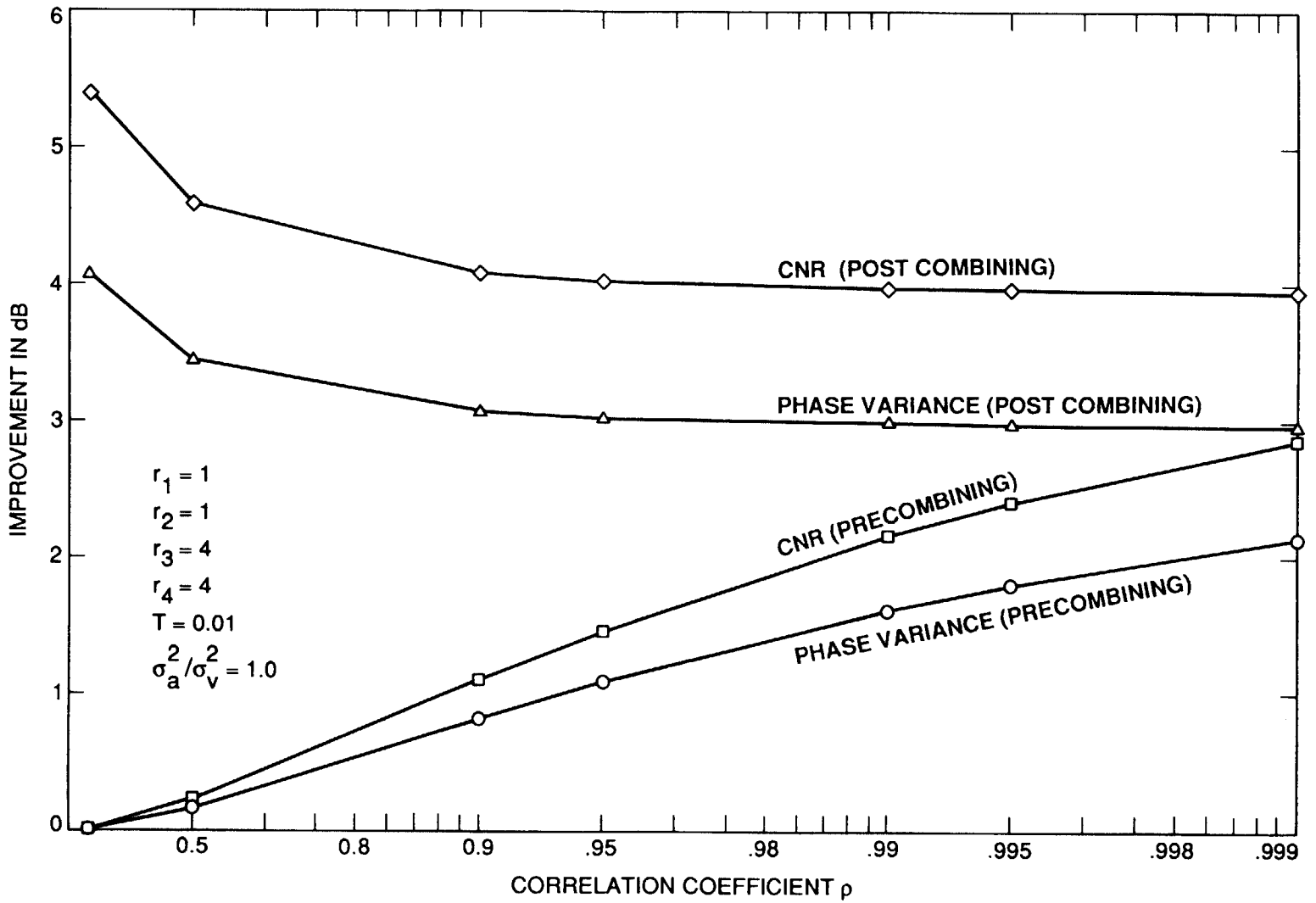

Fig. 28. Improvement Due to Arraying With a Four-Receiver Configuration and a 1:1:4:4 Ratio (Receiver 1).

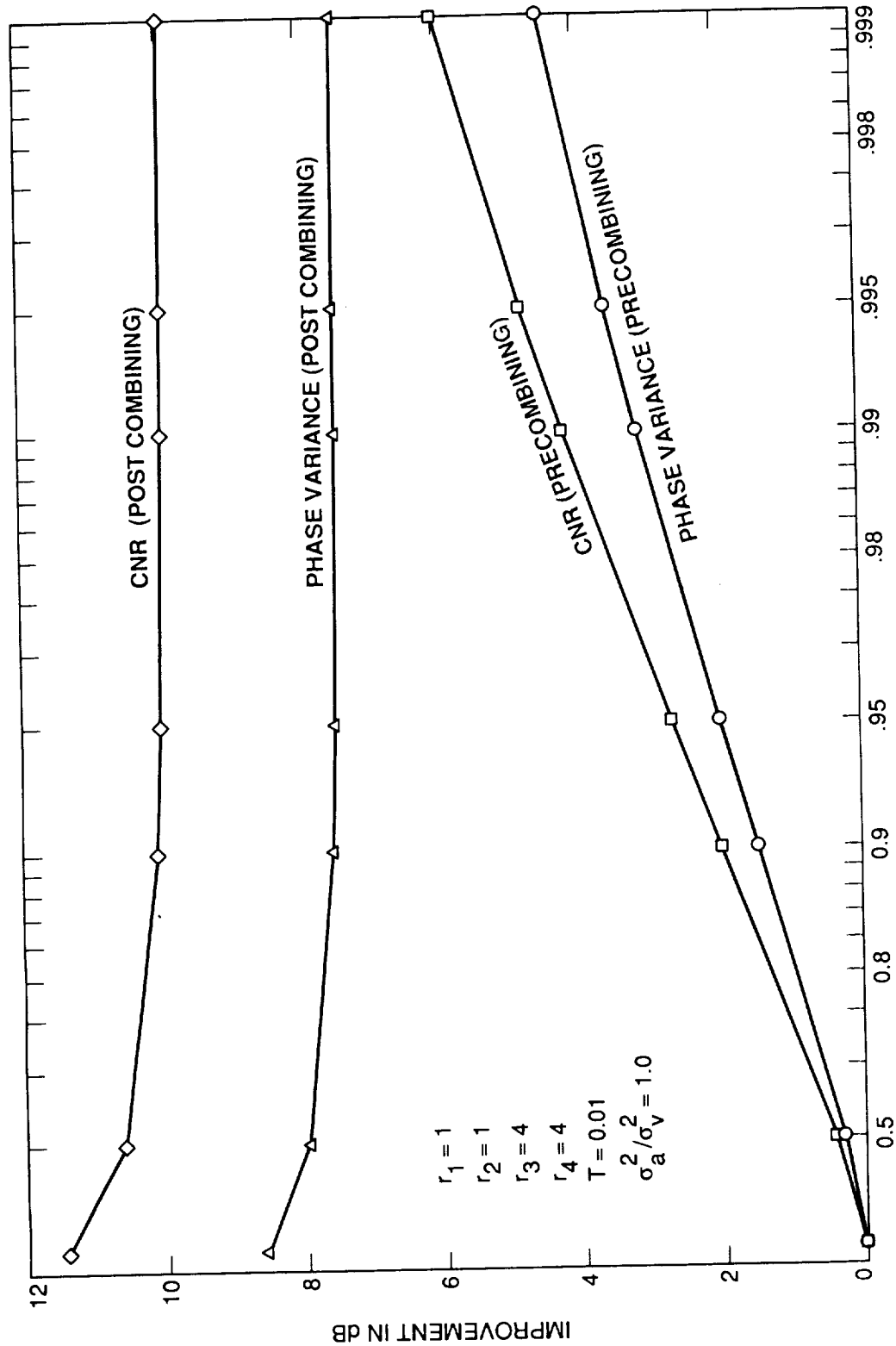

Fig. 29. Improvement Due to Arraying With a Four-Receiver Configuration and a 1:1:4:4 Ratio (Receiver 3).

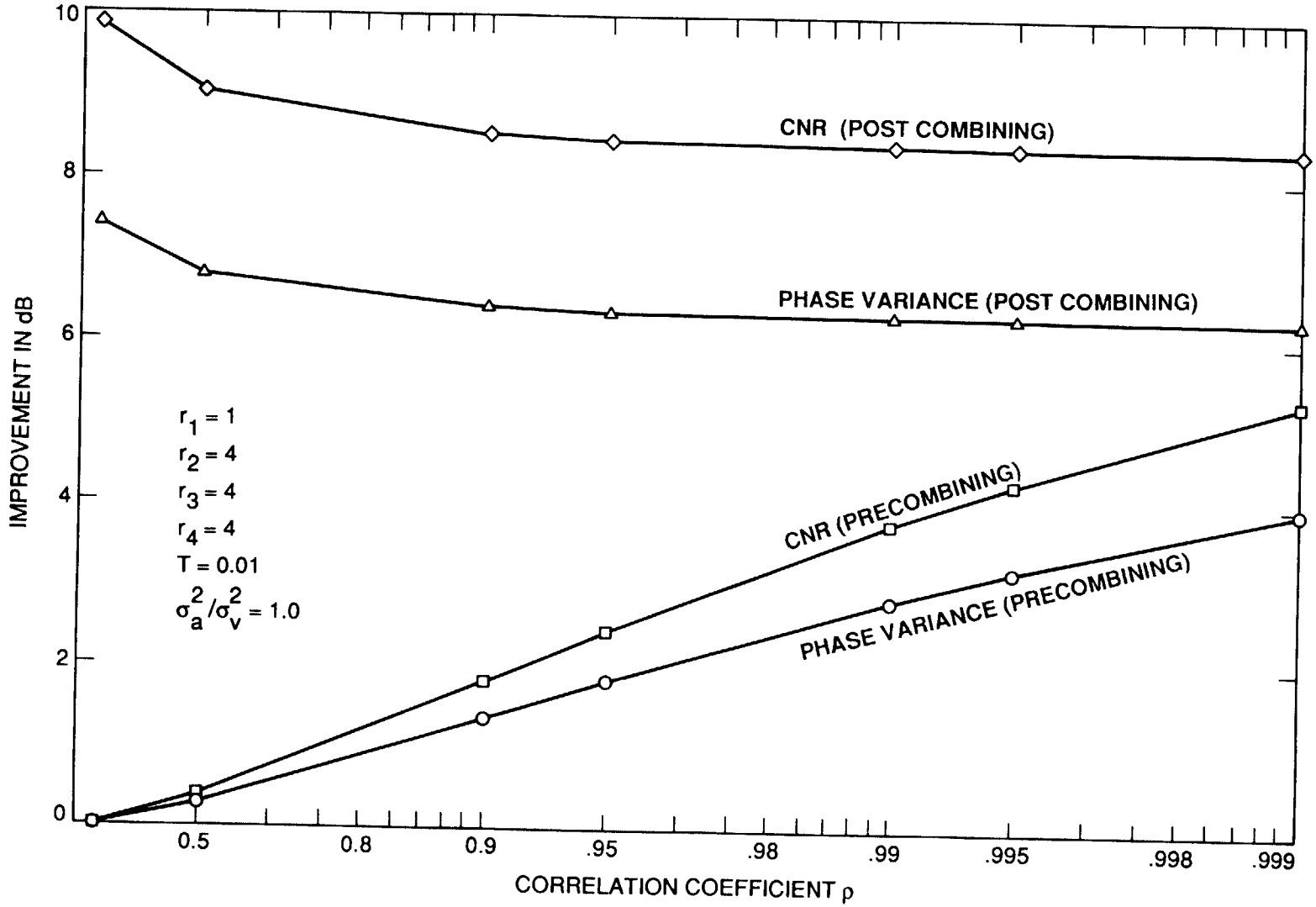

Fig. 30. Improvement Due to Arraying With a Four-Receiver Configuration and a 1:4:4:4 Ratio (Receiver 1).

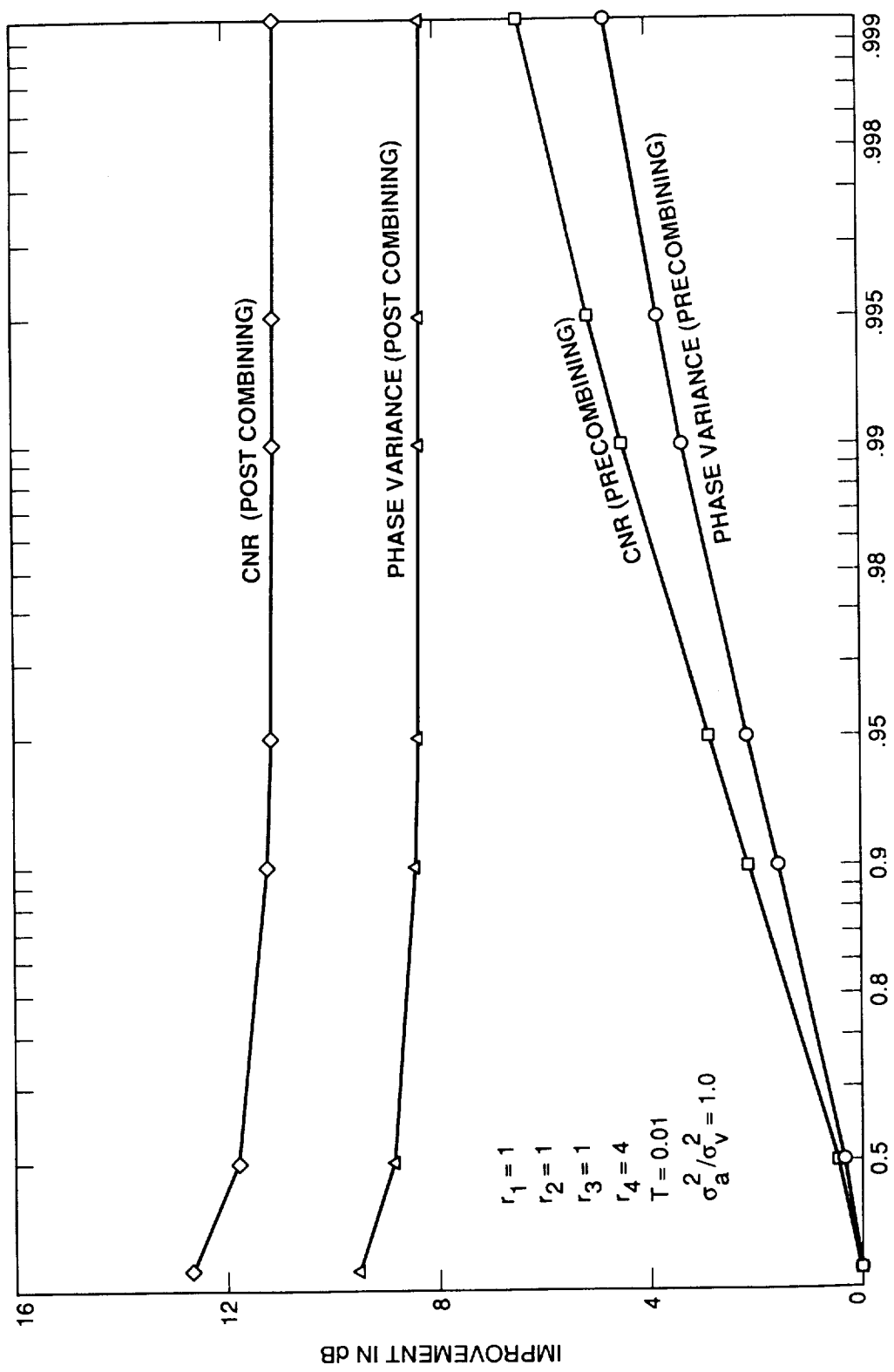

Fig. 31. Improvement Due to Arraying With a Four-Receiver Configuration and a 1:1:1:4 Ratio (Receiver 4).

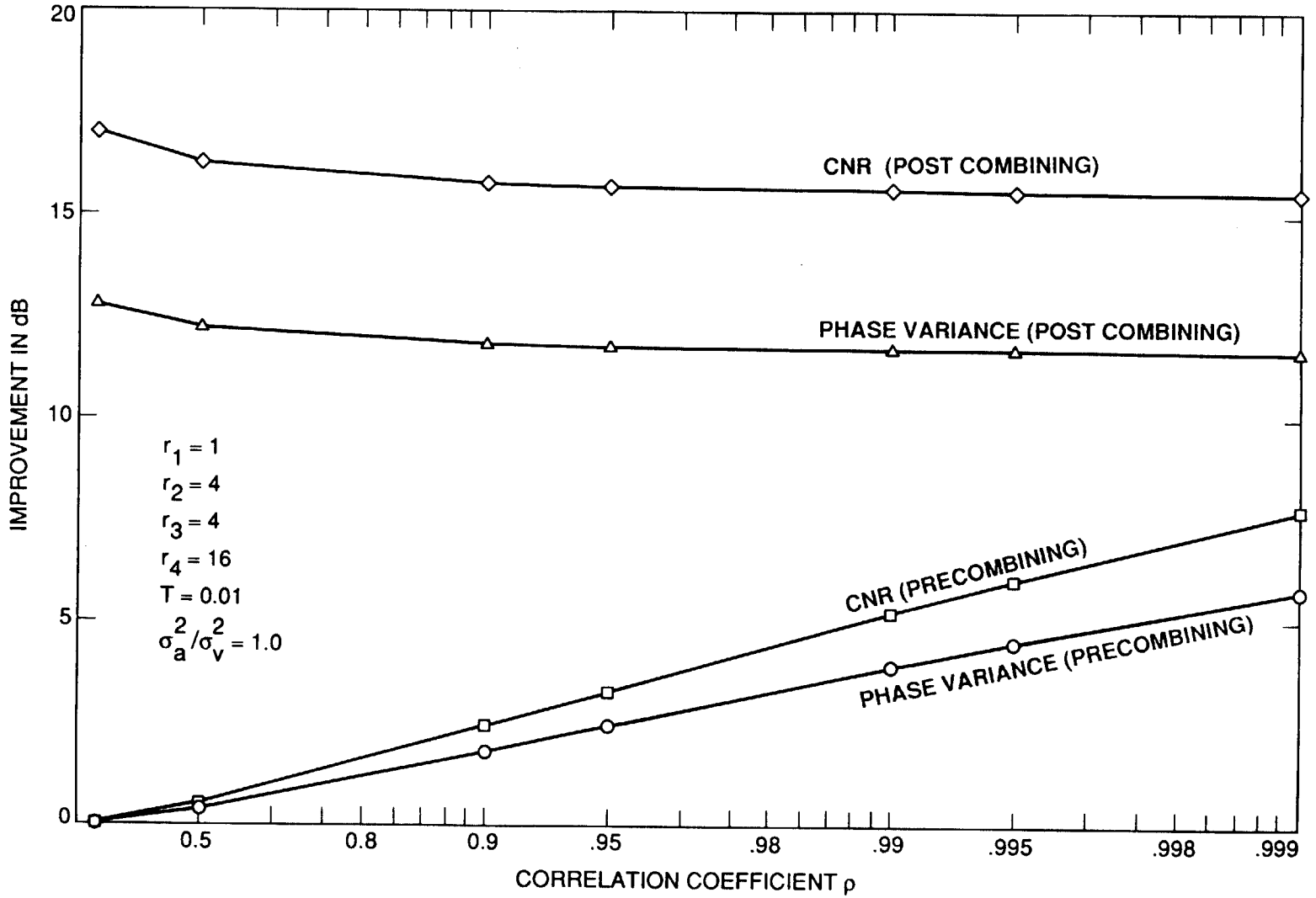

Fig. 32. Improvement Due to Arraying With a Four-Receiver Configuration and a 1:4:4:16 Ratio (Receiver 4).

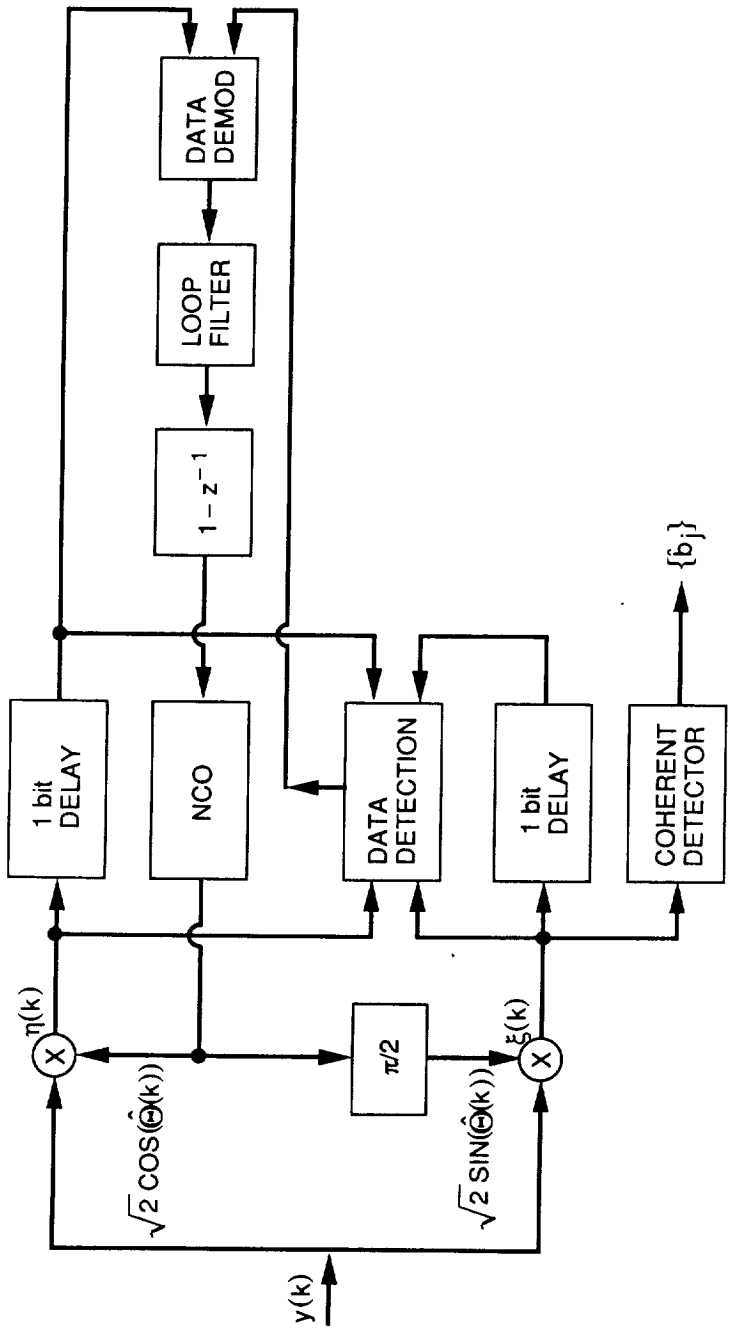

Fig. 33. Decision-Directed Carrier Recovery Loop.

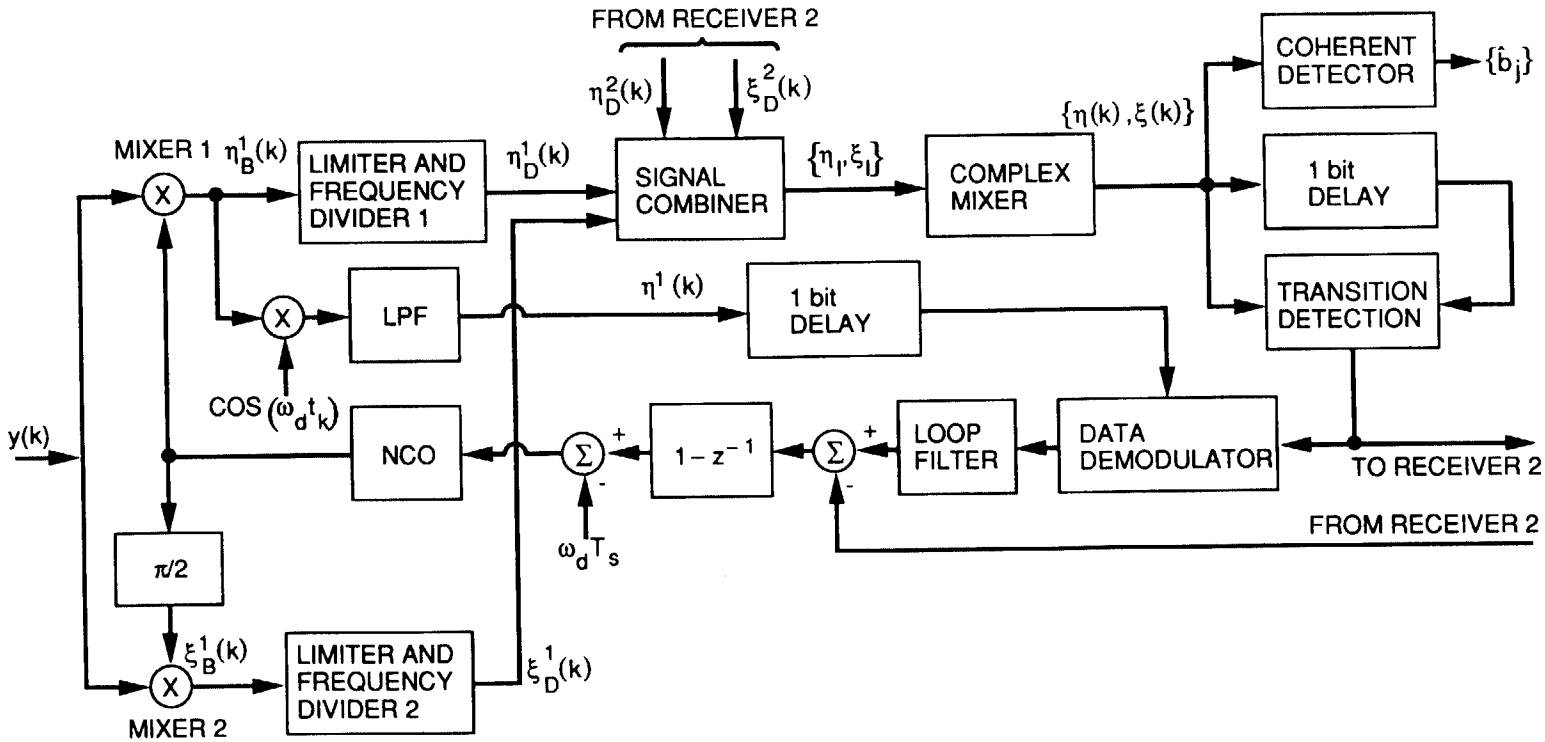

Fig. 34. Decision-Directed and Coupled Receiver Configuration.

TECHNICAL REPORT STANDARD TITLE PAGE

1. Report No. 90-9	2. Government Accession No.	3. Recipient's Catalog No.
4. Title and Subtitle A Novel Multireceiver Communications System Configuration Based on Optimal Estimation Theory		5. Report Date February 1, 1990 6. Performing Organization Code
7. Author(s) R. Kumar		8. Performing Organization Report No.
9. Performing Organization Name and Address JET PROPULSION LABORATORY California Institute of Technology 4800 Oak Grove Drive Pasadena, California 91109		10. Work Unit No. 11. Contract or Grant No. NAS7-918 13. Type of Report and Period Covered JPL External Publication
12. Sponsoring Agency Name and Address NATIONAL AERONAUTICS AND SPACE ADMINISTRATION Washington, D.C. 20546		14. Sponsoring Agency Code

15. Supplementary Notes
Prepared (jointly) for the California State University, Long Beach, and the National Aeronautics and Space Administration.

16. Abstract This publication presents a novel multireceiver configuration for the purpose of carrier arraying and/or signal arraying. Such a problem arises for example, in the NASA Deep Space Network where the same data-modulated signal from a spacecraft is received by a number of geographically separated antennas and the data detection must be efficiently performed on the basis of the various received signals. The proposed configuration is arrived at by formulating the carrier and/or signal arraying problem as an optimal estimation problem. Two specific solutions are proposed.

The first solution is to simultaneously and optimally estimate the various phase processes received at different receivers with coupled phase-locked loops (PLLs) wherein the individual PLLs acquire and track their respective receivers' phase processes, but are aided by each other in an optimal manner...

However, when the phase processes are relatively weakly correlated, ... and for the case of relatively high values of symbol energy-to-noise spectral density ratio (E_s/N_o), we propose a novel configuration for combining the data-modulated, loop-output signals.

The scheme can be extended to the case of low (E_s/N_o) case by performing the combining/detection process over a multisymbol period. Such a configuration results in the minimization of the effective radio loss at the combiner output, and thus a maximization of energy per bit to noise-power spectral density ratio is achieved.

17. Key Words (Selected by Author(s))	18. Distribution Statement
Spacecraft Communications, Command, and Tracking; Communication; Signal Estimation; Data Detection	Unclassified -- Unlimited

19. Security Classif. (of this report)	20. Security Classif. (of this page)	21. No. of Pages	22. Price
Unclassified	Unclassified	86	